Universitat Autònoma de Barcelona

Insights into the CREB-regulated transcription coactivators (CRTCs) in neurons and astrocytes

Laura Rubió Ferrarons

Institut de Neurociències
Departament de Bioquímica i Biologia Molecular
Unitat de Bioquímica i Biologia Molecular, Facultat de Medicina
Universitat Autònoma de Barcelona

Insights into the CREB-regulated transcription coactivators (CRTCs) in neurons and astrocytes

Laura Rubió Ferrarons

TESI DOCTORAL

Bellaterra, Octubre de 2020

Institut de Neurociències
Departament de Bioquímica i Biologia Molecular
Unitat de Bioquímica i Biologia Molecular, Facultat de Medicina
Universitat Autònoma de Barcelona

Insights into the CREB-regulated transcription coactivators (CRTCs) in neurons and astrocytes

Estudi dels coactivadors transcripcionals de CREB (CRTCs) en neurones i astròcits

Memòria de tesi doctoral presentada per Laura Rubió Ferrarons per optar al grau de Doctora en Neurociències per la Universitat Autònoma de Barcelona.

Treball realitzat al Departament de Bioquímica i Biologia Molecular i a l'Institut de Neurociències de la Universitat Autònoma de Barcelona sota la direcció del Dr. Carlos A. Saura Antolín.

El treball realitzat en aquesta tesi doctoral ha estat finançat pels projectes de recerca del Ministerio de Ciencia, Innovación y Universidades (SAF2016-80027-R) i pel Centro de Investigación Biomédica en Red de Enfermedades Neurodegenerativas (CIBERNED) CB06/05/0042.

Bellaterra, 30 d'Octubre de 2020

Doctoranda	Director de tesi
Laura Rubió Ferrarons	Dr. Carlos A. Saura Antolín

I perduts en un desert, caminem buscant petjades,
tot cercant un rumb incert que ens apropi a l'horitzó.
Cada pas que fem ha de ser un pas ferm,
que el rellotge empeny sense compassió.

Obeses (2018)
El nostre temps. Fills de les estrelles.

I Table of contents

II Abstract

The transcriptional function of the cyclic adenosine monophosphate (cAMP)-response element binding protein (CREB) is modulated by the family of CREB regulated transcription coactivators (CRTCs). CRTC isoforms (CRTC1, CRTC2 and CRTC3) are present in the brain, but their specific expression, regulation and function in the distinct cell types of the brain remain largely unclear. In this doctoral thesis, I have investigated the expression pattern, regulatory mechanisms and transcriptional function of the CRTC1 and CRTC2 isoforms in neurons and astrocytes of the mouse cerebral cortex. Using novel *Crtc2-LacZ* reporter mice, I show that CRTC2 is expressed in the adult mouse brain in both neurons and glial cells, including microglia and astrocytes. CRTC1 is abundant in neurons, whereas CRTC2 is highly expressed in cultured astrocytes. Pharmacological analyses reveal differential regulation of CRTC1 and CRTC2 in cultured neurons and astrocytes. In neurons, synaptic activity induces CRTC1 dephosphorylation and activation through protein phosphatase (PP) 2B/calcineurin while CRTC2 dephosphorylation is mediated by PP1. In astrocytes, CRTC1 dephosphorylation is regulated by PP2B/calcineurin, whereas CRTC2 dephosphorylation is independent of PP2B/calcineurin, PP1 and PP2A activities. In agreement, CRTC1 is dephosphorylated upon neuronal activity and translocated to the nucleus where interacts with CREB to enhance gene transcription. CRTC2 is also translocated to the nucleus after neuronal stimulation without affecting CREB-mediated transcription in cortical neurons. In fact, neuronal CRTC2 deletion does not result in global phenotypic alterations in neuron-specific *Crtc2* conditional knockout (cKO) mice. By contrast, CRTC2 is translocated to nucleus and recruited to specific CREB target gene promoters to mediate activity-induced transcription in astrocytes. These results indicate differential expression, regulatory mechanisms and transcriptional roles of CRTC isoforms in neurons and astrocytes of the cerebral cortex.

III List of abbreviations

ACQ	Acquisition
A-CREB	CREB negative mutant
ACTH	Adrenocorticotropic hormone
AD	Alzheimer's Disease
Ad5	Adenoviral vector serotype 5
AMPK	AMP-activated protein kinase
ANLS	Astrocyte-neuron lactate shuttle
ANOVA	Analysis of variance
AP-1	Activator protein 1
aPKC	Atypical PKC
ATF	Activating transcription factor
ATM	Ataxia-telangiectasia mutated
ATP	Adenosine triphosphate
BAT	Brown adipose tissue
Bax	Bcl-2-associated X protein
Bcl-2	B-cell lymphoma 2
BDNF	Brain-derived neurotrophic factor
BSA	Bovine serum albumin
bZIP	Basic leucine zipper
C/EBPβ	CCAAT-enhancer-binding protein beta
CaM	Calmodulin
CaMK	Ca^{2+}/calmodulin-dependent kinase
cAMP	Cyclic AMP
CaN	Calcineurin
CART	Cocaine and amphetamine regulated transcript
CBD	CREB-binding domain
CBP	CREB binding protein
CDB	ChIP Dilution Buffer
CDK	Cyclin-dependent kinase
CGRP	Calcitonin gene-related peptide
ChIP	Chromatin immunoprecipitation
cKO	Conditional knockout
CNS	Central nervous system
CoIP	Co-immunoprecipitation
COP1	Constitutive photomorphogenic 1
COPII	Coat protein complex II
Cre	Cre-recombinase

CRE	cAMP-response element
CREB	cAMP-response element binding protein
CREBH	CRE-binding protein H
CREM	cAMP response element modulator
CRF	Corticotropin Releasing Factor
CRH-1	CREB homolog-1
CRTC	CREB-regulated transcription coactivator
CsA	Cyclosporin A
D:A	Donor:acceptor
DIV	Days *in vitro*
DMEM	Dulbecco's modified eagle medium
DNA	Deoxyribonucleic acid
dNTPs	Deoxynucleotide triphosphates
DTT	Dithiothreitol
ECL	Enhanced chemiluminescence
EDTA	Ethylenediaminetetraacetic acid
E-LTP	Early-phase LTP
ER	Endoplasmic reticulum
ERK	Extracellular signal-regulated kinase
ES	Embryonic stem
f/f	Floxed/floxed
FBS	Fetal bovine serum
FRET	Fluorescence Resonance Energy Transfer
FSK	Forskolin
G6Pase	Glucose-6-phosphatase
GABA	γ-aminobutyric acid
GAPDH	Glyceraldehyde-3-phosphate dehydrogenase
GFAP	Glial fibrillary acidic protein
GFP	Green fluorescent protein
GPx1	Glutathione peroxidase 1
GR	Glucocorticoid receptor
HBS	HEPES Buffered Saline
HEK	Human embryonic kidney
HK2	Hexokinase 2
HRP	Horseradish peroxidase
IL	Interleukin
IP	Immunoprecipitation

Irs2	Insulin receptor substrate 2
KID	Kinase-inducible domain
KIX	Kinase-inducible interacting
LARII	Luciferase assay reagent II
LB	Luria broth
LDHA	Lactate dehydrogenase A
LKB1	Liver kinase B1
L-LTP	Late-phase LTP
LTP	Long-term potentiation
LV	Lentiviral particles
MAPK	Mitogen-activated protein kinase
MAPKAP2	MAP kinase-activated protein kinase 2
MARK	Microtubule affinity regulating kinase
MOI	Multiplicity of infection
mRNA	Messenger RNA
MSK	Mitogen/stress-activated kinase
MWM	Morris Water Maze
NAAG	N-acetylaspartylglutamate
NE	Norepinephrine
NES	Nuclear export sequence
NGS	Normal goat serum
NLS	Nuclear localization sequence
NMDA	N-methyl-D-aspartate
NONO	Non-POU domain-containing octamer-binding
Nr4a1	Nuclear receptor subfamily 4 group A member 1
Nr4a2	Nuclear receptor subfamily 4 group A member 2
OGT	O-glycosyl transferase
OkA	Okadaic Acid
OP	Opposite
PAGE	Polyacrylamide gel electrophoresis
PBG	PBS-Glucose
PBS	Phosphate buffered saline
PCR	Polymerase chain reaction
PDL	Poly-D-lysine
PEPCK	Phosphoenolpyruvate carboxykinase
PFA	Paraformaldehyde
PGC-1α	Peroxisome proliferative-activated receptor gamma coactivator 1α

PKA	Protein kinase A
PKB	Protein kinase B
PKC	Protein kinase C
PMSF	Phenylmethylsulfonyl fluoride
PP1	Protein phosphatase 1
PP2A	Protein phosphatase 2A
PP2B	Protein phosphatase 2B
PP4	Protein phosphatase 4
PRMT6	Protein arginine methyltransferase 6
PTEN	Phosphatase and tensin homolog
PTP1B	Protein tyrosine phosphatase 1B
PVDF	Polyvinylidene fluoride
REG	Regulatory
RIPA	Radioimmunoprecipitation assay
RNA	Ribonucleic acid
ROI	Region of interest
ROS	Reactive oxygen species
RSK	Ribosomal S6 kinase
RT-qPCR	Real-time quantitative PCR
SCN	Suprachiasmatic nucleus
Scr	Scramble
SD	Splicing domain
SD	Standard deviation
SDS	Sodium dodecyl sulfate
SEM	Standard error of the mean
shCRTC1	Short hairpin *Crtc1*
SIK	Salt-inducible kinase
Sirt1	Sirtulin 1
sNPF	Short neuropeptide F
SOD2	Superoxide dismutase 2
SREBP1	Sterol regulatory element-binding protein 1
STP	Short-term potentiation
SUMO	Small ubiquitin-related modifier
TAD	Transactivation domain
TAF4	TATA binding protein-associated factor 4
TBS	Tris-buffered saline
TE	Tris-EDTA

TFIID	Transcription factor IID
TG	Target
Th	T helper cell
TORC	Transducers of regulated CREB activity
TPA	12-O-Tetradecanoylphorbol-13-acetate
TPM	Transcripts per million
TRH	Thyrotropin Releasing Hormone
TRPV1	Transient receptor potential cation channel subfamily V member 1
TSS	Transcription starting site
UCP1	Uncoupling protein 1
WT	Wild type
XPO1	Exportin 1
ΔCre	Non-active mutant Cre-recombinase

IV Introduction

1 The transcription factor CREB

cAMP-response element (CRE) binding protein (CREB) is a transcription factor that mediates cellular responses induced by a wide range of extracellular and intracellular stimuli by enhancing transcription of targeted genes containing CRE sites in their promoter regions. CREB is ubiquitously expressed in most human tissues, where it plays multiple physiological and pathological functions. Among these, CREB regulates neuronal survival, synaptic plasticity and memory, circadian rhythm or glucose homeostasis in the brain (Lonze & Ginty, 2002).

1.1 CREB structure and regulation

CREB belongs to the basic leucine zipper (bZIP) domain large family of transcription factors that also includes the cAMP-response element modulator (CREM) and activating transcription factor 1 (ATF1). CREB structure contains an amino-terminal transactivation domain (TAD), that comprises a central kinase-inducible domain (KID) and two glutamine-rich constitutive activation (Q1 and Q2) domains, and a carboxy-terminal bZIP binding domain (**Figure 1**). The bZIP domain mediates the binding to DNA through CRE sequences, CREB dimerization and the binding to CREB-regulated transcription coactivators (CRTCs), whereas the TAD region regulates the interaction of different components essential for recruiting the transcriptional machinery (Johannessen et al., 2004; Schumacher et al., 2000).

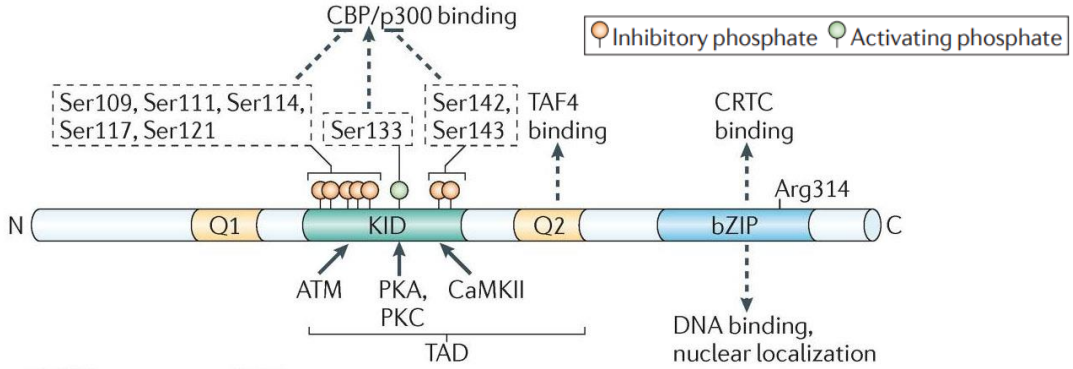

Figure 1. CREB structure. CREB contains two glutamine-rich activation domains (Q1 and Q2), a kinase-inducible domain (KID) and b-ZIP domain. Different kinases regulate phosphorylation of multiple residues at KID which determine CREB binding to CBP/p300. Q2 mediates interaction with the TAF4 and bZIP mediates both DNA and CRTC binding. The KID together with Q2 conform the transactivation domain (TAD). From Altarejos and Montminy 2011.

CREB-dependent transcriptional activity depends on different factors including, among others, the number of CRE sites in a gene promoter, their distance to the TSS, the presence of TATA box and the methylation state of the CRE sequences (X. Zhang et al., 2005). CREB regulates expression of multiple target genes by recognizing conserved palindromic CRE (TGACGTCA) or half-CRE (CGTCA/TGACG) sites (Mayr & Montminy, 2001). In the human genome, ~750,000 palindromic sequences and half-CRE sites have been reported although only about

4,000 CRE sequences are located in the proximal promoter region, that is within 200 base pairs of the TSS, which increases the probability to induce gene transcription (X. Zhang et al., 2005). CREB binding to the gene promoters is regulated by DNA methylation, a mechanism that impairs CREB binding to the DNA (Iguchi-Ariga & Schaffner, 1989; X. Zhang et al., 2005). CRE methylation is more frequently found in intergenic regions, where CREB is presumably non-functional, although CRE sequences in promoter regions can also be methylated (X. Zhang et al., 2005). In fact, differential methylation at promoter regions of CREB target genes could, in part, explain the cell-type specific transcriptional programs. However, the occupancy profile of CREB over the CRE sites is very similar in different tissues. Nonetheless, despite this high CREB occupancy over gene promoters, only a small percentage of the human genome genes, about 100 out of the 4,000 genes harboring CRE sequences proximal to the promoter region, are transcribed after cAMP induction in a cell type-specific manner (X. Zhang et al., 2005). Indeed, promoters with CREB binding sites are transcriptionally more active when are located proximal to TATA boxes, which makes genes more prompt to be regulated by cAMP signalling. On the contrary, CREB transcription becomes weaker when the TATA box(es) is located far upstream from the CRE sequence (Conkright, Guzmán, et al., 2003; Mayr & Montminy, 2001). However, only a 10% of genes occupied by CREB that contain TATA-box are upregulated in a cAMP-dependent manner, suggesting additional regulation by recruitment of coactivators or epigenetic modulation (X. Zhang et al., 2005).

CREB transcriptional activity is modulated by interacting with different binding partners. The CREB glutamine-rich domain interacts with TATA binding protein-associated factor (TAF) 4 through TAFII130 or TAFII135 binding (**Figure 1**). TAF4 is part of the transcription factor IID (TFIID) complex, so this interaction is essential for recruiting the RNA polymerase complex to initiate transcription. (Felinski & Quinn, 2001; Ferreri et al., 1994; Mengus et al., 2005; Saluja et al., 1998). CREB phosphorylation at Ser133 allows the recruitment of CREB coactivators, such as CREB binding protein (CBP) or p300, via their kinase-inducible interacting (KIX) domain (**Figure 1**) (Chrivia et al., 1993; Kwok et al., 1994). CBP and its paralog p300 are histone acetyl-transferases that facilitate the access of the RNA polymerase II transcriptional complex to the transcription starting site (TSS) (Asahara et al., 2001; Kee et al., 1996; Ogryzko et al., 1996).

Different signalling pathways increase intracellular levels of Ca^{2+} or cAMP that finally converge in CREB phosphorylation (**Figure 2**) (Gonzalez & Montminy, 1989; Sheng et al., 1991). Several kinases can recognize and modify multiple phosphorylation sites contained in the TAD region of CREB, which are essential for regulating CREB transcriptional activity (Johannessen et al., 2004). The main regulatory mechanism of CREB function is through phosphorylation at Ser133 by different kinases including Ca^{2+}/calmodulin (CaM)-dependent kinase (CaMK) II and IV,

protein kinase A (PKA), protein kinase C (PKC), mitogen/stress-activated kinase (MSK), ribosomal S6 kinase (RSK), PKB/Akt, mitogen-activated protein kinase (MAPK) and MAP kinase-activated protein kinase 2 (MAPKAP2 or MK2) (Deak et al., 1998; Du & Montminy, 1998; Ginty et al., 1994; Gonzalez & Montminy, 1989; Matsumoto et al., 1998; Pierrat et al., 1998; Sun et al., 1994; Tan et al., 1996; Xing et al., 1996). Structural analysis of CREB and CBP interaction through their KID-KIX domains suggests that CREB phosphorylation at Ser133 is sufficient for CBP/p300 recruitment and CREB target gene transcription in response to stimulus (Cardinaux et al., 2000; Parker et al., 1998; Shaywitz et al., 2000).

Besides Ser133 phosphorylation, other two clusters of phosphorylation flanking Ser133 are important for regulating CREB activity. The first one, phosphorylation at Ser111 and Ser121 by ataxia-telangiectasia mutated (ATM) in response to DNA damage, blocks the CREB-CBP interaction (Shanware et al., 2007; Shi et al., 2004). In addition, phosphorylation at Ser142 and Ser143 mediated by CaMKII and/or casein kinase II destabilize CREB-CBP interaction. However, when this second cluster is phosphorylated together with Ser133, it results in enhancement of activity-induced gene transcription (Kornhauser et al., 2002; Sun et al., 1994). These results suggest that CREB-mediated gene expression can be potentiated independently of CBP interaction (Kornhauser et al., 2002).

CREB dephosphorylation at Ser133 by Ser/Thr protein phosphatase 1 (PP1) and 2A (PP2A) results in a reduced CREB transcriptional activity (**Figure 2**) (Alberts et al., 1994; Wadzinski et al., 1993). Calcineurin/protein phosphatase 2B (CaN/PP2B) has also been implicated in CREB dephosphorylation, presumably through indirect activation of PP1 (Bito et al., 1996). Other phosphatases have been proposed to regulate CREB by inhibiting the kinases responsible for CREB phosphorylation. Some of these phosphatases are phosphatase and tensin homolog (PTEN) that inhibits PKB/Akt or protein tyrosine phosphatase 1B (PTP1B) that blocks the MAPK pathway (Johannessen et al., 2004).

Although, KID phosphorylation seems to play an important role in the CREB-dependent gene transcription, CREB can be active independently of Ser133 phosphorylation. In this case, interaction of CREB with CREB-regulated transcription coactivators (CRTCs) is sufficient to enhance the binding of the CREB bZIP domain to DNA and to recruit the transcriptional complex for potentiating gene transcription (Conkright, Canettieri, et al., 2003).

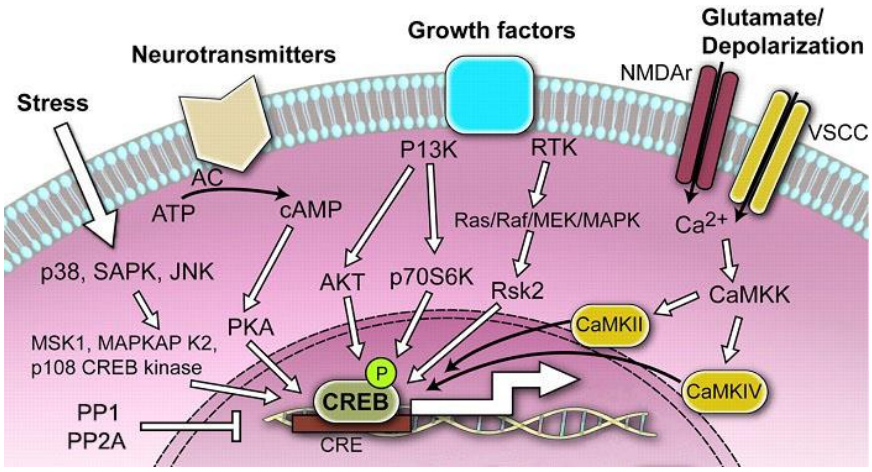

Figure 2: CREB activity regulation. Multiple extracellular stimuli converge in CREB phosphorylation through different pathways and enhance CREB-dependent gene transcription. CREB dephosphorylation is mediated by PP1 and PP2A. Modified from Alberini 2009.

Moreover, CREB activity can be modulated not only by phosphorylation, but also by post-translational modifications, including acetylation, ubiquitination, SUMOylation and glycosylation. CREB is acetylated by CBP/p300 in three different lysines at the TAD domain. Inhibition of CREB acetylation prolongs CREB phosphorylation induced by cAMP and enhances CREB-dependent gene transcription (Q. Lu et al., 2003). Glycosylation of CREB occurs in residues of the Q2 domain, a region responsible for the recruitment of the transcriptional machinery. Glycosylation *β*-*N*-acetylglucosamine (*O*-GlcNAc glycosylation) at these residues leads to destabilization of CREB binding to the transcriptional complex, TAFII130, which results in an impairment of the CREB transcriptional activity (Lamarre-Vincent & Hsieh-Wilson, 2003). Moreover, CREB contains a proteasomal-targeting motif (DSVTDS) that is recognized and dephosphorylated by PP1. When this motif becomes hyperphosphorylated, ubiquitination occur and CREB is targeted to proteasomal degradation (Taylor et al., 2000). CREB can also be post-translationally modified by small ubiquitin-related modifier (SUMO)-1, a process that enhances CREB-dependent gene transcription (Comerford et al., 2003). Site-directed mutagenesis at Lys304 revealed loss of SUMO-1 modifications and also, a loss of CREB nuclear localization suggesting a role for SUMOylation in mediating CREB activation. Additional SUMOylation consensus sequences are present in CREB, although the role of these SUMOylation sites in CREB function are unknown (Comerford et al., 2003).

In summary, CREB transcriptional activity is regulated by a wide range of stimuli and intracellular signals including: 1) the activation of signalling cascades that depend on the cellular type and context, 2) CREB post-translational modifications and 3) the presence of transcriptional coactivators. In addition, CREB transcription depends on the number of CRE sites, their distance to the TSS, the presence of proximal TATA boxes or the methylation state of the promoters.

1.2 Function of CREB in the brain

CREB is expressed in the different cell types found in brain, although its function has been much more investigated in neurons, where plays essential roles such as neuronal survival, synaptic plasticity or memory formation, than in other cell types.

Transcriptomic analysis comparing CREB signature in neurons and astrocytes revealed substantial differences (Pardo et al., 2017). Thus, while 75% of neuronal CREB target genes are related with neurotransmission, signalling and transcription; 75% of the CREB-regulated astrocytic genes are associated with mitochondrial function, lipid metabolism, signalling through MAPK, SNARE function and protective responses such as redox protection and plasticity genes (Pardo et al., 2017). Thus, CREB seems to participate in diverse non-redundant functions in neurons and astrocytes. Nonetheless, it is unknown whether distinct regulatory mechanisms, including post-translational modifications or binding to specific coactivators, are responsible for regulating the singular CREB-dependent transcriptomes in neurons and astrocytes.

1.2.1 CREB function in neuronal survival

CREB family members are essential and critical for nervous system development. CREB knockout mice show defects in the central nervous system (CNS) development including reduction in the corpus callosum and in the anterior commissures that results in death after birth (Rudolph et al., 1998). CREB deficit is also associated with an increase in apoptosis and disrupted axonal growth during development in the peripheral nervous system (Lonze et al., 2002). Moreover, postnatal expression of a negative mutant of CREB induces apoptosis and neurodegeneration indicating CREB function is also required for neuronal survival in the adult brain (Ao et al., 2006). To support these neuroprotective effects, CREB regulates expression of different pro-survival factors such as B-cell lymphoma 2 (Bcl-2) in response to neurotrophic factors (Riccio et al., 1999). Loss of CREB, thus, results in a Bcl-2-associated X protein (Bax)-dependent apoptosis (Lonze et al., 2002). Moreover, the protective role of CREB in neurons involves expression of the peroxisome proliferative-activated receptor gamma coactivator (PGC)-1α, a key regulatory coactivator that enhance expression of reactive oxygen species (ROS)-detoxifying enzymes (Herzig et al., 2001). In particular, PGC-1α can induce expression of anti-ROS genes such as glutathione peroxidase 1 (GPx1) or superoxide dismutase 2 (SOD2) genes and also stimulate mitochondrial electron transport while supressing ROS levels (St-Pierre et al., 2006). More recent studies indicate that chronic expression of a constitutive active CREB induce excitotoxicity in neurons which also leads to neuronal death and epileptic seizures (De Armentia et al., 2007). Altogether, CREB tightly regulates the shift between neuronal survival and death.

1.2.2 CREB function in synaptic plasticity

Synaptic plasticity is the capacity of the brain to adapt to environmental changes by modulating synapse strength according to neuronal activity. Thus, synapses may present an increase or reduction in synaptic transmission, termed as potentiation or depression, respectively. It is assumed that learning and memory are tightly linked with changes in the strength of synaptic connections (i.e. synaptic plasticity) allowing the encoding and storage of memory. Different types of activity-dependent synaptic plasticity are required for memory formation. For instance, short-term potentiation (STP) results in a transiently increase of synaptic transmission which correlates with working memory and allows information storage for a short period of time (P. Park et al., 2014). On the contrary, long-term memory results in long-lasting synaptic plasticity termed as long-term potentiation (LTP). LTP can be divided in two different phases: early phase (E-LTP) and late phase (L-LTP), which present different physiological functions (Baltaci et al., 2019). E-LTP changes are transient and independent of protein synthesis which allow memory retention for a brief period of time, from minutes to few hours (Bliss & Collingridge, 2013; P. Park et al., 2014). By contrast, L-LTP requires gene expression and protein synthesis to structurally remodel the synapses resulting in prolonged memory, covering from several hours to months (Alberini, 2009; Baltaci et al., 2019; Bosch et al., 2014).

Thus, considering that learning and memory processes require gene transcription and *de novo* protein synthesis, activity-dependent transcription factors can be essential for its regulation. Different studies suggest a role of CREB in mediating gene transcription priming for LTP (Benito & Barco, 2010). A first study by Kandel's lab demonstrated that microinjection of CRE sequences into the nucleus of a sensory neurons of *Aplysia* selectively blocked long-term facilitation, a type of long lasting synaptic plasticity, without affecting short-term facilitation (Dash et al., 1990). Studies using *Drosophyla melanogaseter* also supported the role exerted by CREB in gene transcription in the learning and memory process (Yin et al., 1994, 1995). Several studies using CREB loss or gain-of-function strategies in rodents also emerged, demonstrating the involvement of CREB in synaptic plasticity, learning and memory. These results showed that CREB mediates different types of memory such as spatial, contextual fear, conditioned taste aversion and social recognition memories (Bourtchuladze et al., 1994; Kogan et al., 1997, 2000; Lamprecht et al., 1997; Pittenger et al., 2002). Thus, CREB can induce memory consolidation by promoting direct expression of memory-related genes or also enhancing expression of other transcription factors such as *c-fos, nuclear receptor subfamily 4 group A member 1 (Nr4a1), Nr4a2* or *Jun* (Pardo et al., 2017). Another CREB-dependent gene that is transcribed during LTP is the brain-derived neurotrophic factor (*Bdnf*). BDNF is important for the function and the structure of excitatory and inhibitory synapses. *Bdnf* transcription is also required for the conversion of short-term to long-lasting memory in many brain regions (Barco et al., 2005; B. Lu et al., 2015). The regulation of

synaptic plasticity and memory by CREB is also modulated by specific transcriptional coactivators, including CRTCs (see section 2.2.5 of introduction). Alternatively, CREB mediates memory by altering the intrinsic excitability of neurons. CREB induces neuronal excitability by enhancing the transcription of membrane ion channels and modulating their activity by phosphorylation allowing, thus, an increase in the firing rate (Benito & Barco, 2010). By contrast, overactivation of CREB also disturbs memory acquisition (Viosca, De Armentia, et al., 2009; Viosca, Malleret, et al., 2009).

Altogether, these results indicate that CREB favours learning and memory by regulating expression of different genes involved in neuronal excitability and synaptic plasticity (Lisman et al., 2018).

1.2.3 CREB function in neuronal energetic metabolism regulation

CREB regulates glucose homeostasis and energy metabolism in the brain. Hypothalamic neurons coordinate glucose and lipid metabolism by sensing circulating hormones and nutrients through the CREB-dependent pathway (Altarejos & Montminy, 2011). Similarly, disruption of CREB activity in neurons leads to a reduction of glycogen and lipid stores and a higher sensitivity to starvation stress in flies (Iijima et al., 2009). The role of CREB in energy metabolism in the hypothalamus is also dependent on the transcriptional coactivators CRTCs, a topic that will be extended in the CRTCs specific sections.

At the cellular level, CREB modulates energy metabolism by acting at different levels. For instance, synaptic activity favours CREB-dependent transcription of *Glut3*, the main neuronal glucose transporter, and the ubiquitin-ligase *Siah2*. Expression of GLUT3 allows glucose uptake and metabolism, enhancing also lipid synthesis, which is required for plasmatic membrane enlargement during neurite outgrowth (Segarra-Mondejar et al., 2018). Moreover, GLUT3 protein levels are downregulated in Alzheimer's disease (AD) brains, which may explain the impaired brain glucose uptake and metabolism occurring in this neurodegenerative disease (Simpson et al., 1994). On its turn, *Siah2* expression stabilizes the hypoxia-inducible factor 1-α (HIF-1α), a transcription factor that regulates the expression of glycolytic rate-limiting enzymes (Segarra-Mondejar et al., 2018). Also, in cultured hippocampal neurons, CREB enhances transcription of PGC-1α, a master regulator of mitochondrial biogenesis and oxidative metabolism. An increase in mitochondrial biogenesis enhances the capability for cellular energy production. In fact, PGC-1α knock-down reduced the amount of mitochondria in dendrites and the density of dendritic spines and synapses (Cheng et al., 2012). These results sustain the idea that mitochondrial biogenesis is important for sustaining synaptic function and morphology.

1.2.4 CREB function in astrocytes

Astrocytes are key players in multiple brain functions. They can modulate their physiology to adapt to the environmental conditions, for instance, assisting neurons metabolically or modulating neuronal function by the release of gliotransmitters. Although CREB is expressed in astrocytes, its function is largely unknown. Different studies suggest that CREB activation in astrocytes is independent of calcium (Carriba et al., 2012; Murray et al., 2009). For instance, increase of intracellular calcium induces transient phosphorylation of CREB at Ser133 that fails to activate CREB-dependent gene transcription. Lack of calcium-dependent CREB activation in astrocytes correlates with the absence of CaMKIV, the main kinase responsible for CREB phosphorylation and activation in response to calcium in neurons (Murray et al., 2009). Another study showed that activation of CREB transcription in astrocytes in response to norepinephrine (NE) and ATP was mediated via an atypical PKC (aPKC), which activity is independent of calcium and cAMP (**Figure 3**) (Carriba et al., 2012). Conversely, other authors suggest ATP-dependent activation of CREB transcription is via activation of CaM kinase through calcium (Takasaki et al., 2008). Nonetheless, inhibition of CaM kinase had a modest effect on CREB-dependent gene transcription suggesting that alternative pathways mediate CREB activation in astrocytes.

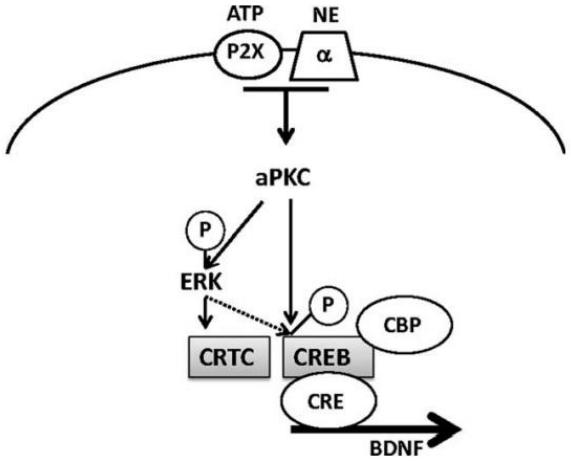

Figure 3. Regulation of CREB in astrocytes. CREB phosphorylation in astrocytes is driven by atypical PKC (aPKC) in response to ATP and NE signalling. From Carriba et al., 2012**.**

The physiological role of CREB in astrocytes is largely unknown, although, similarly to neurons, astrocytic CREB also potentiates protective effects by increasing transcription of neurotrophins. In fact, NE, ATP and dopamine signalling increases BDNF expression via CREB-dependent gene transcription (Koppel et al., 2018; Pardo et al., 2016). Furthermore, CREB activity enhancement in reactive astrocytes after traumatic brain injury prevents from neuronal death and damage, reduce the macrophage infiltration and rescues the expression of genes related with mitochondrial metabolism (Pardo et al., 2016).

1.2.5 CREB in neuron-astrocyte crosstalk

The crosstalk between neurons and astrocytes is essential for brain function. Astrocytes promote neuronal survival, regulate neurotransmission and provide nutrient support for neurons, and, in turns, neurons modulate astrocyte physiology. Thus, the idea that neuronal activity controls astrocytic transcriptome is now emerging.

Astrocytic processes are tightly associated with neurons at synaptic terminals, conforming the tripartite synapse (Araque et al., 1999). It is well known that astrocytes express neurotransmitters receptors that allow astrocytic response to neuronal signalling. This astrocytic response to neurotransmitters generate intracellular calcium waves that result in the release of gliotransmitters, constituting a communication feedback to neurons that can also modulate its synaptic activity (Parpura et al., 1994). As described above, ATP or NE activate CREB in astrocytes, so neuronal activity modulates astrocytic transcriptome and physiological functions (Carriba et al., 2012). Recent evidences also indicate that transmitter-triggered CREB transcriptional activity in astrocytes regulates calcium waves generating an adaptive plasticity-like phenomena that results in reduced intracellular calcium signalling responses upon ATP or NE treatment (Eraso-Pichot et al., 2017). Thus, this astrocytic plasticity can potentially affect neuronal activity by altering gliotransmission (Henneberger et al., 2010; Navarrete & Araque, 2010; Serrano et al., 2006).

Astrocytes express transporters for several neurotransmitters including glutamate, GABA or glycine, which are essential for removing the excess of neurotransmitters at the synaptic cleft after neuronal activity while avoiding neurotransmitter diffusion (Allen, 2014). The uptake of neurotransmitters by astrocytes is essential for the maintenance of neurotransmitters balance since about the 80% of the synaptically-released glutamate is uptaken by astrocytes and a disruption in glutamate balance is associated with several brain disorders (Mahmoud et al., 2019). Importantly, astrocytes modulate glutamate transporters according to neuronal needs. Astrocytic cAMP signalling can affect expression, trafficking and function of glutamate transporters, so CREB activation induced by prolonged cAMP signalling upregulates expression of glutamate transporters (Schlag et al., 1998). Furthermore, a recent study showed that astrocytes, when co-cultured with neurons, change their transcriptome and upregulate genes involved in uptake and metabolism of GABA, glutamate and N-acetylaspartylglutamate (NAAG) (Hasel et al., 2017).

Moreover, synaptic activity induces changes in the metabolic capacity of astrocytes by enhancing the transcription of a large cluster of genes via CREB. Precisely, neuronal activity upregulates genes of glucose oxidation, whereas components of mitochondrial import of pyruvate and NADH are not affected. This indicates that gene expression is focused on glucose oxidation to supply lactate to neurons via astrocyte-neuron lactate shuttle (ANLS). The ANLS hypothesis, first

proposed by Magistretti & Pellerin, 1996, postulates that astrocytes respond to neuronal activity by enhancing glycolysis and release of lactate, which is then uptaken by neurons and used as energy source (**Figure 4**). Traffic of lactate from astrocytes to neurons is necessary for basic neuronal functions such as synaptic plasticity, learning and memory formation (Newman et al., 2011; Steinman et al., 2016; Suzuki et al., 2011; Volkenhoff et al., 2015). Although, at present, it is unclear whether astrocytic CREB regulates synaptic plasticity and memory by affecting ANLS.

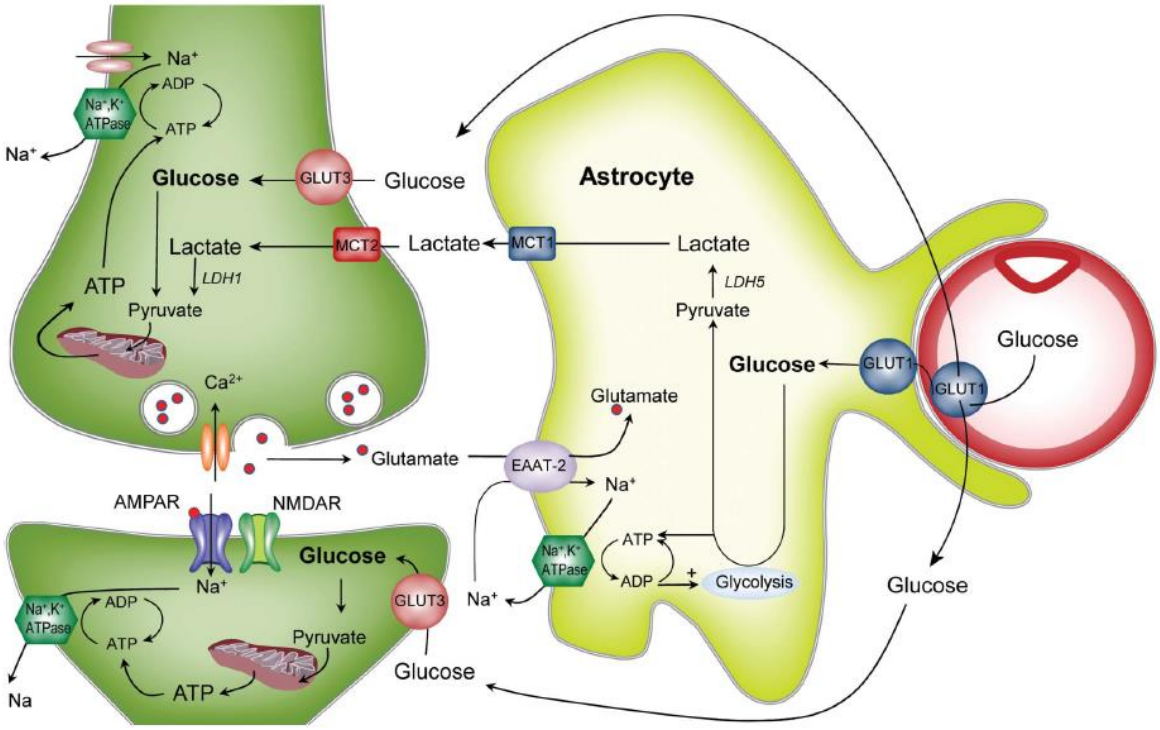

Figure 4. Astrocyte-neuron lactate shuttle. Released glutamate from neurons after synaptic activity is taken up by astrocytes. The co-entrance of glutamate and Na^+ in astrocytes and its association with the Na^+/K^+ ATPase leads to increased glucose consumption and lactate production. Astrocytic lactate is then shuttled to neurons where is used as energy source. From Benarroch, 2014.

2 The role of CRTCs in the brain

Multiple signalling pathways are responsible for CREB phosphorylation and activation, facilitating the recruitment of CREB to CBP or p300 and enhancing gene transcription. However, CREB phosphorylation is not always sufficient for inducing CREB transcription, suggesting that CREB can be activated independently of its phosphorylation. In fact, to regulate the transcription of different and specific sets of gene programs, CREB needs to interact with different coactivators that modulate its transcriptional activity.

Molecular screening studies revealed a new family of CREB coactivators named CREB-regulated transcription coactivators (CRTCs), previously referred as Transducers of Regulated CREB activity (TORCs) (Conkright, Canettieri, et al., 2003; Iourgenko et al., 2003). CRTCs activate the transcription of genes containing CRE consensus sequences in their promoters in response to Ca^{2+} and cAMP (Bittinger et al., 2004; Screaton et al., 2004). Three different CRTC isoforms have been described in mammals: CRTC1, CRTC2 and CRTC3. In humans, CRTC1 is abundant in the brain where plays important functions in synaptic plasticity, memory, circadian rhythm, energy balance and longevity (Saura & Cardinaux, 2017). By contrast, CRTC2 and CRTC3 are more ubiquitously expressed in human tissues (Conkright, Canettieri, et al., 2003). CRTC2 is highly expressed in the liver, where plays a central role in gluconeogenic regulation (Dentin et al., 2007; Koo et al., 2005), in pancreas, where enhances β-cell viability (Eberhard et al., 2013), and in muscle, where favours mitochondrial biogenesis (Wu et al., 2006). Finally, CRTC3 is abundantly found in white and brown adipose tissues where regulates lipid metabolism and participates in the macrophage anti-inflammatory function (MacKenzie et al., 2013; Song et al., 2010).

Crtcs transcripts are detected in different brain regions (Watts et al., 2011). The three CRTC isoforms are widely distributed in the rat brain, being CRTC1 the most expressed followed by CRTC2 and CRTC3 (**Figure 5**). mRNAs of all CRTCs are found in the hippocampus and in the cortex, being *Crtc1* mRNA levels highly expressed. In hypothalamus, *Crtc1* and *Crtc2* transcripts are also found to be abundant, being *Crtc2* levels comparable to those of *Crtc1* in supraoptic nucleus, paraventricular nucleus and suprachiasmatic nucleus of the hypothalamus. All three isoforms are also found in the thalamus, being *Crtc3* the less abundant. *Crtc3*, is, however, prominent in the ventricular ependyma and pia mater (Watts et al., 2011). Myelinated tracts also show low mRNA expression of the three CRTC isoforms, being *Crtc2* the most abundant isoform, which suggests that CRTCs expression is not restricted to neurons (Watts et al., 2011). These results indicate that CRTCs expression may be cell type-specific suggesting also particular regulatory mechanisms and functions for each isoform depending on the cellular context.

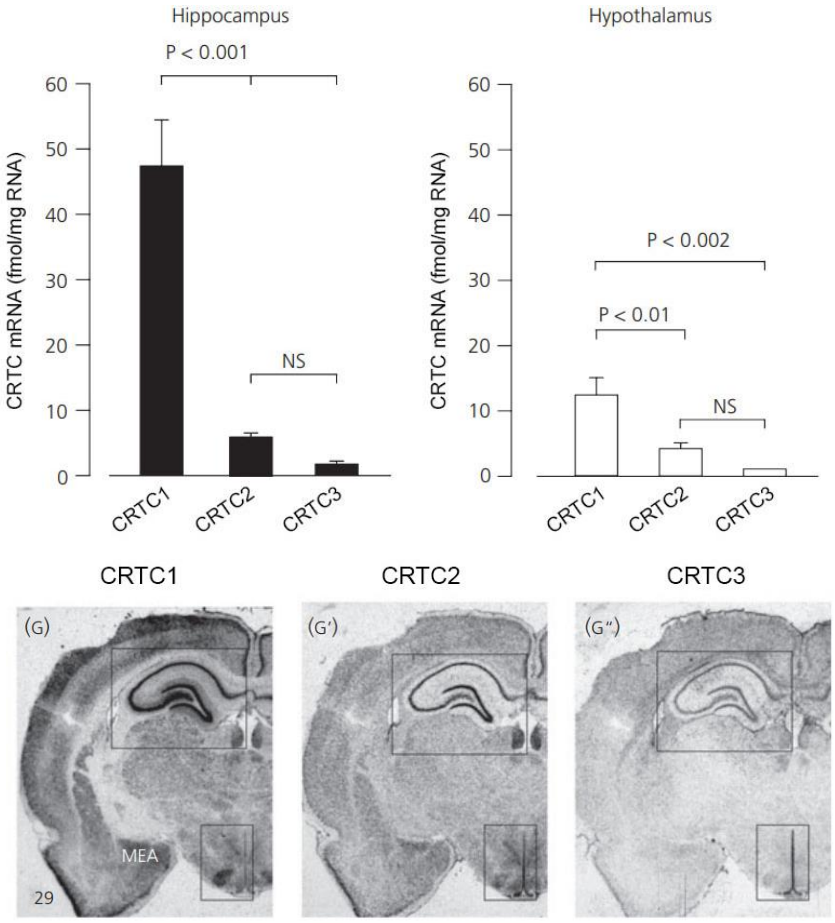

Figure 5: *Crtcs* mRNA levels and localization in the rat brain. (**Top**) mRNA expression levels of the different CRTC isoforms in hippocampal and hypothalamic rat lysates obtained by qRT-PCR. (**Bottom**) *In situ* hybridization analysis of CRTCs in rat brain. Images from Watts et al., 2011.

2.1 CRTC structure and regulation

CRTCs share common and highly conserved domains consisting of a N-terminal coiled-coil domain referred as CREB-binding domain (CBD), a central regulatory (REG) domain that contains a nuclear localization sequence (NLS) and two nuclear export sequences (NES), a splicing domain (SD) and the transactivation domain (TAD), required for transcriptional activation, at the C-terminus (**Figure 6**) (Altarejos & Montminy, 2011; Saura & Cardinaux, 2017).

CRTCs activity is highly regulated by post-translational modifications. The phosphorylation at the REG domain by several protein kinases, specially by the salt-inducible kinase (SIK) family, negatively modulates CRTCs activity (Jansson et al., 2008; Katoh et al., 2006; Koo et al., 2005; Mair et al., 2011; Screaton et al., 2004). In addition, CRTCs activity can also be modulated by acetylation, ubiquitination, glycosylation or methylation (see specific CRTCs sections below) (Saura & Cardinaux, 2017).

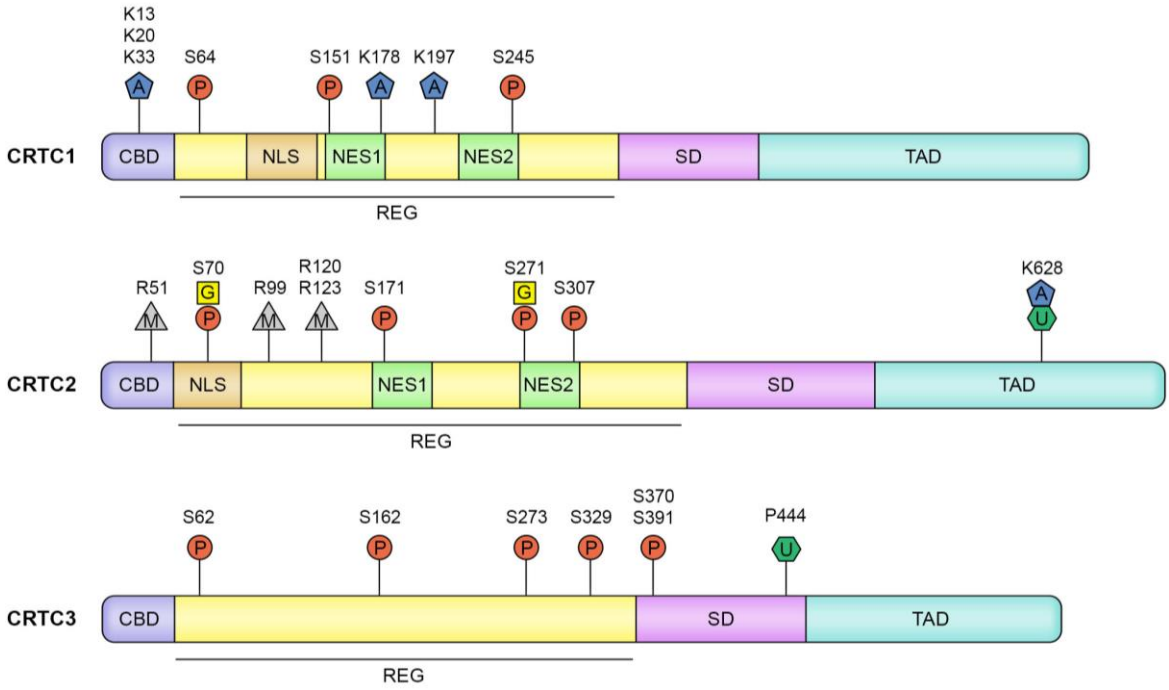

Figure 6. Murine CRTC structures and post-translational modifications. CRTCs contain a CREB-binding domain (CBD), a regulatory domain (REG) containing the nuclear localization sequence (NLS) and nuclear export sequences (NES), a splicing domain (SD) and a transactivation domain (TAD). Post-translational modifications are: acetylation (A), glycosylation (G), methylation (M), phosphorylation (P) and ubiquitination (U). NLS and NES exact location for CRTC3 is not known. Modified from Tasoulas et al., 2019.

In general, the phosphorylation of CRTCs favours its interaction with 14-3-3 protein, which retains CRTCs in the cytoplasm under basal conditions. Upon CRTCs dephosphorylation, CRTCs dissociates from 14-3-3 protein and translocate to the nucleus (**Figure 7**) (Ch'Ng et al., 2012; Screaton et al., 2004). The main regulatory homologous residues that undergo phosphorylation and modulate nuclear translocation are: Ser151 in CRTC1, Ser171 in CRTC2 and Ser162 in CRTC3 (Clark et al., 2012; España et al., 2010; Screaton et al., 2004). These residues have to be dephosphorylated by serine/threonine phosphatases for CRTCs activation. Thus, upon increase of cytosolic Ca^{2+} or cAMP, CRTCs become directly dephosphorylated by calcineurin (CaN)/protein phosphatase 2B (PP2B), or indirectly by PKA-mediated phosphorylation and inhibition of SIK family kinases (Bittinger et al., 2004; Ch'Ng et al., 2012; Screaton et al., 2004). It has been recently shown that the phosphorylation state of CRTCs is modulated by other phosphatases, including PP1 and PP2A (McTague et al., 2012; Ricarte et al., 2018; Sonntag et al., 2019). CRTC dephosphorylation allows its translocation to the nucleus where activates CREB-dependent gene transcription (Bittinger et al., 2004; Ch'Ng et al., 2012; Screaton et al., 2004) (**Figure 7**). Long after stimulation, CRTCs are progressively phosphorylated and returned to the cytosol via exportin 1 (XPO1), which recognizes the leucine-rich NES domain (Bittinger et al., 2004).

Nuclear CRTCs can interact with bZIP transcription factors, including CREB. The CBD of CRTCs directly binds to the CREB bZIP domain that also recognizes the CRE site. Thus, each CREB molecule harbours one binding site for CRTC, resulting in a 2:2:1 stoichiometry conformed by 2 CRTCs, 2 CREBs and 1 CRE sequence (Luo et al., 2012). The interaction of CRTC to CREB favours the occupancy of CREB over CRE binding sites and the recruitment of the TAFII130 and the transcriptional complex in the promoter region, which induce CREB-dependent gene transcription (Bittinger et al., 2004; Conkright, Guzmán, et al., 2003) (**Figure 7**). Accordingly, CRTCs inactivation or suppression of the CBD result in reduction of CREB occupancy over target promoters suggesting a role for CRTCs in stabilizing the bZIP domain of CREB to interact with DNA (Song et al., 2018; Wang et al., 2010). Indeed, mutagenesis of the CRE sequences totally disrupts transcription induced by CRTC overexpression (Conkright, Canettieri, et al., 2003).

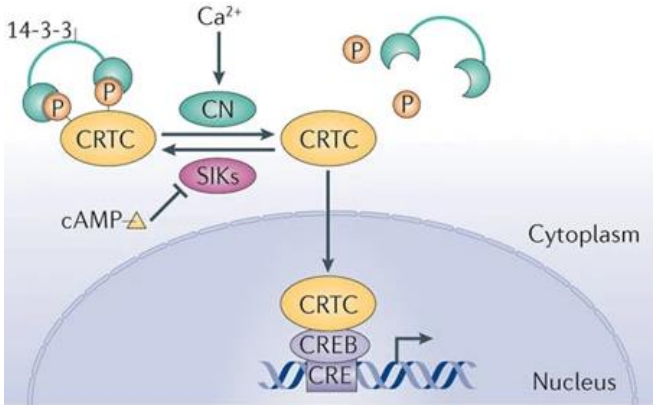

Figure 7. Regulation of CRTCs cytosol-nucleus shuttling. Phosphorylated (P) CRTCs are recruited in the cytoplasm by 14-3-3 protein. Upon cellular stimulation, increased intracellular Ca^{2+} and cAMP induce CRTCs dephosphorylation disrupting interaction with 14-3-3 protein, which allows its nuclear translocation and interaction with CREB to enhance CREB-dependent gene transcription. CN: calcineurin. From Altarejos & Montminy, 2011.

Interestingly, CRTCs potentiate CREB-dependent gene transcription specifically in genes containing CRE sites with proximal TATA boxes in their promoter regions. Genes containing CRE TATA-less promoters show minimal effect in transcription enhancement after CRTC overexpression (Conkright, Canettieri, et al., 2003). A recent study indicates that CREB is constitutively bound to target genes promoters in neurons, and upon stimulation CRTC1 is preferentially recruited to the transcriptional complex in CRE/TATA-containing promoters (Parra-Damas, Rubió-Ferrarons, et al., 2017). These evidences indicate that, contrary to CREB interaction with CBP/p300 or TAFII130, the binding of CRTC to CREB provides a high selective transcription of cAMP-responsive genes. Thus, CRTCs may contribute selectively to gene expression by potentiating CREB binding to specific genome sequences instead of increasing general gene transcription (Conkright, Canettieri, et al., 2003).

In contrast to other CREB coactivators, such as CBP or p300, which overexpression results in minimal effects on gene transcription, CRTC overexpression enhances CREB-dependent gene transcription. These results indicate that while CBP/p300 levels are not limiting factors, CRTCs are main regulators of CREB-dependent gene transcription (Conkright, Canettieri, et al., 2003; Ravnskjaer et al., 2007). Moreover, CREB transcriptional activity mediated by CRTCs can occur independently of CREB phosphorylation (Conkright, Canettieri, et al., 2003). For instance, a mutant mouse expressing a CREB lacking Ser133 phosphorylation site shows no differences in CREB mediated gene transcription compared to control mice (Briand et al., 2015). Nonetheless, when CREB activity is supressed by overexpressing a CREB negative mutant (A-CREB) that blocks the binding of CREB to the DNA, CRTCs overexpression cannot recover the transcriptional activity mediated by CRTCs (Conkright, Canettieri, et al., 2003). In this line, a CREB mutant lacking the CRTC binding domain can bind to DNA but it does not induce CREB-dependent gene transcription (España et al., 2010; Screaton et al., 2004).

CRTCs play also critical roles as transcriptional coactivators beyond CREB-dependent transcription by directly binding and enhancing transcription of other transcription factors containing bZIP domains. These transcription factors include activator protein 1 (AP-1), cAMP-responsive element-binding protein H (CREBH) or activating transcription factors (ATFs) (Canettieri et al., 2009; M. W. Lee et al., 2010; Wang et al., 2009). The physiological roles of CRTCs when regulating these transcription factors is largely unknown although in some cases, they play similar roles than those observed in CRTC/CREB-dependent transcription (see specific sections below).

Besides its role in gene transcription, recent studies have shown that CRTCs participate in the regulation of protein trafficking and RNA splicing (Amelio et al., 2009; Han et al., 2015). CRTCs contain a proline-rich region that resembles the regions found in splicing factors suggesting that they can regulate alternative splicing of transcripts containing CRE promoters, although no conserved RNA-binding domain is found in CRTCs (Amelio et al., 2007, 2009). For instance, CRTC2 can interact with spliceosome factor non-POU domain-containing octamer-binding (NONO) and promote cell-type specific alternative splicing of transcripts by affecting the selection of the pre-mRNA splice site (Amelio et al., 2007). On the other hand, CRTC2 can mediate vesicle trafficking from endoplasmic reticulum (ER) to the Golgi by direct binding with the coat protein complex II (COPII) (Han et al., 2015).

Taking together, CRTCs couple extracellular signals to modulate gene expression through direct regulation of transcription or by directing alternative splicing. Interestingly, regulation of CREB-target genes splicing can be performed independently of gene transcription (Altarejos &

Montminy, 2011; Amelio et al., 2009). Moreover, a new function has been described for CRTCs in the regulation of vesicle trafficking.

2.2 CRTC1 regulation in neurons

CRTC1 is highly expressed in the brain, especially in neurons, were plays diverse physiological functions. CRTC1 activity is mainly regulated by phosphorylation at different sites. The CRTC1 regulatory residues Ser64, Ser151 and Ser245 can undergo phosphorylation by SIK, AMP-activated protein kinase (AMPK) and microtubule affinity regulating kinase (MARK)2 whereas activity-dependent dephosphorylation is mediated by the PP2B/CaN (Nonaka et al., 2014). In neurons, CRTC1 phosphorylation, nuclear localization and transcriptional activity is regulated by synaptic activity. In silenced hippocampal neurons, phosphorylated CRTC1 is located at dendrites and upon neuronal activity, CRTC1 is rapidly dephosphorylated and translocated to nucleus (Ch'Ng et al., 2012). Increased intracellular levels of calcium after synaptic activation induce CRTC1 dephosphorylation through CaN. These dephosphorylations at the above regulatory serines are required for CRTC1 dissociation from 14-3-3 protein, allowing CRTC1 nuclear transport (Ch'ng et al., 2015). After synaptic activity, CRTC1 is accumulated in the nucleus where remains as long as excitatory synaptic activity lasts. In fact, basal nuclear CRTC1 levels are restored upon 20 min after the removal of the synaptic stimulus (Ch'Ng et al., 2012).

CRTC1 activity can also be modulated by other post-translational modifications such as acetylation. Mass spectrometry analysis has revealed several acetylated residues, including Lys13, Lys20, Lys33, Lys178 and Lys197 (Jeong et al., 2012). Acetylation at Lys13 and Lys20 reduces interaction to CREB, whereas sirtulin 1 (Sirt1)-mediated CRTC1 deacetylation enhances CRTC1 activation by promoting its interaction with CREB (Jeong et al., 2012).

As described above, CRTC1 also interacts with other transcription factors belonging to the CREB family. For instance, CRTC1 can induce AP-1-dependent gene transcription of *c-Jun* and *c-Fos* in response to 12-O-Tetradecanoylphorbol-13-acetate (TPA) (Canettieri et al., 2009). Moreover, CRTC1 binding to AP-1 induces cellular proliferation, suggesting a new biological function for this coactivator.

2.2.1 CRTC1 in neuronal development

CRTC1 is highly expressed in the developing brain with a maximum expression peak that correlates with dendritic sprouting (Li et al., 2009). Both *in vitro* and *in vivo* studies demonstrate increase of dendritic growth after CRTC1 overexpression in neurons. By contrast, expression of a dominant negative CRTC1 or CRTC1 downregulation severely affects dendritic development (Li et al., 2009). These results suggest that CRTC1/CREB-dependent gene transcription mediates dendritic morphology during development of cortical neurons. The mechanisms underlying

CRTC1-dependent dendrite morphology involve glutamate signalling and BDNF. BDNF can induce CREB phosphorylation although it is not sufficient to enhance dendritic growth. It also requires the function of CRTC1 triggered by activation of NMDA receptors (Finsterwald et al., 2010). Interestingly, there is a co-regulation of glutamate and BNDF since glutamate signalling increases expression of BDNF and, on its turn, BDNF enhances glutamate release (Mattson, 2008). These results demonstrate that BNDF and NMDA-dependent signalling converge in mediating expression of genes involved in dendritic development via CRTC1/CREB-dependent pathway (Finsterwald et al., 2010).

2.2.2 CRTC1 in energy balance

The hypothalamus is the main brain region responsible for orchestrating the response to peripheral signals by coordinating systemic metabolism, in particular the glucose and lipid metabolism, after sensing circulating nutrients and hormonal signals. Leptin, a hormone responsible for the maintenance of energy balance, is secreted by white adipocytes after feeding. Circulating leptin can bind to leptin receptor found in brain, more precisely in neurons from the arcuate nucleus of the hypothalamus. Leptin activates a CRTC1 signalling cascade leading to expression of neuropeptides that inhibits feeding and promotes energy expenditure. After feeding, increase of circulatory leptin leads to CRTC1 dephosphorylation and nuclear translocation in hypothalamic arcuate neurons. Nuclear CRTC1 enhances expression of the CREB-dependent genes *cocaine and amphetamine regulated transcript* (CART), which encodes a hypothalamic neuropeptide that mediates satiety (Altarejos et al., 2008). Apart from leptin, intraperitoneal glucose injection in mice also resulted in CRTC1 nuclear translocation in neurons of the arcuate nucleus, but not in other brain regions (Altarejos et al., 2008). These results suggest that both hormonal and nutrient sensing are able to inhibit food intake via CRTC1. In fact, mice lacking CRTC1 are hyperphagic and obese (Altarejos et al., 2008).

2.2.3 CRTC1 in longevity

Energy metabolism and aging have been related by the AMPK signalling, which mediates its crosstalk. In *C. elegans*, AMPK activation or CaN inhibition lead to increased lifespan by inactivating the nematode CRTC homolog, CRTC-1. CRTC-1 directly interacts with the CREB homolog-1 (CRH-1) and induces transcription of genes involved in peripheral mitochondrial metabolism and dynamics (Burkewitz et al., 2015; Mair et al., 2011). Neuronal CRTC-1 enhances the signalling of octopamine, the invertebrate equivalent to the catecholamines adrenaline and noradrenaline. Octopamine treatment demonstrated to increase the mitochondrial fragmentation in *C. elegans* muscle, suggesting that neuronal CRTC-1 can mediate octopamine signalling to peripheral tissues and modulate systemic metabolism and longevity (Burkewitz et al., 2015). AMPK is active during low energy status, such as in fasting conditions. This establishes that

neuronal CRTC-1 communicate energy status and regulates metabolism in distal tissues (Burkewitz et al., 2015). Moreover, deletion of transient receptor potential cation channel subfamily V member 1 (TRPV1), a pain receptor that regulates CRTC-1 activity in peripheral sensory neurons, also extends lifespan in *C. elegans* (Riera et al., 2014).

If downregulation of CRTC-1 increases lifespan in a CRH-1 dependent manner in *C. elegans*, CRTCs and CREB may also play similar roles in mammals. Similarly, inactivation of TRPV1 in mice sensory neurons also increases lifespan via CRTCs dependent mechanism. Sensory neurons integrate different sensory inputs and transduce them into neuroendocrine signals to adjust the metabolic activity. Neuronal TRPV1 activation enhance CRTC1-dependent transcription and release of neuropeptide calcitonin gene-related peptide (CGRP). Importantly, levels of CGRP are increased with age. Moreover, CGRP can antagonize insulin secretion in pancreatic β cells contributing to development of age-associated type 2 diabetes (Riera et al., 2014). In summary, CRTC1 plays an important role in longevity by mediating metabolic activity.

2.2.4 CRTC1 in circadian clock regulation

The suprachiasmatic nuclei (SCN) of the hypothalamus coordinates the circadian clock by responding to light/dark cycles. Circadian regulation is modulated by activation of the retinal photoreceptors, responsible to regulate the physiological, metabolic and behavioural rhythmic processes. Neurons from the SCN are well known for its implication in the sustainment of the circadian rhythm. A cyclic activity-dependent expression of multiple transcription factors, which are auto-regulated by negative feedback loops, are the responsible to give rhythmicity in these SCN neurons (Ding et al., 2018). CREB has been involved in circadian clock sustainment by regulating circadian clock genes (B. Lee et al., 2010).

In SCN neurons, CRTC1 display a rhythmic expression pattern. An increase of nuclear CRTC1 is detected after light exposure, whereas CRTC2 is also highly expressed in the SCN but without rhythmic dependence. This rhythmicity in CRTC1 protein levels and nuclear localization may be responsible for the circadian regulation modulated by CREB (Sakamoto et al., 2013). CRTC1 translocation to the nucleus results in an enhanced expression of *Per1* and *Sik1* genes responsible for regulating circadian rhythm. PER1 is a major regulator of circadian rhythm, while SIK1 is responsible for CRTC1 phosphorylation and deactivation, which represents a negative feedback that would lead to a reduction of *Per1* expression (Jagannath et al., 2013; Sakamoto et al., 2013).

2.2.5 CRTC1 in synaptic plasticity and memory

CREB is essential for synaptic plasticity and memory, presumably by mediating expression of genes during L-LTP. In this process, synapse-to-nucleus communication is critical for enhancing gene transcription underlying cognition and memory. Several synaptonuclear factors are

transported from active synapses to the nucleus to induce transcription in an activity-dependent manner (Kaushik et al., 2014; Parra-Damas & Saura, 2019). Among them, the CRTC1 coactivator translocates from synapses to the nucleus in response to Ca^{2+} or cAMP and enhances CREB-dependent gene transcription (Ch'Ng et al., 2012), which is critical for plasticity mechanisms underlying memory and emotional processes (Parra-Damas & Saura, 2019). In fact, nuclear accumulation of CRTC1, but not CREB phosphorylation, correlates with L-LTP induction (Kovács et al., 2007; Zhou et al., 2006). Experiments performed in hippocampal slices show that overexpression of a dominant negative form of CRTC1 prevents activity-dependent CREB transcription and supresses the maintenance of L-LTP without affecting E-LTP (Zhou et al., 2006). Moreover, CRTC1 overexpression enhances L-LTP induction, indicating that CRTC1 mediates activity-dependent gene transcription during L-LTP (Zhou et al., 2006).

Recent studies support the idea for activity-dependent CRTC1/CREB-mediated synaptic plasticity and memory. Contextual fear conditioning, spatial memory and object-location memory tasks induce CRTC1 dephosphorylation and nuclear translocation in hippocampal pyramidal neurons (Parra-Damas et al., 2014; Parra-Damas, Chen, et al., 2017; Uchida et al., 2017). CRTC1 nuclear accumulation is also found in the basolateral amygdala after contextual fear conditioning (Nonaka et al., 2014). Interestingly, silencing CRTC1 in the hippocampus or in the basolateral amygdala reduces CREB-mediated gene transcription and fear memory (Nonaka et al., 2014; Uchida et al., 2017), indicating that CRTC1 plays a crucial role by inducing CREB-dependent gene transcription during consolidation of different memory types. The mechanisms underlying this effect could be by upregulating genes required for synaptic plasticity and long-term memory, such as, *c-fos, Bdnf, Arc, Nr4a1, Nr4a2, Dusp1, Ptg2* or *Fgf1* (**Figure 8**) (Nonaka et al., 2014; Parra-Damas, Chen, et al., 2017; Parra-Damas, Rubió-Ferrarons, et al., 2017; Uchida et al., 2017).

Supporting this idea, CRTC1 activation, nuclear translocation and CRTC1-dependent transcriptional activity are disrupted in the brains of Alzheimer's disease (AD) murine models (**Figure 8**) (España et al., 2010; Parra-Damas et al., 2014; Wilson et al., 2017). β-amyloid reduces calcium influx into neurons, impairing CRTC1 dephosphorylation and CRTC1/CREB-dependent gene transcription, which results in memory impairment. Conversely, memory deficits are ameliorated after CRTC1 overexpression in the hippocampus of an AD mouse model (España et al., 2010). In summary, CRTC1 is essential for coupling synaptic activity with gene transcription underlying hippocampal-dependent long-term memory.

2.3 CRTC2 regulation

CRTC2 is less expressed than CRTC1 in the brain, but it is abundant in peripheral organs. For instance, CRTC2 is highly expressed in liver where plays an essential role in the regulation of energy balance and glucose metabolism. CRTC2 activation is regulated by post-translational

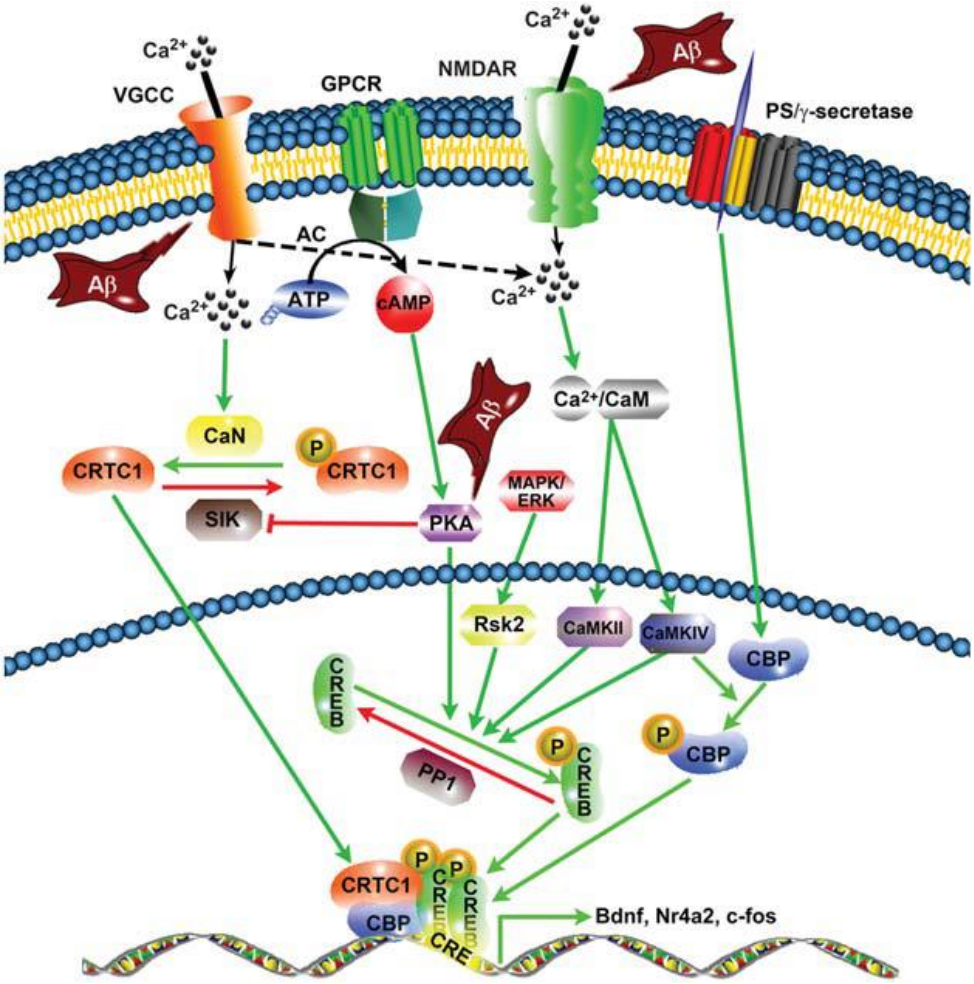

Figure 8. Signaling pathways regulating CREB/CRTC1 transcription for long-term memory in neurons. Multiple signaling pathways favours CREB phosphorylation and CRTC1 nuclear translocation to enhance CREB-dependent gene transcription necessary for memory formation. In AD brains, β-amyloid disrupts CREB transcription by interfering at different steps. From Saura & Valero, 2011.

mechanisms, including phosphorylation, acetylation, ubiquitination, glycosylation and methylation. Many phosphorylation sites in CRTC2, including Ser70, Ser171, Ser275 and Ser307, stabilize CRTC2/14-3-3 protein interaction, which regulates CRTC2 nuclear trafficking (Koo et al., 2005; Sonntag et al., 2017; Uebi et al., 2010). As CRTC1, phosphorylation of CRTC2, especially at Ser171, negatively affects nuclear translocation. Although the regulatory mechanisms underlying CRTC2 phosphorylation and dephosphorylation are not fully understood, different kinases have been reported for its regulation including SIK, AMPK and MARK families (Dentin et al., 2007; Koo et al., 2005; Patel et al., 2014) as well as different phosphatases such as PP1, PP2A, CaN and PP4 (McTague et al., 2012; Sonntag et al., 2019; Uebi et al., 2010; Yoon et al., 2010).

Besides phosphorylation, CRTC2 localization is also affected by glycosylation. O-glycosylation at Ser70 and Ser171 by O-glycosyl transferase (OGT) compete for phosphorylation and thus,

favours nuclear translocation (Dentin et al., 2008). CRTC2 function is also controlled by modulating protein levels through acetylation and ubiquitination. In response to glucagon, hepatic CRTC2 translocates to the nucleus where can be acetylated at Lys628 by CBP/p300, which stabilizes CRTC2-p300 binding. During re-feeding, SIK2 phosphorylates CBP/p300, destabilizing CRTC2-p300 binding, and then CRTC2 is phosphorylated and translocated to the cytosol. Noteworthy, SIK2 is responsible for both CRTC2 and CBP/p300 phosphorylation (Liu et al., 2008). Moreover, deacetylation of CRTC2 by Sirt1 allows ubiquitination of Lys628 by E3 ligase constitutive photomorphogenic protein (COP1), which targets CRTC2 to proteasomal degradation (Dentin et al., 2007; Liu et al., 2008; Lv et al., 2016). Finally, methylation of CRTC2 can enhance gene transcription. CRTC2 is methylated at Arg-conserved residues by the arginine methyltransferase PRMT6. CRTC2 methylation enhances the association of CRTC2/CREB over gene promoters to induce transcription. In mice, overexpression of PRMT6 was associated with an increase in blood glucose concentration as a result of higher expression of gluconeogenic enzymes. In this case, methylation of CRTC2 enhances gene transcription although, it does not affect its subcellular localization (Han et al., 2014).

2.3.1 CRTC2 in glucose homeostasis

CRTC2 plays a crucial function in glucose homeostasis. Under feeding conditions, insulin induces CRTC2 phosphorylation and recruitment to the cytoplasm in hepatocytes, which blocks gluconeogenic gene programs (**Figure 9**) (Altarejos & Montminy, 2011; Dentin et al., 2007). On the contrary, upon fasting, glucagon induces CRTC2 dephosphorylation and translocation to the nucleus, which enhances transcription of gluconeogenic genes such as phosphoenolpyruvate carboxykinase (PEPCK), glucose-6-phosphatase (G6Pase) or PGC-1α (**Figure 9**) (Altarejos & Montminy, 2011; Koo et al., 2005; Le Lay et al., 2009; Yoon et al., 2010). Thus, mice with constitutively active CRTC2 in the liver cannot reduce glucose concentration in blood leading to insulin resistance (Hogan et al., 2015). Conversely, *Crtc2* knockout mice show a reduction in gluconeogenic genes as well as low levels of glucose in blood (Wang et al., 2010). Also, CRTC2 strongly coactivates the transcription factors CREBH and glucocorticoid receptor (GR) enhancing expression of the regulatory enzymes PEPCK and G6Pase (Hill et al., 2016; M. W. Lee et al., 2010).

CRTC2 regulates glucose levels, also, by responding to ER stress. Precisely, after ER stress, CRTC2 interacts with ATF6α and enhances expression of ER quality control genes in liver (Wang et al., 2009). In response to acute ER stress, ATF6α translocates to the nucleus and disrupts CREB/CRTC2 interaction, which leads to a reduction of CRTC2 occupancy over gluconeogenic genes that results in a decreased hepatic glucose release.

Moreover, CRTC2 mediates glucose homeostasis in other tissues. In white adipose tissue, CRTC2/CREB-dependent gene transcription is induced after fasting, which leads to ATF3 expression that subsequently downregulates the expression of glucose transporter GLUT4 and adiponectin. These changes results in reduced glucose uptake in adipocytes leading to insulin resistance (Henriksson et al., 2015; J. Park et al., 2014). In pancreas, CRTC2 plays a protective role facilitating insulin secretion by enhancing the transcription of the β-cell type restricted factor MAF bZIP transcription factor A (MafA) (Eberhard et al., 2013).

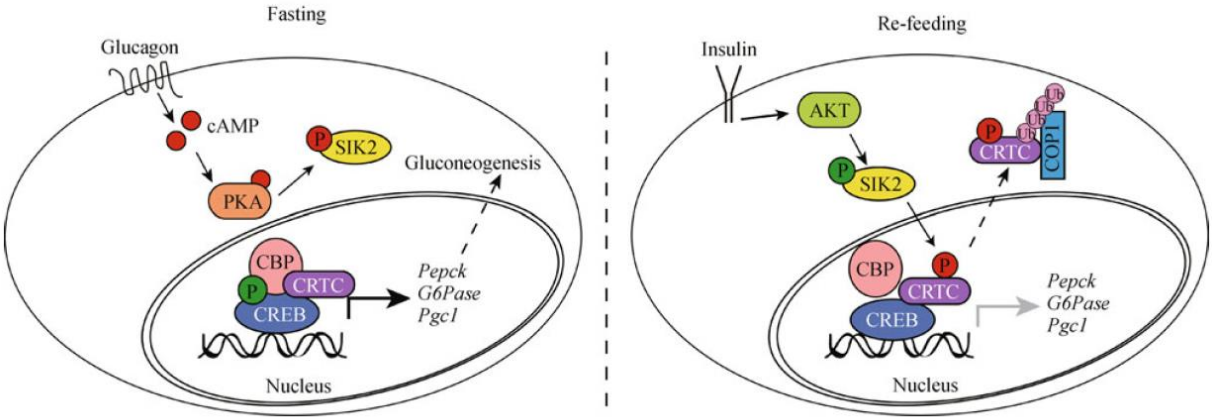

Figure 9. Signaling pathways regulating CREB/CRTC2 gluconeogenic transcription in hepatocytes. CRTC2 regulation in fasting (left) and feeding (right) conditions. Upon fasting, glucagon favours CRTC2 nuclear localization that enhances CREB-dependent transcription of gluconeogenic genes. After feeding, insulin leads to CRTC2 phosphorylation and cytoplasmatic localization, blocking the CREB-dependent gluconeogenic transcription. Cytosolic CRTC2 can undergo ubiquitination by COP1. From Berdeaux, 2011.

2.3.2 CRTC2 and energy sensing

The role of neuronal CRTCs in energy sensing seems to be mediated by the maintenance of peripheral metabolic homeostasis. In *Drosophila* neurons, the CREB-CRTC complex enhances expression of the short neuropeptide F (sNPF), ortholog of the mammalian neuropeptide Y. Neuronal sNPF promote energy homeostasis via the gut receptor of sNPF, which maintains gut epithelial integrity. Loss of CRTC-sNPF signalling disrupts gut epithelial tight junctions compromising energy balance (Shen et al., 2016).

In mammals, CRTC2 is highly expressed in the hypothalamus and its phosphorylation state reflects the nutritional status. In contrast to the liver, hypothalamic CRTC2 is dephosphorylated after feeding and phosphorylated after fasting (Lerner et al., 2009). CRTC2 translocates into nuclei of hypothalamic cells in response to high glucose exposure to enhance expression of CREB-dependent target genes, such as corticotropin releasing factor (CRF), insulin receptor substrate 2 (Irs2) and thyrotropin releasing hormone (TRH) (Breit et al., 2016; Lerner et al., 2009). Although different genes have been identified as targets for CRTC2/CREB-dependent

transcription in response to nutrient state in hypothalamus, its physiological function remains still unknown.

2.3.3 CRTC2 in lipid metabolism

CRTC2 controls hepatic regulation of sterol regulatory element-binding protein 1 (SREBP1). The transcription factor SREBP1 is synthetized and rests as an inactive precursor bound to ER that will be transported to Golgi in response to insulin signalling for a posterior shuttling into the nucleus. Nuclear SREBP1 enhances expression of genes that modulate cholesterol and the fatty acid synthesis (Horton et al., 2002). In this process, CRTC2 modulates the trafficking of SREBP1 from ER to Golgi through COPII complex-mediated vesicle trafficking. In response to insulin or nutrient sensing, CRTC2 is phosphorylated by mTOR and dissociates from the COPII complex favouring SREBP1 transport to Golgi for a posterior nuclear shuttling. Nuclear SREBP1 enhances transcription of regulatory lipid enzymes leading to lipogenesis (Han et al., 2015).

2.3.4 CRTC2 and immune response

CREB mediates important functions in immune system such as regulating proliferation, survival and activation of T cells. In response to inflammatory signals, CREB mediates the production of different cytokines by T cells, which promotes the differentiation of naïve T cells into the different T helper (Th) cell subtypes. Thus, mice overexpressing a dominant negative CREB mutant in T cells resulted in impaired T cell proliferation and function. These data suggest that CREB activity is essential for T cell activation and proliferation (Wen et al., 2010).

Recent findings indicate that CRTC2 also modulates immune responses. In this case, naïve T cells differentiate to T helper (Th)17 cells via CRTC2/CREB-dependent gene transcription which enhances interleukin (IL)-17 cytokine production. Sustaining this idea, a T cell-specific *Crtc2* knockout mutant mouse shows reduced levels of Th17 cells. Moreover, these mutant mice show resistance in experimental autoimmune encephalomyelitis, an experimental autoimmune mouse model for multiple sclerosis. These results, offer a new vision of CRTC2 in the autoimmune disease field (Hernandez et al., 2015). Nonetheless, as previously seen, CRTC2 can also contribute to glucose-dependent insulin resistance, which in turns, may cause autoimmune problems.

2.4 CRTC3 regulation

CRTC3 plays a crucial role in energy balance in adipose tissue. Different kinases, including liver kinase B1 (LKB1), SIKs, AMPK, MAPK, cyclin-dependent kinases (CDKs) and extracellular signal-regulated kinases (ERKs) phosphorylate CRTC3 at Ser62, Ser162, Ser273, Ser329, Ser 370 and Ser391 (Clark et al., 2012; Henriksson et al., 2015; Shan et al., 2016; Sonntag et al.,

2019). On the other hand, CRTC3 dephosphorylation and nuclear translocation is mediated by PP2A (Sonntag et al., 2019). In contrast to the activity-regulation of CRTC1 and CRTC2 dephosphorylation, CRTC3 binding to PP2A is independent of cAMP signalling and is induced by CRTC3 phosphorylation in HEK293T cells (Sonntag et al., 2019). CRTC3 is also regulated by other post-translational modifications. For instance, CRTC3 is ubiquitinated and proteasomal degraded in response to prolonged cAMP signalling, a process mediated by the ubiquitin ligase NEDD4L. This regulatory mechanism controls CRTC3 activation by limiting CRTC3 protein levels in adipose tissue (Y. H. Kim et al., 2018).

2.4.1 CRTC3 in lipid metabolism and thermogenesis

CRTC3 is abundant in adipose tissue where plays an important role in mediating energy homeostasis. The CNS regulates energy balance through the release of catecholamines from the sympathetic nervous system that enhance energy expenditure by increasing lipolysis and fatty-acid oxidation in the peripheral tissues. In obesity, there is a disruption of the catecholamine signalling, that leads to insulin resistance. In response to catecholamines signalling, CRTC3 is activated and upregulates the expression of the GTPase regulator of G protein signalling 2 (RGS2) in adipocytes. Expression of RGS2 leads to downregulation of the catecholamine signalling by acting as negative feedback (Song et al., 2010). Thus, CRTC3 promotes obesity by attenuating catecholamine signalling. In humans, elevated CRTC3 levels or expressing a CRTC3 gene variant with increased transcriptional activity have been associated with obesity (Prats-Puig et al., 2016; Song et al., 2010). On the contrary, *Crtc3* knockout mice show enhanced energy consumption and ectopic lipid accumulation (Song et al., 2010).

CRTC3 plays an important role in thermogenesis in adipose tissue. Brown adipose tissue (BAT) dissipates energy through uncoupling protein 1 (UCP1)-mediated respiration. High levels of UCP1 allows high energy expenditure and facilitates glucose tolerance, insulin sensitivity and resistance to high-fat diet-induced obesity. Interestingly, different studies investigated the role of CRTC3 in thermogenesis although some controversial results came up. On one hand, exposure to cold results in a decreased expression of LKB1 that induces nuclear translocation of CRTC3 in brown adipocytes. Nuclear CRTC3 interacts with C/EBPβ, a bZip transcription family member, and enhances *Ucp1* transcription in brown adipocytes (Shan et al., 2016). Thus, nuclear translocation of CRTC3 correlates with higher expression of UCP1 and lower body weight and fat mass (Xu et al., 2019). On the other hand, and contrarily to Shan's results, *Crtc3* knockout mice show higher levels of UCP1 in brown adipose tissue, presumably because CRTC3 inhibits UCP1 transcription by associating with PRDM16. PRDM16 is a transcriptional coregulator that enhances the thermogenic program by associating with C/EBPβ. Thus, binding of CRTC3 to PRDM16 disrupts its interaction with C/EBPβ reducing *Ucp1* transcription (Yoon et al., 2018).

In the same direction, another study reported that brown adipocytes obtained from *Crtc3* knockout mice showed increased *Ucp1* mRNA levels. These results indicate that loss of CRTC3 increases fat burning, in part, through increased thermogenesis (Song et al., 2010).

In summary, loss of *Crtc3* function increases insulin sensitivity, reduces lipid store and weight gain, increases oxygen consumption and energy expenditure, and enhances cold tolerance. (Song et al., 2010; Yoon et al., 2018).

2.4.2 CRTC3 in the immune system

CREB mediates immune responses by potentiating different functions. For instance, CREB promotes antiapoptotic survival signaling in macrophages, leading to enhanced host immune responses, but also induces IL-10 production, potentiating anti-inflammatory effects (Wen et al., 2010).

There are different subtypes of macrophages. Among them, there are the classical activated macrophages (M1), that induce a pro-inflammatory response to combat pathogens, and the regulatory macrophages (M2b), that drive an anti-inflammatory response by secreting high levels of IL-10 to regulate immune response and tissue repair. Although CREB enhances IL-10 transcription, activation of CREB alone is not sufficient to induce IL-10 production (MacKenzie et al., 2013). In macrophages, inhibition of SIK induces CRTC3 dephosphorylation and nuclear translocation resulting in increased IL-10 production and enhanced M2b phenotype (Clark et al., 2012; MacKenzie et al., 2013).

Interestingly, there is a correlation between obesity and the activation of the immune system, two systems regulated by CRTC3. Although the pathway linking these two phenomena has not been described.

2.4.3 CRTC3 and stress

Corticotropin releasing factor (CRF) is a hypothalamic neuropeptide that mediates the stress-induced activation of the hypothalamic–pituitary–adrenal system. In response to stress, CRF mediates adrenocorticotropic hormone (ACTH) and cortisol release. Regulation of CRF expression is mediated by CREB in response to cAMP signalling in hypothalamic cells (Kageyama & Suda, 2010). Indeed, in the paraventricular nucleus (PVN) of the hypothalamus, CRTC3 translocates to the nucleus and enhance CREB-dependent *Crf* transcription in response to stress (Jurek et al., 2015).

At the cellular level, stress response is mediated by the activation of transcription factors that regulate sets of genes involved in the control of organelle biogenesis and organelle-specific

protective chaperones. Some of these genes are PGC-1α, a master regulator of mitochondrial biogenesis, or different mitochondrial oxidative-phosphorylation genes. Transcription of these genes is enhanced by CREB/CRTC activity in response to low ATP levels. In fact, CRTC3 plays a role in mediating stress response in hepatocytes by enhancing PGC-1α expression in response to mitochondrial stress (Than et al., 2011). Thus, treatment with the stressor rotenone, a blocker of the electron transport chain in mitochondria, results in upregulation of genes related with mitochondrial biogenesis through PGC-1α. Surprisingly, after rotenone treatment a small fraction of CRTC3, but not CRTC2, remains into mitochondria. The biological function of CRTC3 in the mitochondria is unknown (Than et al., 2011).

Table 1. Summary of CRTC roles in the brain.

Isoform	Organism	Cell type / brain region	Physiological process	References
CRTC1	Rat	Cortical neurons	Neuronal development	Li et al., 2009
	Mouse	Hypothalamus	Energy balance	Altarejos et al., 2008
		Sensory neurons	Metabolic health	Riera et al., 2014
			Lifespan	
		Suprachiasmatic nucleus	Circadian rhythm	Jagannath et al., 2013; Sakamoto et al., 2013
	Rodents	Hippocampus / amygdala	Memory formation / synaptic plasticity	Nonaka et al., 2014; Parra-Damas et al., 2014; Uchida et al., 2017
CRTC2	Mouse	Hypothalamus	Glucose sensing	Lerner et al., 2009
CRTC3	Rodents	Hypothalamus	Stress response	Jurek et al., 2015
CRTC	*Drosophila*	Neurons	Energy balance	Shen et al., 2016
CRTC-1	*C. Elegans*	Neurons	Metabolic health	Burkewitz et al., 2015; Mair et al., 2011
			Lifespan	

Table modified from Saura & Cardinaux, 2017

In conclusion, CRTCs mediate distinct functions in specific tissues while, in other cases, they can cooperate to mediate a physiological response in the organism. In particular, CRTC isoforms are differently expressed in the mammalian brain where regulate multiple and diverse biological functions as summarized in **Table 1**. However, the specific regulatory mechanisms and physiological functions of CRTC1 and CRTC2 activation in neurons and astrocytes, remain largely unknown. This raises several important questions: Are cerebral CRTC isoforms regulated by similar mechanisms than those of peripheral tissues? Are CRTC isoforms similarly regulated in neurons and astrocytes? Do CRTC isoforms play similar or distinct functions in gene transcription in the cell types of the nervous system? This opens the door to study the regulation and function of CRTC1 and CRTC2 isoforms in the main cerebral cell types, that are neurons and astrocytes.

V Working hypothesis and objectives

The working hypothesis of this doctoral thesis postulates that CRTC isoforms play particular biological functions in distinct cell types of the brain. To address this hypothesis, we propose the following objectives:

1. To investigate the regional and cellular expression pattern of CRTC2 in the adult mouse brain
2. To study the molecular mechanisms of CRTC1 and CRTC2 regulation in neurons and astrocytes
3. To investigate the role of CRTC1 and CRTC2 on CREB-mediated transcription in neurons and astrocytes
4. To generate and characterize a novel neuronal-specific *Crtc2* conditional knockout mouse

VI Materials and methods

1 Reagents and general buffers

Table 2: Reagents and resources used in this work

Reagent or Resource	Source	Identifier
Bacterial and virus strains		
DH5α competent cells	Invitrogen	18265-017
Adenoviral vector serotype 5 (Ad)5-GFP	Viral Vector Unit Production; CBATEG	UPV-776
Adenoviral vector serotype 5 (Ad5)-Cre recombinase	Viral Vector Unit Production; CBATEG	UPV-757
Experimental models		
Crtc2 embryonic stem (ES) cells	European Mouse mutant Archive (EMMA)	EPD0197_3_G07 clon, parental line JM8.N4
Flp transgenic mice	Jackson Laboratory	B6;SJL-Tg(ACTFLPe)92005Dym/J
Cre-recombinase transgenic mice	Dr. J. Shen laboratory (Yu et al., 2001)	
Biological samples		
Fetal bovine serum (FBS)	Life Technologies	10270106
Normal goat serum (NGS)	Sigma	S6-100ML
Chemical compounds, peptides and recombinant proteins		
Ampicillin sodium salt	Sigma	A0166
B27 supplement	Life Technologies	17504-044
Bovine serum albumin (BSA)	Sigma	A7906
Deoxyribonuclease I from bovine pancreas (DNAse)	Sigma	D5025
DNA polymerase 5U/µL	Biotools	10049-4111
dNTPs mix 10 mM	Biotools	20038
DPX Mountant	Sigma	06522
Dulbecco's Modified Eagle Medium (DMEM)	Sigma	D5796
Dynabeads protein G	Life Technologies	10004-D
Ethylene glycol-bis (succinic acid N-hydroxysuccinimide ester) (EGS)	Sigma	E3257
FluorSave	Calbiochem	345789-20ML
Forskolin (FSK)	Sigma	F6886
Glutamine (200 mM)	Life Technologies	25030081
Hoechst33258	Invitrogen	H3569
Hydrogen peroxide	Sigma	216763
L-(-)-norepinephrine (+)-bitartrate (NE)	Sigma	A95112
Lipofectamine 2000 reagent	Life Technologies	11668-079
Luminol	Sigma	09253
Luria Broth base (LB)	Invitrogen	12795027

LB agar	Sigma	L2897
Molecular weight marker	BioRad	161-0373
Mowiol 4-88	Sigma	81381
Neurobasal medium	Life Technologies	21103-049
Oligo(dT) primers	Life Technologies	18418012
OptiMEM medium	Thermo Fisher Scientific	31985070
Paraformaldehyde (PFA) 16%	Thermo Fisher Scientific	28908
Penicillin-Streptomycin (500 U/mL)	Life Technologies	15070-063
Phosphatase inhibitor tablets (PhosSTOP)	Roche	4906837001
Poly-D-lysine (PDL)	Sigma	P7658
Power SYBR green PCR master mix	Life Technologies	4367659
Protease inhibitor cocktail tablets	Roche	11697498001
Protein A Plus beads	Thermo Fisher Scientific	22811
Proteinase K	Roche	3115879001
p-Coumaric acid	Sigma	28200
Random hexamers	Invitrogen	N8080127
RNAse Out Recombinant Ribonuclease inhibitor	Invitrogen	10777019
RNase-free DNAse set	Qiagen	79254
Super Script II reverse transcriptase	Invitrogen	18064014
Sybr-Safe DNA gel stain	Life Thechnologies	S33102
Tissue-Tek O.C.T Compound	Sakura	4583
Trypsin	Sigma	T4665
Trypsin/EDTA	Life Technologies	5200-056
Trypsin inhibitor	Life Technologies	17075-029
UltraPure Glycogen	Life Technologies	10814010
UltraPure Phenol:Chloroform:IsoamylAlcohol(25:24:1,v/v)	ThermoFisher Scientific	15593031
Comercial assays and kits		
Actin Green 488 Ready Probes reagent	ThermoFisher Scientific	R37110
BCA Protein Assay Kit	Pierce	23225
β-Galactosidase Reporter Gene Staining Kit	Sigma	GALS
DAB Peroxidase (HRP) Substrate kit	Vector Laboratories	SK-4100
Dual-Luciferase Reporter Assay System	Promega	E1910
Polyvinylidene fluoride (PVDF) membrane	BioRad	162-0177
PureLink HiPure Plasmid Filter kit	Invitrogen	K-210017
PureLink RNA Mini Kit	Thermo Fisher Scientific	12183025
Superfrost Plus slides	Thermo Fisher Scientific	J1800AMNT
Vectastain ABC HRP kit	Vector Laboratories	PK-6100
Zenon Rabbit Alexa Fluor 488 Rabbit IgG kit	Molecular Probes	Z25302
Zenon Rabbit Alexa Fluor 568 Rabbit IgG kit	Molecular Probes	Z25306

Recombinant DNA		
pcDNA3-FLAG-TORC2 WT	Montminy Lab (Screaton et al., 2004)	
pCre-luc	Stratagene	
pMD2.G	Addgene	12259
pRL-TK reporter vector	Promega	E2241
pRL-null reporter vector	Promega	E2271
psPAX2	Addgene	12260

Table 3: List of antibodies used in this work

Antibody	Supplier	Ref.	Host	Dilution				
				WB	IHC	ICC	CoIP	ChIP
β-actin (AC-15)	Sigma	A1978	Mouse	1:60000				
Alexa Fluor 568 anti-mouse	Thermo Fisher Scientific	A-21134	Goat			1:300		
Alexa Fluor 568 anti-rabbit	Thermo Fisher Scientific	A-11036	Goat			1:300		
Biotin anti-rabbit	Vector Laboratories	BA-1000	Goat		1:200			
CREB	Cell Signaling	9197	Rabbit	1:700			1:100	1:300
pCREB (Ser 133)	Cell Signaling	9198	Rabbit	1:1500				
CRTC1	Cell Signaling	2587	Rabbit	1:10000		1:250	1:65	
CRTC1	Merk Millipore	MABE4 61	Mouse	1:1000				
CRTC2	Merk Millipore	ST1099	Rabbit	1:4000				
CRTC2	Proteintech	12497-1-AP	Rabbit				1:80	1:90
GAPDH	Ambion	AM4300	Mouse	1:200000				
GFAP	Dako	Z0334	Rabbit		1:500			
HRP anti-mouse	Bio-Rad	1706516	Goat	1:3000				
HRP anti-rabbit	Bio-Rad	1706515	Goat	1:3000				
Iba1	Wako	019-19741	Rabbit		1:100			
Lamin B1	Zymed	33-2000	Mouse	1:1000				
NeuN	Sigma	ABN78	Rabbit		1:500			
OctA-Probe (H5)	Santa Cruz	sc-166355	Mouse			1:100		
β-tubulin (SAP.4G5)	Sigma	T7816	Mouse	1:20000				

WB: Western blotting; IHC: Immunohistochemistry; ICC: Immunocytochemistry; CoIP: co-immunoprecipitation; ChIP: Chromatin immunoprecipitation. FRET dilutions are specified in results section. Dilutions are only indicated for the confirmed used applications.

Table 4: Primers used for PCR genotyping

Gene	Primer	Direction	Sequence	Product size
WT *Crtc2*	Crtc2-5'arm	Forward	5'-TTGTGTCCCTTACCCTACTCAGGC-3'	732 bp
	Crtc2-3'arm	Reverse	5'-TGTAATCCCAACATAGTGAGATGTCG-3'	
Floxed *Crtc2*	Crtc2-For	Forward	5'-GGCTGGCGAAGGTGAGTCCAGAGC-3'	306 bp
	Crtc2-Rev	Reverse	5'-TGAACTGATGGCGAGCTCAGACC-3'	
Floxed *Crtc2-LacZ*	Crtc2-5'arm	Forward	5'-TTGTGTCCCTTACCCTACTCAGGC-3'	417 bp
	LAR3	Reverse	5'-CAACGGGTTCTTCTGTTAGTCC-3'	
Cre-recombinase	P156	Forward	5'-GCCTGCATTACCGGTCGATGCAACGA-3'	720 bp
	P157	Reverse	5'-GTGGCAGATGGCGCGGCAACACCATT-3'	

Table 5: Primers used for qPCR gene expression analysis of mouse genes

Gene	RefSeq accession	Direction	Sequence	Amplicon size
Actb	NM_007393	Forward	5'-CTTCTTGGGTATGGAATCCT-3'	97 bp
		Reverse	5'-ATAGAGGTCTTTACGGATGTC-3'	
Bdnf	NM_007540	Forward	5'-GAAAGTCCCGGTATCCAAAG-3'	140 bp
		Reverse	5'-CATACGATTGGGTAGTTCGG-3'	
Crtc1	NM_001004062	Forward	5'-GTCACCTGTCCGATAATACC-3'	184 bp
		Reverse	5'-GTCTAAGCCTGTCCTGAGAG-3'	
Crtc2	NM_028881	Forward	5'-ACTCACCTTTGGATTCATCTCG-3	123 bp
		Reverse	5'- TATGGAGAACTGTCAATGTGGC-3'	
Crtc3	NM_173863	Forward	5'-TGAGACCAAACCCATATTCC-3'	64 bp
		Reverse	5'-TTTGTATCTTCTGTCAGGATGG-3'	
c-fos	NM_010234	Forward	5'-CAAAGTAGAGCAGCTATCTCCT-3'	71 bp
		Reverse	5'-CAGCCATCTTATTCCGTTCC-3'	
Gapdh	NM_008084	Forward	5'-AAGCTCATTTCCTGGTATGAC-3'	97 bp
		Reverse	5'-TGGTCCAGGGTTTCTTACTC-3'	
Hprt1	NM_013556	Forward	5'-TTGTTGGATATGCCCTTGAC-3'	56 bp
		Reverse	5'-ACAAACGTGATTCAAATCCC-3'	
HK2	NM_013820	Forward	5'-GCTTCATCCTCACTTTGCCA-3'	53 bp
		Reverse	5'-AGGACACGTCACATTTCGGA-3'	
Ldha	NM_001136069	Forward	5'-CTGAGAGCATAATGAAGAACC-3'	65 bp
		Reverse	5'-ATAGAGACCCTTAATCATGGTG-3'	
Nr4a1	NM_010444	Forward	5'-GGTGAAGGAAGTTGTACGGA-3'	107 bp
		Reverse	5'-AGGGAAGTGAGAAGATTGGT-3'	
Nr4a2	NM_013613	Forward	5'-CTATTCCAGGTTCCAGGCA-3'	56 bp
		Reverse	5'-TGTTGGGTATCATCTCCACTC-3'	
Ppia	NM_008907	Forward	5'-GACTGAATGGCTGGATGG-3'	124 bp
		Reverse	5'-GGAAATGGTGATCTTCTTGCT-3'	

Table 6: Primers used for ChIP-qPCR analysis of endogenous mouse gene promoters.

Gene	Primer	Direction	Sequence	Position from TSS
c-fos	*c-fos*_P1	Forward	5'-TAGGTGAAAGATGTATGCCAAG-3'	-180 bp
		Reverse	5'-GCTGTGAATGGATGGACTTC-3'	-38 bp
	*c-fos*_P2	Forward	5'-CGCTGGGTTTGGATCTCTAAG-3'	-1802 bp
		Reverse	5'-CTGCTCCCTAGGAACCTCTG-3'	-1662 bp
Nr4a2	*Nr4a2*_P1	Forward	5'-CGCGGTGGGTCATTGTTTCC-3'	-245 bp
		Reverse	5'-TGCAGCCGGCGCTATAAATAA-3'	-146 bp
	*Nr4a2*_P2	Forward	5'-GAGGCGTTCGATAGGAAAGG-3'	-2017 bp
		Reverse	5'-AGAAACAGGACAGGTTTGGAG-3'	-1884 bp
	Irrelevant Region	Forward	5'-ACTGCCTCCCTTGTACTACAC-3'	-
		Reverse	5'-TGGTGAACCTGTGAGTTAGTG-3'	-

Table 7: General buffers and culture media recipes

General buffers and culture media	Composition
Complete neurobasal medium	Neurobasal medium supplemented with B27, 2 mM glutamine, 25 U/ml penicillin and 25 µg/mL streptomycin
Full DMEM	DMEM containing 10% FBS, penicillin/ streptomycin (25 U/mL, 25 µg/ml respectively)
Loading buffer (1X)	62.5 mM Tris-HCl pH 6.8, 10% glycerol, 2% SDS, 5% β-mercaptoethanol and 0.01% bromophenol blue
PBG	PBS supplemented with 30 mM glucose
Phosphate Buffer Saline (PBS)	136.87 mM NaCl, 2.9 mM KCl, 8 mM Na_2HPO_4, 1.47 mM KH_2PO_4, pH 7.4
Tris Buffer Saline (TBS)	20 mM Tris base, 136.87 mM NaCl, pH 7.6

2 Mouse models

Mice used in these experiments were in a C57BL/6 background. Generation of *Crtc2-LacZ* reporter, *Crtc2* f/f and *Crtc2* cKO mice was performed as described in results (section 1.1). Mice were maintained in standard conditions at the Animal Care Facility of the Universitat Autònoma de Barcelona, with food and water available *ad libitum* and on a 12 h light/dark cycle. All behavioural experiments were performed during the light phase. Littermates were housed together, with a maximum of six mice per cage, keeping males and females separated after weaning. Experimental procedures were conducted according to the Animal and Human Ethical Committee of the Universitat Autònoma de Barcelona (CEEAH 2896) and Generalitat de Catalunya (DMAH 8787) following the experimental European Union guidelines and regulations (2010/63/EU).

3 Cell culture

3.1 Cell lines

Human embryonic kidney (HEK293T) cells were cultured in full DMEM. Cells were maintained in a humidified incubator at 37ºC with 5% CO_2. Culture medium was changed every 3-4 days and cell passages were performed once a week. For passages, cells were washed twice with PBS and trypsinized for 3 min at 37ºC with 1 ml of 0.25% Trypsin/EDTA. Flasks were manually shaken and pre-warmed full DMEM was added. Detached cells were centrifuged at 250 g for 5 min. Cell pellet was resuspended at the desired dilution and plated.

3.2 Primary neuronal culture

Cortical and hippocampal neurons were obtained from E15.5 mouse embryos. Embryos were extracted and placed in a p100 petri dish with cold PBG where dissection was performed. Brains were extracted, hemispheres were separated, and meninges were removed. Cortices and hippocampi were transferred to a tube containing Solution 1 (120 mM NaCl, 4.8 mM KCl, 1.2 mM KH_2PO_4, 25 mM $NaHCO_3$, 14.3 mM glucose, 0.3% BSA and 0.15% $MgSO_4$) and centrifuged at 300 g for 1 min. Tissue was incubated in Solution 2 (0.025% trypsin in Solution 1) at 37ºC for 10 min. Solution 3 (0.052% trypsin inhibitor, 0.008% DNAse and 0.038% $MgSO_4$ in Solution 1) was added and cells were centrifuged at 300 g for 1 min. The pellet was resuspended in Solution 4 (16% Solution 3 in Solution 1), mechanically disgregated using a Pasteur pipette and filtered through a 40 µm pore size nylon mesh. Filtered cells were transferred into Solution 5 (0.03% $MgSO_4$ and 0.0014% $CaCl_2$ in Solution 1) and centrifuged at 250 g for 5 min. The pellet was resuspended in pre-warmed complete neurobasal medium and cells were seeded in Poly-D-lysine (PDL)-coated 24 well plates (35.000 cells/well for immunocytochemistry and 150.000 cells/well for luciferase assay), 12-well plates (250.000 cells/well for mRNA analysis), 6-well plates

(500.000 cells/well for biochemical assays), 100 mm diameter dishes (4-5 x 10^6 cells/dish for co-immunoprecipitation assays). Neurons were maintained in a humidified incubator at 37ºC and 5% CO_2, and the medium was changed every 4 days by replacing half of the conditioned medium with fresh medium.

3.3 Primary astrocytic culture

Astrocyte cultures were prepared from cortices from mice at postnatal day 1. Mice were decapitated and the cortices were isolated, minced and processed in the same way as with primary neuronal culture. Filtered cells were resuspended in pre-warmed full DMEM and plated at 300.000 cells /ml in 24-well plates for luciferase assay and immunocytochemistry, 12-well plates for mRNA analysis, 6-well plates for biochemical assays and 100 mm dishes for chromatin immunoprecipitation assay and co-immunoprecipitation analysis. Astrocytes were maintained at 37ºC in an incubator with a humidified atmosphere with 5% CO_2. Medium was changed two hours after plated to avoid excessive microglial growth. Cells were maintained until cultures reached confluency (about 12 days) replacing the medium every 7 days.

3.4 Pharmacological treatments

Cultured cells were directly treated by adding the pharmacological reagent to the medium. Treatments used were: forskolin (FSK) at 1 or 20 μM, KCl at 30 or 55 mM, cyclosporin A (CsA) at 1 μM, okadaic acid (OkA) at 1 μM and norepinephrine (NE) at 10 μM.

3.5 Cellular transduction

For neuronal transduction, 4 days *in vitro* (DIV) cultured neurons were left with half of the medium and transduced with lentiviral particles (LV) overnight using 2 infective particles/cell. The following day medium was replaced with a mix of conditioned medium with fresh medium (1:1).

Astrocytes were transduced when reached 60% confluency with adenoviral vectors serotype 5 (Ad5) in DMEM containing 1% FBS for 3 h using 100 multiplicity of infection (MOI). Afterwards, medium was replaced for full DMEM.

3.6 Cellular transfection

Cultured neurons were transfected using Lipofectamine 2000 reagent according to manufacturer's instructions. Briefly, plasmidic DNA diluted in OptiMEM medium was mixed with Lipofectamine 2000 reagent diluted in OptiMEM medium and incubated for 20 min at room temperature. Meanwhile, half of cultured media was removed. Next, the mixture was added to

cell culture medium and incubated for 50 min. Finally, medium was all replaced by conditioned medium diluted in fresh medium (1:1).

For astrocytic transfection, the same protocol performed in neurons was used except that all medium was replaced for DMEM without FBS before transfection and the mixture of DNA-Lipofectamine was incubated for 4 h. Next all medium was replaced for full DMEM.

For HEK293T transfection the calcium phosphate method was used for lentiviral particles generation. A mix of DNA plasmids to be transfected were mixed in HEPES buffered saline (HBS) buffer (140 mM NaCl, 0.75 mM Na_2HPO_4, 25 mM HEPES; pH 7.05) containing 125 mM $CaCl_2$ and incubated for 25 min at room temperature. Meanwhile HEK293T media was replaced for DMEM without FBS. Next, mixture was added to media and incubated for 7 h. Finally, transfection media was replaced for full DMEM.

4 Biochemical methods

4.1 Cellular and tissue lysis and protein quantification

Cell cultures were washed twice with ice-cold PBS and lysed in cold RIPA lysis buffer (50 mM Tris pH 7.4, 150 mM NaCl, 2.5 mM EDTA, 1% NP40, 0.5% sodium deoxycholate, 0.1% SDS, 1 mM Na_3VO_4, 25 mM NaF, 1mM PMSF) supplemented with protease and phosphatase inhibitors. Samples were sonicated for 10 seconds and centrifuged at 20,000 g for 10 min at 4ºC. Supernatant was kept at -20ºC.

For tissue preparation, mice were euthanised by cervical dislocation, tissue was dissected on ice and kept at -80ºC until processing. Tissue was homogenized using a Dounce homogenizer in RIPA lysis buffer containing protease and phosphatase inhibitors. Homogenized tissue was incubated for 1 h at 4ºC and sonicated 20 seconds three times. Lysates were centrifuged at 20,000 g for 10 min at 4ºC and supernatant was stored at -20ºC.

Protein concentration was determined with BCA Protein Assay Kit following manufacturer's instructions.

4.2 SDS-PAGE and Western blotting

Equal amounts of protein extracts were diluted with loading buffer and heated at 95ºC for 5 min before loading the polyacrylamide gels (PAGE) (6-8%). A molecular weight marker was included in the gel. Electrophoresis was performed at 25 mA per gel in running buffer (25 mM Tris pH 8.3, 200 mM glycine, 0.1% SDS) and proteins were transferred to methanol-activated polyvinylidene fluoride (PVDF) membranes at 110V for 1 h and 15 min in transfer buffer (10 mM Tris base pH 8.3, 100 mM glycine). Transferred membranes were incubated with blocking

buffer (10% skimmed milk powder and 0.1% BSA in TBS) for 1 h at room temperature and with primary antibody (**Table 3**) diluted in antibody solution (0.1% BSA and 0.02% thimerosal in TBS) overnight at 4ºC. Membranes were incubated with secondary antibodies conjugated to horseradish peroxidase (HRP) diluted 1:3000 in blocking buffer for 1 h. Finally, membranes were revealed by chemiluminescence reaction using ECL substrate (mixing ECL1:ECL2 in 1:1 ratio; ECL1: 0.1 M Tris-HCl pH 8.5, 10 mM Luminol and 0.4 mM p-Coumaric acid; ECL2: 0.1 M Tris-HCl pH 8.5, 0.064 % 8.8M Hydrogen Peroxide). Bands were detected on ChemiDoc MP System (BioRad) and quantified with Image Lab 5.2.1 software (BioRad).

4.3 Cellular fractionation

Cultured cortical neurons were washed twice with cold PBS and cell fractionation lysis buffer (10 mM HEPES, 1.5 mM $MgCl_2$, 10 mM KCl, pH7.9) supplemented with 0.1% Triton X-100, protease and phosphatase inhibitors was added to plates. Neurons were collected, mechanically homogenized and centrifuged at 1,200 g for 10 min at 4ºC to pellet nuclear fraction. Nuclei were washed thrice in the same buffer. Supernatant was centrifuged at 7,000 g for 10 min at 4ºC to discard organelles and centrifuged again at 100,000 g for 1 h at 4ºC to obtain the cytosolic fraction (supernatant) without membranes (pelleted).

Cultured astrocytes were washed twice with cold PBS and cell fractionation lysis buffer without Triton X-100 and supplemented with protease and phosphatase inhibitors was added to the plates. The following processing was performed as neuronal cellular fractionation.

For the Western blot analysis, equal amount of total protein was loaded in the gel for each fraction.

4.4 Co-immunoprecipitation (CoIP)

Cultured neurons or astrocytes were crosslinked with 1% PFA for 10 min at room temperature and quenched by adding glycine (125 mM). Cells were washed twice in cold PBS and were lysed in CoIP buffer (50 mM Tris-HCl pH8, 100 mM NaCl, 1 mM $MgCl_2$, 1% triton X-100, 1mM PMSF) supplemented with protease and phosphatase inhibitors. Samples were sonicated for 15 seconds (x3) and centrifuged at 14,000 g for 10 min at 4ºC. Neuronal supernatants (2 mg of protein) were incubated with anti-CREB or anti-CRTC1 antibodies while astrocytic samples were incubated with anti-CREB or anti-CRTC2 antibodies (see **Table 3**) overnight in a rotating wheel at 4ºC. Dynabeads protein G (Life Technologies) were added to samples and incubated for 15 min at room temperature in a rotating wheel. Tubes were transferred to the magnet and beads were washed 4 times in CoIP buffer. Finally, beads were resuspended in loading buffer. To reverse crosslinking, before loading samples in SDS-PAGE, they were incubated at 96ºC with shacking (1,000 rpm) for 30 min.

4.5 CREB transcriptional activity analysis

CREB-dependent transcriptional activity was determined using the commercial kit Dual-Luciferase Reporter Assay System by transfecting cells with the pCre-luc and the pRL reporter vectors. Neurons were transfected with pCre-luc and pRL-TK reporter vectors with Lipofectamine 2000 as described above. Treatment was performed 24 h post transfection with FSK (20 µM) plus KCl (30 mM) for 4 h.

Astrocytes were transfected with pCre-luc and pRL-null reporter vector. Treatment was performed 48 hours post-transfection with NE (10 µM) for 8h.

After treatment, cells were washed twice with PBS and lysed using 100 µl of Passive Lysis Buffer per well. For neuronal analysis, 20 µl of lysate was loaded in an opaque 96-well plate adding 25 µL of Luciferase Assay Reagent II (LAR II) and 25 µl of Stop & Glo reagent. For astrocytic measurements, 40 µl of lysate was analysed adding 40 µl of LAR II and 40 µl of Stop & Glo. Signal was measured using CLARITY luminometer (BIOTEK).

5 Molecular biology methods

5.1 Plasmidic DNA: amplification and purification

For plasmid amplification, 20 µl of DH5α competent cells were transformed with 1 µg of purified DNA plasmid. Briefly, DNA was incubated with the cells at 4ºC for 30 min, afterwards a heat shock was performed (42ºC for 45 seconds) and incubated again at 4ºC for 5 min. Bacteria were resuspended in 500 µL luria broth (LB) and incubated at 37ºC with shacking for 1 h. Finally, cells were pleated onto LB agar plates containing 100 µg/ml of ampicillin and incubated upside-down at 37ºC overnight.

For large-scale DNA purification, one transformed colony was grown in 250 ml of LB containing 100 µg/ml ampicillin at 37ºC with agitation overnight. Bacteria were lysed and the plasmidic DNA was purified using the PureLink HiPure Plasmid Filter kit following the manufacturer's instructions. Purified DNA was stored at -20ºC.

5.2 Genotyping

For genotyping, genomic DNA was extracted from a 1-2 mm portion of mouse tail. Tissue was incubated overnight at 56ºC in digestion buffer (100 mM Tris-HCl pH 8.5, 200 mM NaCl, 5 mM EDTA and 0.2% SDS) containing 0.1 mg/mL proteinase K (Roche). Samples were centrifuged at 15,000 g for 5 min and the supernatant was transferred into a new tube containing 500 µl of isopropanol, mixed and centrifuged at 15,000 g for 10 min. DNA pellet was washed with 500 µl of 70% ethanol and centrifuged again. Supernatant was removed and the DNA pellet was

resuspended in 100 µl TE buffer (10 mM Tris-HCl pH 7.4, 1 mM EDTA pH 8) at room temperature overnight with shacking. For genotyping, 2 µl of DNA were added to 23 µl PCR mix containing 0.2 mM dNTPs mix, 2 mM $MgCl_2$, 0.5 µM of each primer (Life Technologies) (**Table 4**) and 1U DNA polymerase in PCR Buffer. PCR conditions were as follow: 94ºC for 4 min, 40 cycles of 94ºC for 1 min, 60ºC for 1 min, 72ºC for 1 min and followed by a final step of amplification at 72ºC for 7 min. PCR products were resolved in a 2 % agarose gel containing 1X Sybr-Safe in TAE buffer (40 mM Tris-acetate and 1 mM EDTA at pH 8.2). Gel electrophoresis was performed at 110V for 45 min and DNA bands were visualized in the UV transilluminator (GeneGenius, Syngene).

5.3 RNA extraction and reverse transcription

Total RNA from frozen tissue or cultured cells was extracted by using the PureLink RNA Mini Kit according to manufacturer's instructions. To avoid genomic DNA contamination, a DNAse digestion step was performed in the column using the RNase-free DNAse set according to manufacturer's instructions. Purified RNA (0.5 – 1 µg) was reverse transcribed in a 50 µl mix containing Oligo(dT) primers (1 µM), random hexamers (1µM), dNTPs (0.5 mM), DTT (0.45 mM), RNAse Out (10 U), reaction buffer (1X) and Super Script II reverse transcriptase (200 U). First, a 25 µl mix containing RNA, dNTPs, Oligo(dT) primers and random hexamers was incubated at 65ºC for 10 minutes before adding the rest of reagents. Samples were incubated at 25ºC for 10 min, 42ºC for 1 h and finally 72ºC for 15 min. The resultant cDNA was stored at -20ºC.

5.4 Quantitative PCR

For gene expression analysis, reverse transcribed cDNA was diluted 1:100 and analysed using real-time quantitative PCR (RT-qPCR). RT-qPCR reactions were performed in duplicate using the Power SYBR green PCR master mix and custom designed primers (0.4 µM; Life Technologies) (**Table 5**) using the 7500 Fast instrument (Applied Biosystems) with the following parameters: 95ºC for 10 min, 40 cycles at 95ºC for 15 seconds, 60ºC for 1 min followed by 95ºC for 30 seconds and 60ºC for 15 min. Amplification data was acquired using the 7500 Software v2.0.6 (Applied Biosystems), analysed using LinRegPCR software (Ruijter et al., 2009) to extract the Cq values and the PCR efficiencies and finally analysed using the comparative Cq method (Pfaffl, 2001).

In the case of quantitative chromatin immunoprecipitation (ChIP-qPCR) analysis, no previous dilution of the samples was performed.

5.5 Generation of lentiviral particles

Lentiviral particles (LV) were generated in HEK293T cells. HEK293T cells were co-transfected using the calcium phosphate method with psPAX2 packaging vector, pMD2.G envelope vector and the plasmid of interest: pFUGW-EGFP-NLS-Cre, pFUGW-EGFP-NLS-ΔCre (Ho et al., 2006), pLVTHM-shCRTC1 or pLVTHM-Scr (España et al., 2010) that express Cre-recombinase (Cre), a non-active mutant Cre-recombinase (ΔCre), short hairpin *Crtc1* (shCRTC1) and its control scramble (Scr) respectively.

48 h after transfection, medium was centrifuged at 100,000 g for 2 h at 4ºC to precipitate the lentiviral particles. The pellet was then resuspended in PBS and kept at -80ºC. For titration, HEK293T cells were transduced with different dilutions of the lentiviral particles and GFP positive cells were quantified using the flow cytometer (Cytomics FC 500, Beckman Coulter) 72 h after transduction.

5.6 Generation of adenoviral vectors

Adenoviral vectors serotype 5 (Ad5) expressing GFP (Ad5-GFP) or Cre-recombinase (Ad5-Cre) under the CMV promoter were generated at the Viral Vector Unit Production (UPV) from Centre de Biotecnologia Animal i Teràpia Gènica (CBATEG).

5.7 Quantitative chromatin immunoprecipitation (ChIP-qPCR)

Confluent cultured astrocytes in 100 mm dish were crosslinked with 1% PFA for 10 min at room temperature with gentle agitation and quenched with glycine (125 mM) for 5 min. In case of performing the IP against the transcriptional coactivator (CRTC2), astrocytes were also crosslinked using 6 mM ethylene glycol-bis(succinic acid N-hydroxysuccinimide ester) (EGS) for 30 min. Pleated cells were then placed on ice and washed twice with cold PBS. Astrocytes were collected in PBS supplemented with protease inhibitors and 1 µM PMSF, transferred to an eppendof and centrifuged at 10,000 g for 10 min. The resultant cell pellets were stored at -80ºC. For ChIP, frozen pellets were thaw on ice and lysed in 50 µl of SDS-Lysis Buffer (50 mM Tris-HCl pH 8.1, 100 mM NaCl, 5 mM EDTA, 1% SDS, 0.1% Na-deoxycholate, 1 µM PMSF and protease inhibitors) for 1 h in a tube rotator at 4ºC. Lysates (120 µl corresponding to 2 pellets) were transferred to a new eppendorf and 180 µl of ChIP Dilution Buffer (CDB) (16.7 mM Tris-HCl, pH 8.1, 167 mM NaCl, 1.2 mM EDTA, 1.1% Triton X-100, 0.01% SDS, 0.1% Na-deoxycholate, 1 µM PMSF and protease inhibitors) were added before sonication in the Bioruptor Plus (Diagenode, Seraing, Belgium). Chromatin was sheared between 200 and 500 bp. 700 µl of CDB were added to the fragmented chromatin and centrifuged at 12,000 g for 10 min at 4ºC. Part of the resultant supernatant was kept as input (25 µl) and the rest was transferred to a new eppendorf and incubated at 4ºC in a tube rotator overnight with anti-CREB or anti-CRTC2

antibodies (see **Table 3**) or without antibodies as a negative control. Each sample was incubated with 50 µl of Protein A Plus beads for 1 h in a tube rotator at 4ºC and centrifuged at 350 g for 2 min at 4ºC. Beads were washed twice with 700 µl Low-salt wash buffer (20 mM Tris-HCl pH 8.1, 150 mM NaCl, 2 mM EDTA, 1% Triton X-100, 0.1% SDS), 700 µL LiCl wash buffer (10 mM Tris-HCl pH8.1, 250 mM LiCl, 1% NP40, 1% Na-deoxycholate, 1mM EDTA) and 700 µl Tris-EDTA (TE) (10 mM Tris pH 8, 1mM EDTA). Immunoprecipitated chromatin was eluted in 200 µl of Elution Buffer (20 mM Tris-HCl pH 7.5, 5 mM EDTA, 70 mM NaCl supplemented with 1% SDS and 5 mM DTT) incubating at 65ºC in agitation (1000 rpm) for 15 min. To each immunoprecipitated sample (200 µl) were added 100 µl of Elution Buffer without DTT nor SDS before proceeding to reverse de crosslinking. To each input sample (25 µl) were added 225 µl CDB, 25 µl NaCl 2M, 20 µl SDS 10% and 12.5 µl DTT 100 mM. Input and immunoprecipitated samples were incubated at 65ºC for 3 h in agitation (600 rpm) followed by a 3 h proteinase K digestion (125 µg) at 65 ºC agitating at 600 rpm. 500 µL of UltraPure Phenol:Chloroform:Isoamyl Alcohol (25:24:1, v/v) were added to samples, mixed vigorously and centrifuged at 16,000 g for 10 min at room temperature. The upper face was then transferred to a new eppendorf and a mix containing 1 ml of Absolute Ethanol (stored at -20 ºC), 40 µl NaAc 3M and 0.2 µl UltraPure Glycogen was added to each sample before storing them overnight at -20ºC. Samples were centrifuged at 20,000 g for 20 min at 2ºC to precipitate the DNA, supernatant was removed, and the precipitated DNA was washed with 70% ethanol. Purified chromatin was resuspended in 60 µl TE incubating at 37ºC in agitation (650 rpm) for 20 min and amplified by real-time qPCR using primers for specific gene promoter regions (**Table 6**).

6 Histological and immunostaining methods

6.1 Immunohistological staining

To analyse expression of the reporter gene *LacZ,* a protocol combining an enzymatic β-galactosidase assay with an immunohistochemistry with peroxidase was used. Brains of 12 months-old male mice were dissected out, OCT embedded (Tissue-Tek O.C.T Compound) and fresh-frozen in isopentane. Sections of 8 µm were obtained in a cryostat (Leica) and collected on Superfrost Plus slides. Samples were stained using the β-Galactosidase Reporter Gene Staining Kit according to manufacturer's instructions. Briefly, slides were fixed with the fixing solution provided in the kit for 10 min at room temperature and incubated with the Staining Solution for 16 h at 37ºC. Next, slides were fixed with 3% PFA for 15 min at room temperature and incubated with 1% hydrogen peroxide in methanol for 15 min. Slices were blocked with 5% NGS and 0.3% Triton X-100 in TBS. Primary antibodies NeuN, GFAP or Iba1 (see **Table 3**) were diluted in blocking solution and applied to the sections for 2 h at room temperature. Sections were then incubated with secondary biotinylated anti-rabbit antibody (1:200) in blocking solution for 30

min at room temperature and incubated with the avidin-biotin peroxidase (HRP) complex using the Vectastain ABC HRP kit. After 2 washes of 50 mM Tris-HCl pH 7.5 for 10 min, sections were incubated with DAB Peroxidase (HRP) Substrate kit following manufacturer's instructions. Sections were dehydrated: incubated in distilled water for 10 min (twice) and 3 min in each alcohol dilution (50%, 70%, 96%, 100% (twice), xilol (twice)). Finally, slices were mounted using DPX Mountant.

6.2 Immunofluorescence staining

Cultured cells plated on glass coverslips were washed twice with PBS, fixed with 4% PFA for 15 min and washed again with PBS. Fixed cells were blocked and permeabilized incubating coverslips in blocking solution (1.5% NGS, 0.1% Triton X-100 in PBS) for 30 min at room temperature. Primary antibodies anti-OctA-Probe FLAG tag or anti-CRTC1 (**Table 3**) were incubated overnight at 4ºC in blocking solution and 3 washes of PBS (5 min) were performed. Secondary antibodies Alexa Fluor 568 anti-mouse or anti-rabbit (see **Table 3**) were diluted in PBS and incubated with the samples for 45 min at room temperature. If necessary, fixed cells were incubated with Actin Green 488 Ready Probes reagent for 30 min at room temperature following manufacturer's instructions. Finally, nuclei were stained using Hoechst33258 (1 µg/ml) diluted in PBS and incubated for 20 min at room temperature. Coverslips were finally washed with PBS and mounted using FluorSave Reagent.

6.2.1 Fluorescence resonance energy transfer (FRET)

FRET refers to the transfer of nonradiative energy from an excited state of a fluorophore (donor) to an adjacent fluorophore (acceptor). Thus, exciting a donor results in emission of the acceptor despite it has not been directly excited (**Figure 10A**).

For FRET, protein interaction is considered when the two molecules are less than 10 nm apart (Mátyus, 1992). Distance is an important factor because FRET efficiency (E) between a single pair of donor and acceptor is determined by $E=1/[1+(r/R_0)^6]$, were r is the distance between the two fluorophores and R_0 corresponds to the distance when 50% of energy is transferred (Snapp & Hegde, 2006; Wouters et al., 2001). The R_0 value is fluorophore-dependent and is determined by the amount of overlap between emission spectra of the donor and the excitation spectra of the acceptor and the relative orientation of the fluorophores. Thus, an important factor to consider for FRET analysis is the pair of fluorophores chosen. In this case, Alexa Fluor 488 was used as donor while Alexa Fluor 568 was determined as acceptor because their emission spectra and excitation spectra, respectively, overlap and have an R_0 of 62 Å (Group & Microsystems, 2006) (**Figure 10C**).

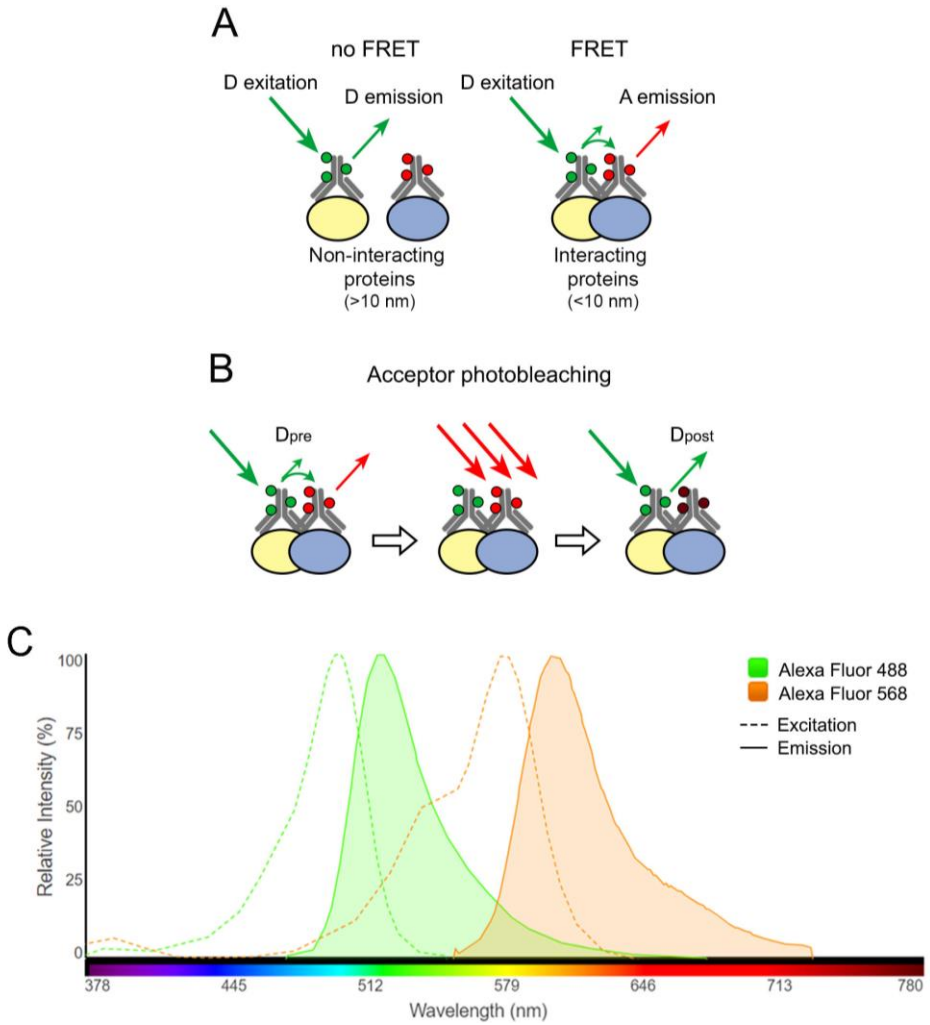

Figure 10. FRET approach principles

(A) FRET principle. In the absence of protein interaction, energy emission of donor (D, yellow) fluorophores (green circles) cannot excite acceptor (A, blue) fluorophores (red circles). When proteins are close enough, part of D emission is transferred to A fluorophores which emit energy (A emission). **(B)** FRET measurement by acceptor photobleaching. First, donor (D) fluorophores are excited and D emission is quantified as D prebleaching (Dpre). Second, acceptor fluorophores are photobleached. Third, D fluorophores are excited and D emission is quantified as D postbleaching (Dpost). **(C)** Excitation (dotted lines) and emission (solid line) spectra of Alexa Fluor 488 (green), used as donor, and 568 (orange) used as acceptor. Note that 488 emission spectra overlap with 568 excitation spectra. Figure obtained from Fluorescence Spectra Viewer, Thermo Fisher Scientific: https://www.thermofisher.com/order/spectra-viewer.

Different techniques can be implemented to determine FRET (Broussard et al., 2013). In this work, experiments have been analysed using the acceptor-photobleaching. In this case, acceptor is photobleached and the donor emission before bleaching (D_{pre}) is compared to the donor emission after bleaching (D_{post}) (Kenworthy, 2001) (**Figure 10B**). Before acceptor-photobleaching, donor emission energy is partially transferred to acceptor but, after acceptor-photobleaching no energy transference takes place and all donor energy is emitted. Thus, if the donor emission is higher after acceptor-photobleaching, one can assume that fluorophores are close enough to undergo FRET. FRET efficiency ($FRET_{eff}$) is then determined by $FRET_{eff} = (D_{post} - D_{pre})/D_{post}$ (Snapp & Hegde, 2006).

Cultured hippocampal neurons plated on glass coverslips were washed twice with PBS, fixed with fresh 4% PFA for 15 min at room temperature, and washed again with PBS. Cells were permeabilized and blocked for 30 min at room temperature with blocking solution (1.5% NGS, 0.1% Triton X-100 in PBS). Primary antibodies were directly conjugated to fluorophores using Zenon Rabbit Alexa Fluor 488 Rabbit IgG kit or Zenon Rabbit Alexa Fluor 568 Rabbit IgG kit following manufacturer's instructions. Primary antibodies were conjugated using 1:6 molar ratio (1 primary antibody to 6 Fab Zenon labelling reagent) as proceeds: 1 µg of primary antibody was incubated with 10 µl of reagent A for 5 min at room temperature and then blocked with 10 µl of reagent B for 5 more min. For 1:3 molar ratio, 1 µg of primary antibody was incubated with 5 µl of reagent A and B. Conjugated primary antibodies were used within a maximum of 30 min. Fixed neurons were incubated with conjugated primary antibodies (diluted in blocking solution) for 1 h at room temperature and washed thrice with PBS for 5 min. Cells were fixed again with 4% PFA for 15 min at room temperature and washed thrice in PBS for 5 min. When necessary, an incubation of 45 min at room temperature with Alexa Fluor 568 anti-mouse or anti-rabbit secondary antibody diluted in blocking solution was performed. Coverslips were then washed with PBS and mounted on slides using Mowiol. Primary and secondary antibody dilutions are specified in the results (section 2.4.2).

6.3 Image acquisition and processing

For histological staining, images were captured with Nikon Eclipse 90i series microscope using the DXM 1200F camera with ACT-1 software (Nikon). For immunofluorescence staining and CRTC1 and 2 translocation analysis, images were taken using a laser scanning confocal microscope (Zeiss LMS700, Carl Zeiss Microscopy) with a 40x objective and a zoom of 0.5. For the analysis of the CRTCs translocation, quantifications were performed with ImageJ software (National Institutes of Health). First, a sum projection was performed for multiple stacks and nuclear and cytosolic ROIs were established. Nuclear/cytosolic intensity of CRTCs staining was calculated as integrated density (IntDen).

For FRET experiments, slides were examined using a laser scanning confocal microscope (Leica TCS-SP5, Leica Microsystems). Images were taken using FRET wizard Leica software with a 63x objective, a zoom of 1.5x and 512x512 pixel resolution. For donor excitation was used 488 nm laser line with 30% intensity and emission was collected from 500-555 nm. For acceptor excitation, 568 nm laser line with 20% intensity was used and emission was collected from 585-700 nm. Prebleach images were acquired first. Then, bleaching was performed with the 561 nm laser at 100% intensity with 5 iterations in a 3x3 ROI established in the nucleus of neurons. Then, postbleach images were acquired. FRET analysis was performed using FRETcalc v5.0 plugin of ImageJ 1.5i (Stepensky, 2007). First, stacks of 8-bit files containing pre- and postbleach images

for donor and acceptor were prepared. Background was subtracted using a ROI adjacent to cell and a smooth filter (3x3) was applied to eliminate noise. Donor and acceptor thresholds were set as the mean of intensity values of samples without labelling. For the analysis, only the pixels that were bleached over 50% were considered. FRET analysis was performed on the pixels in the selected ROI that passed the established threshold values.

7 Behavioural experiments

For the transgenic mice phenotypic characterization, we used a battery of different tests. First, observation assessments were performed and then, more sophisticated tasks such as Morris water maze and contextual fear conditioning were analysed.

7.1 Observation assessment

The primary observations that were evaluated are summarized in the **Table 8**. Each parameter is scored to provide a quantitative value to compare between genotypes. Individual observations can be compared as well as a global value obtained from all observations. For the attainment of the global punctuation individual values were summed or subtracted depending on if the evaluated parameter was defining a positive (P) or a negative (N) aspect of the general condition of the mice health respectively.

Table 8: List of primary observation parameters evaluated

Parameter	Range	Range of scores	Condition
Body Position	0-5	Incorrect to correct	P
Spontaneous Activity	0-3	None to repeated vigorous movement	P
Tremor	0-2	None to marked	N
Urination	0-1	Absent or present	N
Defaecation	n		N
Piloerection	0-1	Absent or present	N
Gait	0-3	Incapacity to normal	P
Injury	n		N
Righting Reflex	0-3	From impairment to no impairment to fails to right when placed on back	P
Body tone	0-2	None to strong	P
Pinna Reflex	0-2	Response to ear light tactile stimulus	P
Fur	0-2	From many bald areas to normal fur	P
Whiskers	0-1	Absent or present	P
Lacrimation	0-1	Absent or present	N
Tail elevation	0-2	Flattened to Straub tail	N
Skin colour	0-2	Blanched to normal	P
Hump	0-1	Absent or present	N
Right eye opening	0-2	From shut eye to wide opened eye	P

Left eye opening	0-2	From shut eye to wide opened eye	P
Weight	g		

Modified from Hatcher et al., 2001. P: positive; N: negative

7.2 Morris water maze (MWM)

Morris water maze (MWM) experiments were performed in a circular pool of 120 cm diameter full of white-coloured water at 20-22 ºC. During the first day, animals were trained (4 trials; 60 s each) to learn there is a platform (11 cm diameter) indicated with a visual cue, submerged (1.5-2 cm) in the pool. For the following days, 4 visual cues were situated at the virtual cardinal points of the pool, dividing the pool with 4 virtual quadrants. The hidden platform was situated at the middle of one quadrant (target, TG) and was maintained at the same position during all training. During acquisition (ACQ), mice were trained for 5 or 8 consecutive days (4 or 6 trials daily; 60 s per trial). In each trial, animals were individually introduced at the pool for each virtual cardinal point, entering for all different cardinal points each day and changing the entrance order each day of acquisition. Mice were put in the pool facing the wall and were left for free swimming for a maximum of 1 min or until animal found platform. Mice that couldn't find platform were guided to platform and were left on the platform for 10 seconds. After each trial, mice were returned at the home cage for 15 min before proceeding to the following trial. Mice were probed 2 h and 24 h post-acquisition. For the probe trial, platform was removed, and animals were introduced to the pool from the adjacent right quadrant of the target quadrant (2 h) and the adjacent left quadrant of the target quadrant (24 h). Animals freely swam for 60 seconds during each probe. Mice behaviour during acquisition and probe was recorded and automatically analysed using ANY-maze software (Version 5.1; Stoelting).

7.3 Contextual fear conditioning (CFC)

Mice were individually placed in a conditioning chamber (15.9 cm x 14 cm x 12.7 cm; Med Associates Inc.) for 3 min allowing them to explore and develop a representation of the context before applying the unconditioned stimulus, consisting on a foot shock (1s/0.8mA). Mice were then maintained in the chamber for 2 min and immediate freezing after shock was analysed. The conditioning chamber was cleaned before placing each mouse using 70% ethanol. Mice were re-exposed to the same chamber 2 h (short-term memory), 24 h (long-term memory) or 7 days (extinction) after the foot shock, and contextual fear memory was assessed by measuring the freezing response during 4 min. Freezing response is defined as total movement cessation except for respiration and was automatically measured using the Video Freeze Software (Med Associates Inc.).

8 Statistical analyses

Experiments were performed using at least three independent experiments, otherwise stated, and data are represented as mean ± standard deviation (SD) or standard error of the mean (SEM). Statistical analyses were performed using GraphPad Prism 6 (GraphPad Software). Analysis of t-test and one or two-way analysis of variance (ANOVA) were performed followed by Bonferroni's, Sidak's or Tukey's *post hoc* test. Differences with P value < 0.05 were considered significant.

VII Results

1 CRTC2 expression in the adult mouse brain

1.1 Generation of *Crtc2* cKO mice

Crtc2-LacZ reporter mice were obtained by injecting *Crtc2* embryonic stem (ES) cells into C57BL/6J-Tyr c-Brd blastocysts (Pettitt et al., 2009). The *Crtc2* ES cells contain a knock-in insertion into the endogenous *Crtc2* gene containing a *LacZ* reporter gene and a *Neo* resistance gene between short flippase (Flp) recognition target (*FRT*) sites, and loxP sequences flanking the *Crtc2* exon 4 (**Figure 11A**). The resultant chimeric mice were crossed with C57BL/6J-Tyr c-Brd females and the offspring carrying the genetic allele (heterozygous) were crossed to set up the colony. These *Crtc2-LacZ* reporter mice were crossed with Flp transgenic mice to remove the *LacZ* and *Neo* sequences. The Flp transgenic mice expresses a *Flp* recombinase gene under the human β-actin (*Actb)* promoter that allows the recombination of the two FRT sequences to obtain the *Crtc2* f/f mutant mouse which have the wild-type *Crtc2* gene containing two loxP sequences flanking exon 4 (**Figure 11B**). *Crtc2* f/f mice were crossed with calcium/calmodulin-dependent protein kinase IIα (*CamKIIα*)-*Cre-recombinase* transgenic mice (Yu et al., 2001). The obtained *Crtc2* conditional knockout (cKO) mice (*Crtc2* f/f; *CamKIIα-Cre-recombinase*) are expected to recombine the loxP sequences eliminating *Crtc2* exon 4 in postmitotic neurons (**Figure 11B**).

1.2 Expression of CRTC2 in neurons and glia in the adult mouse brain

Previous *in situ* hybridization analyses revealed that all CRTC isoforms, CRTC1, 2 and 3 are widely and differentially expressed in the rat brain (Watts et al., 2011). To examine the regional and cellular expression of CRTC2 in the adult brain, histoenzymatic analyses of β-galactosidase (*LacZ*) were used in brain slices of control (WT) and *Crtc2-LacZ* reporter mice at 12 months of age. This approach allows to study basal CRTC2 expression since the lacZ gene is under the endogenous *Crtc2* promoter. Stained images show abundant β-galactosidase staining in the hippocampus, spread and doted staining in the cortex and hypothalamus and less abundant staining in the thalamus (**Figure 12A**). As expected, staining was absent in f/f control (WT) mice not harbouring the β-galactosidase gene.

To determine the cellular types where CRTC2 is expressed, the histoenzymatic assay was combined with immunohistochemical staining using markers for neurons (NeuN), astrocytes (GFAP) and microglia (Iba1). Imaging analysis revealed that CRTC2 (blue staining) is expressed both in neurons and astrocytes (brown staining) although not all neurons and astrocytes express CRTC2 (**Figure 12B**). Notably, few microglia also express CRTC2 (**Figure 12B**). Again, β-galactosidase staining is absent in the brain of WT mice. These results indicate that CRTC2 is mainly expressed in neurons and astrocytes in different regions of the adult mouse brain.

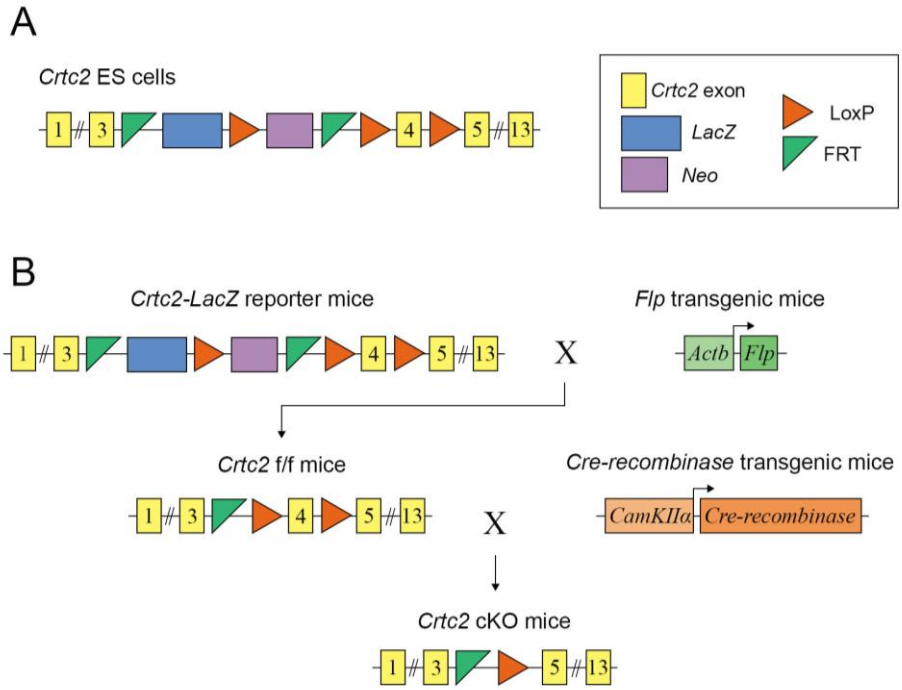

Figure 11. Generation of mutant *Crtc2* f/f and *Crtc2* cKO mice

(A) Schematic representation of the modified *Crtc2* allele in embryonic stem (ES) cells used for generating the *Crtc2-LacZ* reporter mice showing location of the *LacZ* reporter and neomycin (*Neo)* resistance genes and the critical floxed (f) exon 4, flanked by loxP sequences. FRT: flippase recognition target. **(B)** Scheme showing generation of the *Crtc2* f/f and *Crtc2* cKO mice. *Crtc2-LacZ* reporter mice and Flip (*Flp*) transgenic mice were crossed to obtain the *Crtc2* f/f mice after recombination of the FRT sequences. *Crtc2* f/f is crossed with CamKIIα-*Cre-recombinase* transgenic mice to obtain the *Crtc2* f/f; *CamKIIα-Cre-recombinase* (*Crtc2* cKO) mice after recombination of the loxP sequences.

1.3 Cellular expression of CRTCs in the brain

To analyse the cell-type expression of the three *Crtc* isoforms in the mouse brain, we re-analysed free available cell type-specific transcriptomic data from the mouse cerebral cortex obtained from the expression atlas database (Ref. 25186741; E-GEOD-52564; Y. Zhang et al., 2014). To compare the expression of the different *Crtc* isoforms, data were expressed as Log2 transcripts per million (TPM) (**Figure 13A**). *Crtc1* mRNA levels are more abundant in neurons (5.52), followed by oligodendrocytes precursor cells (OPCs) (4.91), astrocytes (4.7), microglia (3.58) and endothelial cells (2). *Crtc2* mRNA was predominantly abundant in all cell types analysed except for oligodendrocytes. *Crtc2* was highly detected in microglia (6.39) and astrocytes (6.21), followed by endothelial cells (5.98) and neurons (5.86). By contrast, *Crtc3* mRNAs were the less abundant isoform in the cerebral cortex but its expression was relatively high in astrocytes (5), neurons (4.58), OPCs (4) and microglia (3.32).

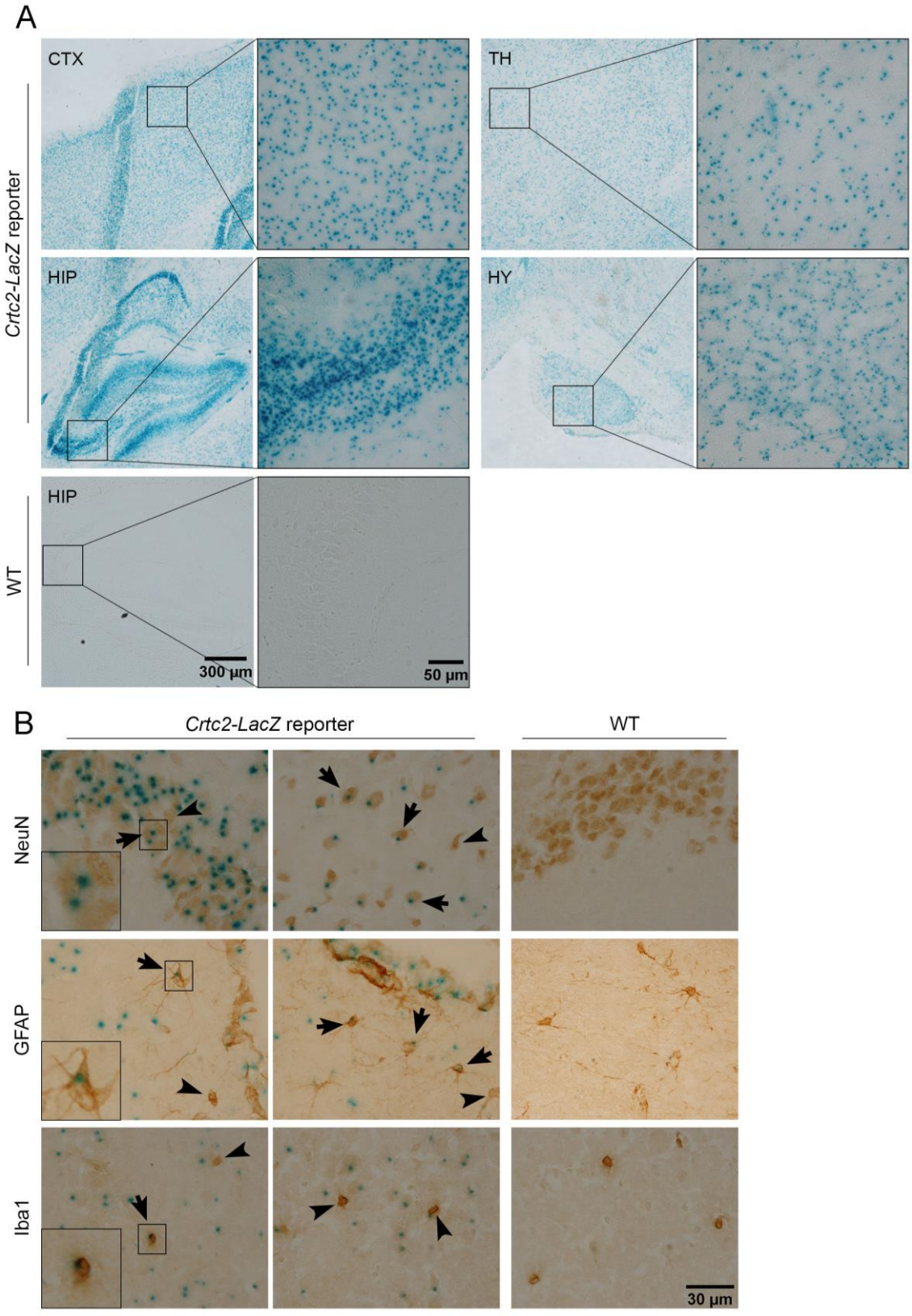

Figure 12. Expression of CRTC2 in the adult mouse brain

(A) X-gal staining of brain sagittal sections of *Crtc2-LacZ* reporter and control (WT) mice at 12 months of age showing X-gal staining in the cortex (CTX), hippocampus (HIP), thalamus (TH) and hypothalamus (HY). **(B)** X-gal staining combined with immunohistochemical staining of markers for neurons (NeuN), astrocytes (GFAP) and microglia (Iba1) in brain sections of *Crtc2-LacZ* reporter and WT mice. NeuN staining images correspond to CA1 (left and right images) and cortex (middle). Arrows indicate colocalization, while arrowheads show non-expressing β-galactosidase cells.

We next performed biochemical analysis to study the expression of the most abundant brain CRTC isoforms, CRTC1 and CRTC2, in cultured mouse cortical neurons and astrocytes (**Figure 13B**). This allows us to quantify the relative levels of CRTC isoforms normalized to β-actin. CRTC1 is highly expressed (~1 fold) in cortical neurons (12 DIV) compared to cortical astrocytes (80% confluency; ~0.1 fold; $P < 0.001$). On the contrary, CRTC2 expression is much higher in astrocytes (~2 fold) than in cortical neurons (~1 fold; $P < 0.001$; **Figure 13B**). These results indicate differential and cell-type specific expression of CRTC isoforms in the mouse cerebral cortex.

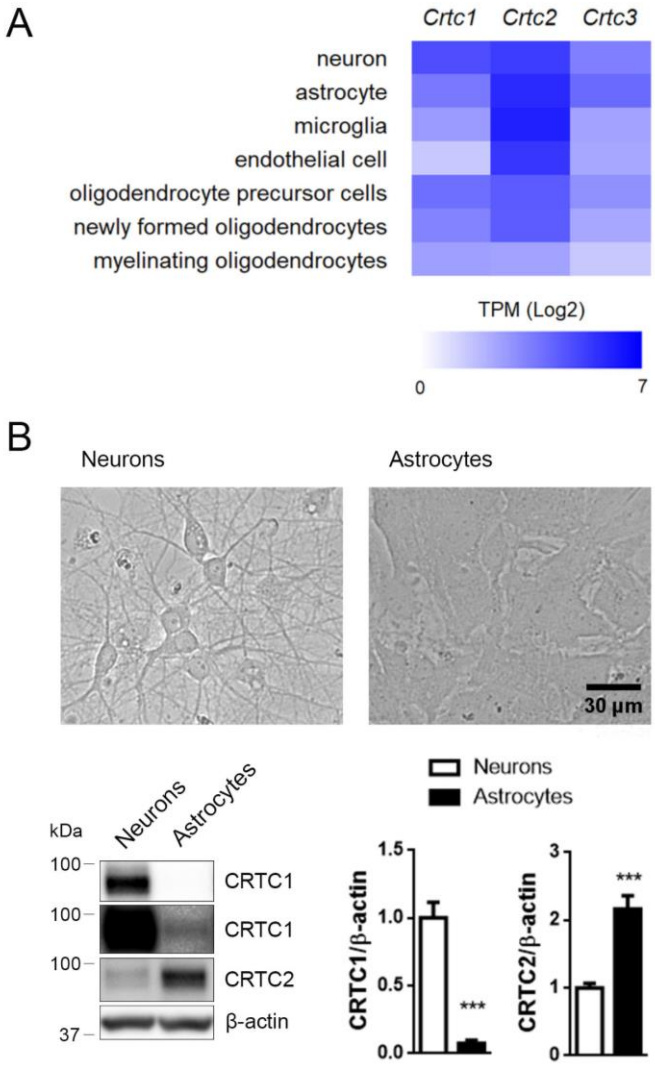

Figure 13. Cellular expression of CRTC isoforms in the mouse cerebral cortex

(A) Relative expression of *Crtc* isoforms analyzed by RNA-sequencing in different cell types of the mouse cerebral cortex. Data extracted from the Expression Atlas database Ref. 25186741; E-GEOD-52564 (Zhang et al., 2014). **(B) Top:** Representative images of primary mouse cortical neurons and astrocytes in culture. **Bottom:** Western blot images (left) and quantification (right) of CRTC1 (two different exposures) and CRTC2 protein levels normalized to β-actin in cultured mouse cortical neurons (12 DIV) and astrocytes. Data are mean ± SD of three independent cultures. ***$P < 0.001$ determined by t-test.

2 Characterization of CRTC1 and CRTC2 in neurons

2.1 Expression of CRTCs in cultured cortical neurons

We next studied the expression pattern of CRTC1 and CRTC2 in cultured neurons at different stages of neuronal differentiation. Cultured mouse embryonic (E15.5) cortical and hippocampal neurons were lysed at 2, 4, 7 and 12 DIV and CRTCs protein levels were analysed by Western blotting and qRT-PCR (**Figure 14A**). CRTC1 protein levels rapidly rises at 4 DIV and then stabilize. Levels of CRTC2 increase at 2 DIV and then progressively decline. Similar results were obtained when analysing mRNA levels of *Crtc1* and *Crtc2* in cortical and hippocampal neurons (**Figure 14B**). *Crtc1* mRNAs are constant in cultured cortical neurons but decline in hippocampal neurons at 2-12 DIV ($P < 0.05$). By contrast *Crtc2* and *Crtc3* mRNAs decline constantly during differentiation of cortical and hippocampal neurons (**Figure 14B**). These results reveal that CRTCs show specific patterns of expression during neuronal differentiation.

2.2 Differential regulation of CRTC phosphorylation in neurons

CRTCs are retained in the cytosol in basal conditions, and upon cellular stimuli they are dephosphorylated and translocated to the nucleus to mediate CREB-dependent gene transcription (Saura & Cardinaux, 2017). Previous studies demonstrated that CRTC1 is dephosphorylated after neuronal stimulation with forskolin (FSK), an adenylate cyclase activator, and depolarizing concentrations of potassium chloride (KCl), which promote increase of intracellular cAMP and Ca^{2+} levels, respectively (Kovács et al., 2007; Parra-Damas, Rubió-Ferrarons, et al., 2017). Protein phosphatase (PP)2B/calcineurin is responsible for CRTC1 dephosphorylation in neurons in response to Ca^{2+} (Ch'Ng et al., 2012), but other studies suggest that dephosphorylation of CRTC1 and CRTC2 depend on different protein phosphatases as showed in rat pinealocytes (McTague et al., 2012).

Here, we examined the molecular mechanisms that regulate CRTC1 and CRTC2 dephosphorylation in cultured cortical neurons (12 DIV). We evaluated the effect of FSK, KCl or both in CRTCs phosphorylation in the presence or absence of cyclosporin A (CsA), a PP2B/calcineurin inhibitor, and okadaic acid (OkA), at doses that inhibit PP1 (Cohen et al., 1990). To investigate the phosphorylation status of CRTC1 and CRTC2, an optimized SDS-PAGE was performed to properly separate the different bands corresponding to the different phosphorylated forms of CRTCs, obtaining a fastest migrating band that corresponds to the dephosphorylated form and three (CRTC1) or two (CRTC2) slowly migrating species corresponding to different phosphorylated forms. Our results show that the percentage of the dephosphorylated CRTC1 form is not affected by FSK and/or KCl treatments (**Figure 15**). However, total levels of CRTC1 were elevated by KCl and FSK/KCl treatments ($P < 0.01$). On the contrary, the percentage of

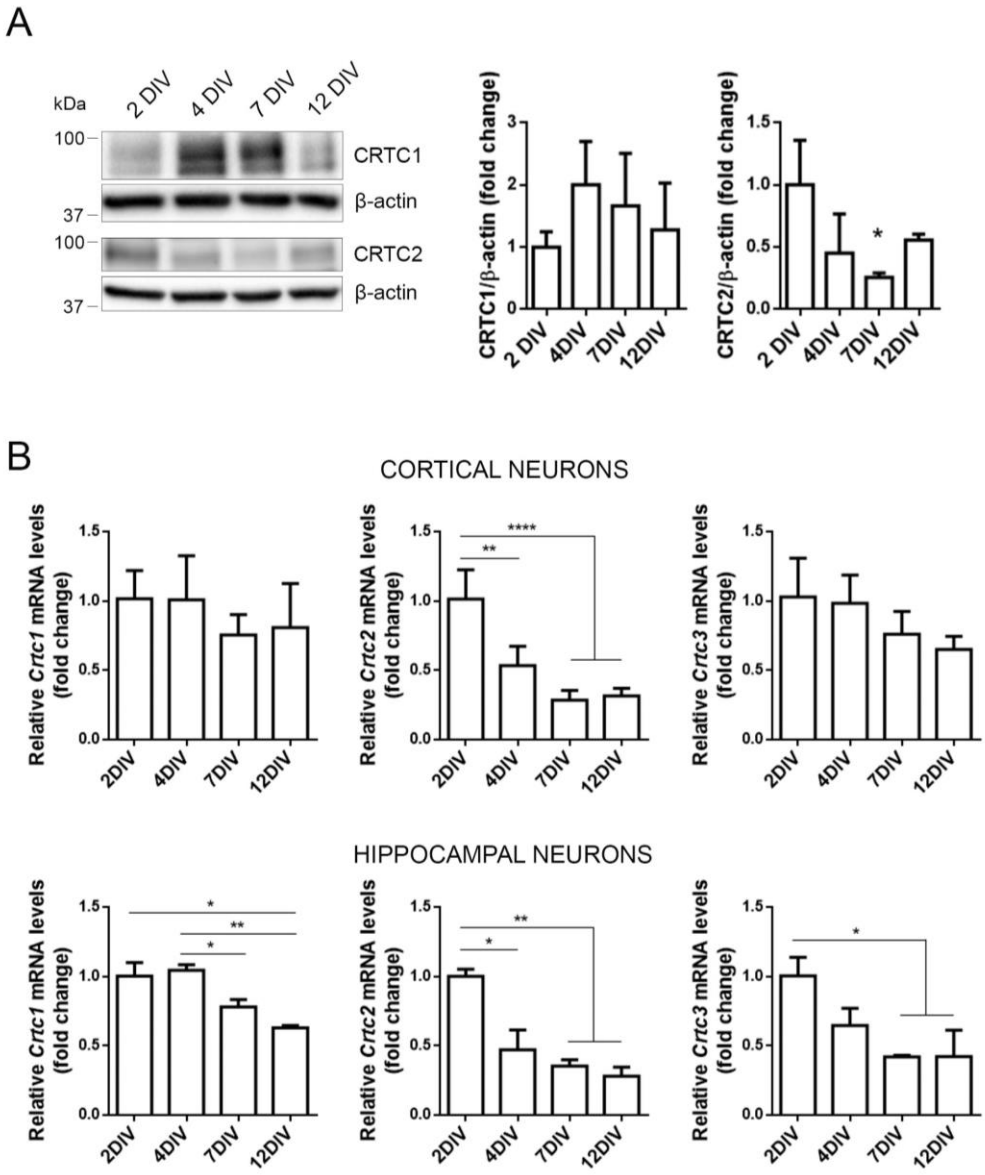

Figure 14. CRTCs expression in cultured cortical and hippocampal neurons

(A) Western blotting analysis of CRTC1 and CRTC2 normalized to β-actin in cultured mouse cortical neurons at 2, 4, 7 and 12 *days in vitro* (DIV). Data represent mean ± SD of three independent cultures. **P* < 0.05 determined by one-way ANOVA followed by Bonferroni's *post hoc* test. **(B)** Analysis of *Crtc1*, *Crtc2* and *Crtc3* mRNA levels in primary mouse cortical and hippocampal neurons at 2-12 DIV. Transcript levels were normalized to *Gapdh* levels. Data represent mean ± SD of three independent experiments. **P* < 0.05, ***P* < 0.01, *****P* < 0.0001 as determined by one-way ANOVA followed by Tukey's *post hoc* test.

dephosphorylated CRTC2 was significantly increased after treatment with FSK ($P < 0.0001$), KCl ($P < 0.001$) and FSK plus KCl ($P < 0.0001$), without changes in total CRTC2 levels (**Figure 15**). Cultured neurons were also treated with CsA or OkA prior to stimuli to inhibit PP2B and PP1, respectively. CsA application resulted in a total blockade of CRTC1 dephosphorylation in all tested conditions ($P < 0.05$ - 0.0001), whereas OkA treatment had no effect on dephosphorylated CRTC1 species (**Figure 15**). Moreover, CsA treatment, but not OkA, inhibited

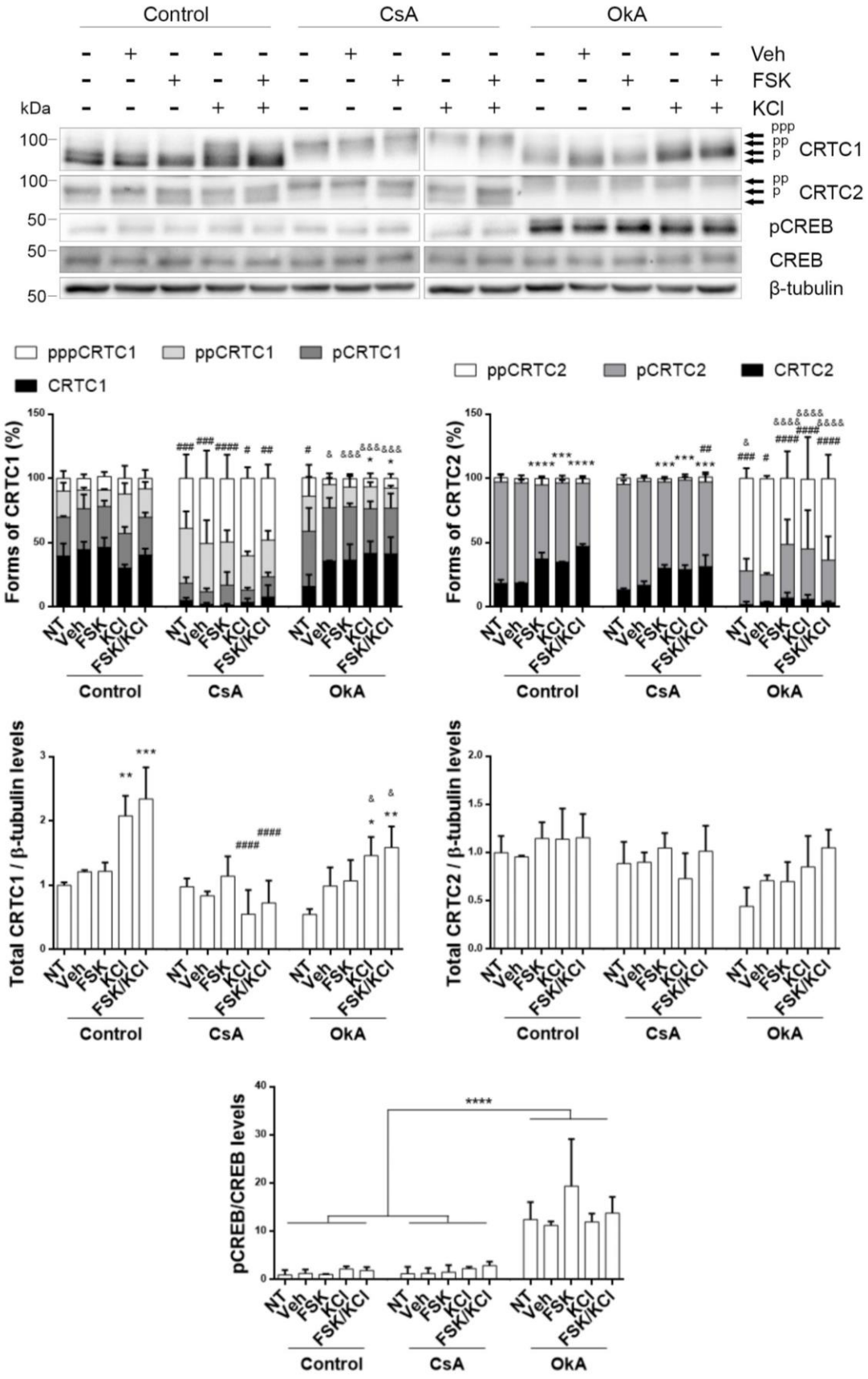
Control
CsA
OkA
Veh
FSK
KCl
kDa
100
100
50
50
50
CRTC1
CRTC2
pCREB
CREB
β-tubulin
pppCRTC1
ppCRTC1
pCRTC1
CRTC1
Forms of CRTC1 (%)
ppCRTC2
pCRTC2
CRTC2
Forms of CRTC2 (%)
NT
Veh
FSK
KCl
FSK/KCl
Control
CsA
OkA
Total CRTC1 / β-tubulin levels
Total CRTC2 / β-tubulin levels
pCREB/CREB levels

Figure 15. Activity-dependent CRTC1 and CRTC2 dephosphorylation in cultured cortical neurons

Images of Western blot analysis showing activity-dependent CRTC1 and CRTC2 dephosphorylation and CREB phosphorylation in cultured cortical neurons. 12 DIV neurons were pre-treated (15 min) with the protein phosphatase inhibitors cyclosporine A (CsA, 1 μM) or okadaic acid (OkA, 1 μM) before cultured in the absence (non-treated; NT) or presence (15 min) of vehicle (DMSO), forskolin (FSK, 20 μM), KCl (30 mM) and FSK/KCl. Unphosphorylated (black bars) and phosphorylated (p, pp, ppp; gray/white bars) CRTC1/2 forms (indicated by arrows at the right of the blot images and at the top part of the graphs). Data represent percentage of the different phosphorylated and non-phosphorylated forms of CRTC1 and CRTC2, total CRTC1 and CRTC2 protein levels and quantification of pCREB (Ser133)/CREB levels ratio. Data are mean ± SD of three independent experiments. Dephosphorylated forms of CRTCs, total CRTC levels and the ratio pCREB/CREB were analyzed by two-way ANOVA followed by Tukey's *post hoc* test. **P* < 0.05, ***P* < 0.01, ****P* < 0.001, *****P* < 0.0001. * To NT within each group; # To its control condition; & To its CsA condition; n.s: non-significant.

the increase of CRTC1 after KCl and FSK/KCl treatments. On the contrary, CRTC2 dephosphorylation was completely inhibited by OkA ($P < 0.05$ - 0.0001), whereas only partial dephosphorylation blockade was detected after CsA treatment in FSK/KCl condition ($P < 0.01$). These results demonstrate that CRTC1 dephosphorylation in neurons is dependent on PP2B, whereas CRTC2 dephosphorylation depends mainly on PP1. In addition, it seems that CRTC1 protein levels, but not CRTC2, are upregulated upon neuronal stimulation, and this increase depends on PP2B. In these experimental conditions, CREB phosphorylation (Ser133) was only enhanced by OkA in all treated conditions ($P < 0.0001$) (**Figure 15**) reinforcing the idea that CREB dephosphorylation is mainly regulated by PP1 in neurons, as previously reported in other cell types (Alberts et al., 1994; Hagiwara et al., 1992).

PP1 and PP2A can be differently inhibited by OkA, depending on its concentration. Cohen and colleagues showed that PP2A was inhibited at >1 nM of OkA, while blockade of PP1 requires doses of > 1 μM (Cohen et al., 1990). To demonstrate whether CRTC2 dephosphorylation depends on PP1 and/or PP2A, we analysed CRTCs dephosphorylation at different doses of OkA (**Figure 16**). CRTC2 dephosphorylation was not affected at low OkA doses (1-500 nM) but it was totally blocked at 1 μM OkA (compare **Figures 15 and 16**). Similarly, pCREB is increased at 500 nM OkA treatment. Dephosphorylated CRTC1 is not affected by OkA at any tested OkA concentration. These results strongly suggest that dephosphorylation of both CREB and CRTC2 depends on PP1.

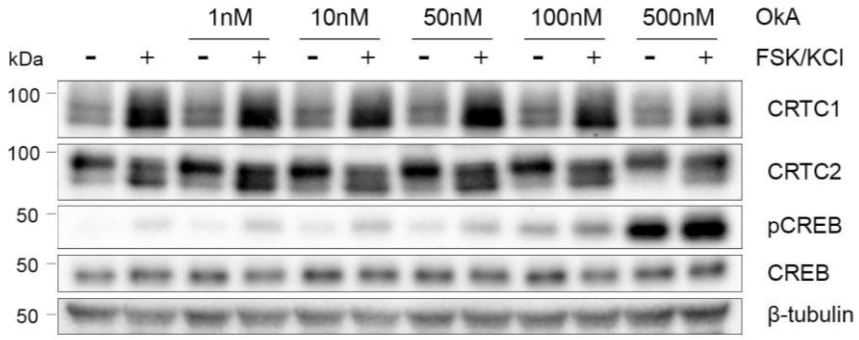

Figure 16. PP1, but not PP2A, regulates CRTC2 and CREB dephosphorylation

Western blot analysis of CRTC1 and CRTC2 dephosphorylation and CREB phosphorylation (Ser133) in cultured cortical neurons (12 DIV) treated with increased doses of okadaic acid (OkA). Cortical neurons were pre-treated with OkA for 15 min and then cultured in the presence of vehicle (DMSO) or FSK/KCl (20 µM, 30 mM) for 15 min. Low OkA doses (< 500 nM) do not affect CRTC1 nor CRTC2 dephosphorylation.

2.3 Regulation of CRTCs cytosolic-nuclear trafficking

We next studied CRTCs cytosolic-nuclear translocation in cultured cortical neurons in basal and stimulated (FSK/KCl) conditions. Subcellular fractionation was performed to obtain total, nuclear and cytosolic fractions and levels of CRTC1 and CRTC2 were analysed by Western blotting (**Figure 17A**). A significant increase of CRTC1 and CRTC2 were detected in total fractions after FSK/KCl treatment ($P < 0.01$ and 0.05, respectively), while no significant changes were observed in the cytosolic fraction. Indeed, neuronal stimulation induced an increase of CRTCs in nuclear fractions ($P < 0.05$) (**Figure 17A**). Unexpectedly, nuclear levels of CRTCs are very low compared to total or cytosolic fractions, suggesting minor CRTCs translocation to the nucleus after neuronal stimulation. CRTC1 nuclear translocation was also analysed by immunocytochemistry. Cultured hippocampal neurons were stained with CRTC1 antibody after FSK/KCl treatment and CRTC1 nuclear/cytosolic signal was quantified (**Figure 17B**). An increase of CRTC1 nuclear intensity after neuronal stimulation was detected when compared to control (basal) conditions ($P < 0.05$).

2.4 CRTC1-CREB interaction in neurons

2.4.1 Co-immunoprecipitation of CREB and CRTC1 in neurons

It has been previously proposed that CRTC2 interacts with the CREB/CBP complex to regulate gene transcription (Luo et al., 2012; Ravnskjaer et al., 2007; Screaton et al., 2004). Since we have demonstrated that CRTC1 is the main isoform found in neurons, we next examined binding of endogenous CRTC1 to CREB upon neuronal activity. Co-immunoprecipitation (CoIP) assays were performed in cortical neurons (12 DIV) in vehicle (Veh) and activity-stimulated conditions (FSK/KCl). FSK/KCl induced CRTC1 dephosphorylation and CREB phosphorylation at Ser 133 (**Figure 18**). Biochemical analysis revealed an increase of CRTC1 (~35%) in CREB

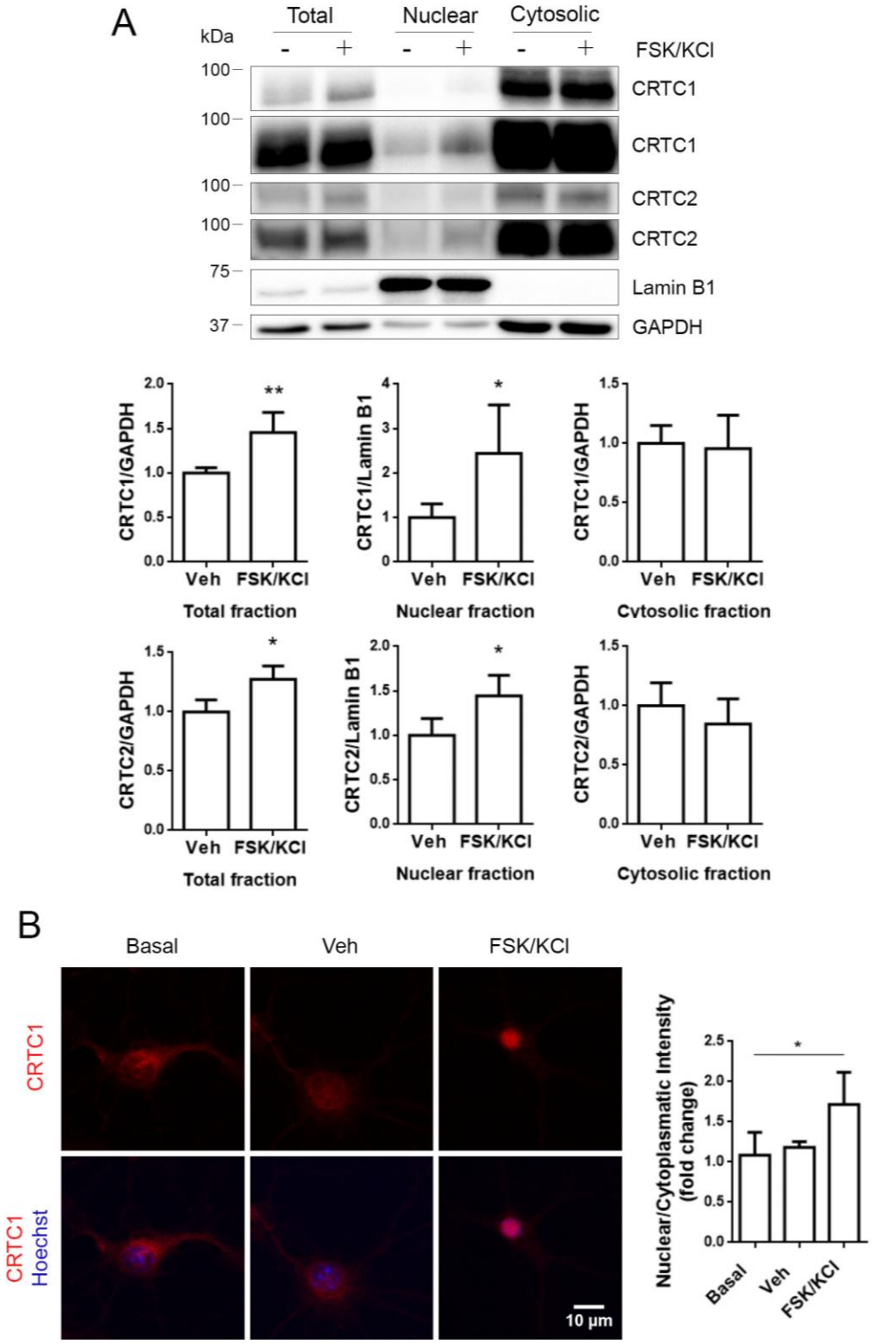

Figure 17. Activity-dependent CRTC1 and CRTC2 nuclear translocation in cultured neurons

(A) Subcellular fractionation showing two different exposures of CRTC1 and CRTC2 in total, nuclear and cytosolic fractions of cortical neurons (12 DIV) treated with FSK/KCl (20 µM, 30 mM) for 15 min. CRTCs levels were quantified and represented as mean ± SD of four independent experiments. *$P < 0.05$, **$P < 0.01$ as determined by t-test. **(B)** Immunostaining of endogenous CRTC1 in cultured hippocampal primary neurons in basal, vehicle (Veh) and FSK/KCl (20 µM, 55 mM) conditions. Representative images of neurons showing localization of CRTC1 (red) in the nucleus (Hoechst) in FSK/KCl-treated neurons. Data represent mean ± SD of nuclear/cytosolic CRTC1 intensity of several independent experiments (n=4; 30-54 neurons per condition and experiment). Statistical analysis was determined by one-way ANOVA followed by Bonferroni's *post hoc*.

immunoprecipitates in stimulated neurons compared with vehicle conditions (~15%). pCREB (50%) was also present in CRTC1 immunoprecipitates upon stimulation. These results demonstrate the presence of CRTC1/CREB complexes upon neuronal activity in cortical neurons.

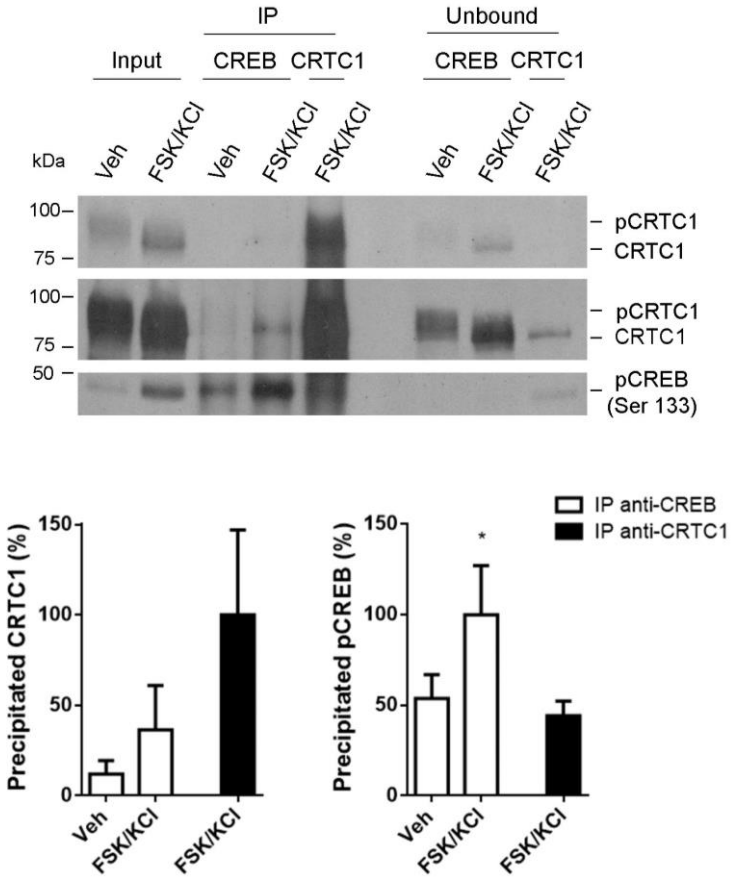

Figure 18. Activity-dependent binding of CRTC1 to CREB in primary cortical neurons

Coimmunoprecipitation experiments showing activity-dependent binding of endogenous CRTC1 to CREB in cultured cortical neurons (12 DIV). Representative immunoblots of CRTC1 (two different exposures) and pCREB in the lysate (input), immunoprecipitated (IP) and unbound fractions. Endogenous CRTC1 is immunoprecipitated with an anti-CREB antibody, and pCREB is efficiently immunoprecipitated with the anti-CRTC1 antibody in neurons treated with FSK/KCl (20 µM; 55 mM). The graphs represent the percentage of immunoprecipitated CRTC1 and pCREB normalized to the maximum immunoprecipitation with their specific antibodies in FSK/KCl conditions, which is considered 100%. Data represent percentage of immunoprecipitation ± SEM of four independent experiments. *$P < 0.05$ by one-tailed t-test.

2.4.2 CREB/CRTC1 interaction detected by Fluorescence Resonance Energy Transfer (FRET)

We also examined CRTC1/CREB interaction by FRET, using the acceptor photobleaching technique. To study CRTC1/CREB interaction in cultured neurons, we first set up the experimental conditions for the protein labelling. CREB primary antibody was conjugated to Alexa Fluor 488, while CRTC1 primary antibody was conjugated to Alexa Fluor 568. For the antibody conjugation different molar ratios (1:3 and 1:6) of antibody:fluorophore were analysed by immunocytochemistry (**Figure 19A**). CREB and CRTC1 antibodies were conjugated with

fluorophores and then diluted 1:250 and 1:55 respectively for sample incubation. Compared to 1:6 antibody:fluorophore molar ratio, the 1:3 molar ratio was barely detected (**Figure 19A**), so all antibody conjugations were performed with 1:6 molar ratio.

We next set up the donor:acceptor (D:A) ratio. For FRET, it is important to have more acceptor than donor fluorophores since one donor is able to excite different acceptors and if donor:acceptor ratio is higher, acceptor fluorophores can be bleached by emission of all donors. Thus, a donor:acceptor ratio at 1:4 or below (usually 1:8) would maximize $FRET_{eff}$ (Snapp & Hegde, 2006). For this study, two different donor:acceptor ratios were tested in a positive control, consisting of CREB primary antibody (diluted 1:250) conjugated with Alexa Fluor 488 and recognized with an anti-rabbit secondary antibody conjugated with Alexa Fluor 568 (diluted 1:370 or 1:600) representing D:A ratios of 1:8 or 1:5 respectively (**Figure 19B**). Since there is a physical interaction between the CREB primary antibody and the rabbit secondary antibody, the expected $FRET_{eff}$ should be the maximum. As a negative control we used CREB primary antibody conjugated with Alexa Fluor 488 (1:250) as donor, and a primary mouse antibody (1:50) against NeuN, a nuclear protein that does not interact with CREB, that is recognized by an anti-mouse secondary antibody Alexa Fluor 568 (1:370) to obtain a 1:8 D:A ratio. Indeed, $FRET_{eff}$ for the negative control is minimum (-1.13% ± 4.83). For the positive control a 1:8 D:A ratio yield a $FRET_{eff}$ of 22.52% ± 1.53 (mean ± SEM), whereas for 1:5 D:A ratio $FRET_{eff}$ was 21.71 ± 2.31 (**Figure 19B**). The $FRET_{eff}$ values for the positive controls were very similar, so we next proceed with the 1:8 D:A ratio to favour $FRET_{eff}$.

To examine how endogenous CREB-CRTC1 interaction is affected by neuronal activity, cultured hippocampal neurons were treated with vehicle (control) or stimulated with FSK/KCl for 5 or 15 min to mimic neuronal activity. Neurons were stained with anti-CREB antibody conjugated with Alexa Fluor 488 (1:250; donor) and anti-CRTC1 antibody conjugated with Alexa Fluor 568, (1:55; acceptor). The resulting conditions were 1:8 D:A ratio. For FRET positive control, FSK/KCl-treated hippocampal neurons (15 min) were stained with the primary rabbit antibody anti-CREB conjugated with Alexa Fluor 488 (1:250) and an anti-rabbit secondary Alexa Fluor 568 antibody; 1:370). Two different FRET negative controls were used: 1) the NeuN negative control, which consisted of the primary antibody anti-CREB (1:250) conjugated with Alexa Fluor 488 and anti-NeuN (1:50) labelled by a secondary anti-mouse Alexa Fluor 568 antibody; 2) the only donor negative control, which consisted on the primary antibody anti-CREB (1:250) conjugated with Alexa Fluor 488 without any acceptor molecule (**Figure 19C**). It should be noticed that determining good positive and negative FRET controls is important because they would define the limits of the experimental $FRET_{eff}$ values. For this experiment, 60 regions of interest (ROIs) per condition corresponding to three coverslips (20 ROIs per coverslip) were

analysed. $FRET_{eff}$ was calculated as the mean of the median of each coverslip (mean ± SEM). As expected, positive control $FRET_{eff}$ was high, reaching a 26.30% ± 0.64, whereas the NeuN negative control $FRET_{eff}$ was very low, 0.54% ± 2.37. The only donor negative control $FRET_{eff}$ could not be calculated since no pixel reached to the established threshold. Interestingly, the $FRET_{eff}$ of the tested conditions was 1.38% ± 0.2 for vehicle, and 3.64% ± 0.58 and 4.46% ± 1.39 for 5 and 15 min FSK/KCl treatment, respectively (**Figure 19D**). These results suggest increased interaction of endogenous CRTC1 and CREB upon neuronal activity.

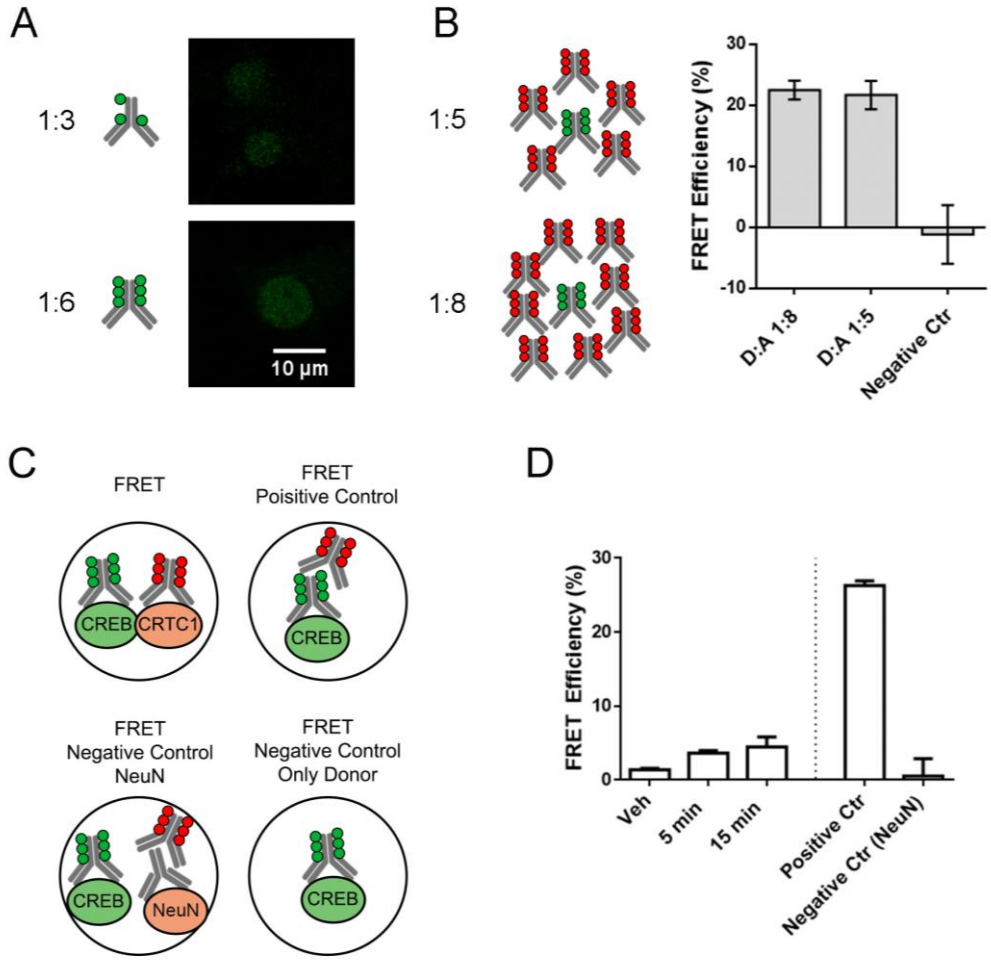

Figure 19. Activity-dependent CRTC1 binding to CREB in cultured hippocampal neurons assayed by FRET

(**A) Left:** Scheme of a primary antibody to fluorophore conjugation with molar ratio of 1:3 and 1:6. **Right:** representative immunocytochemistry images of cultured hippocampal neurons stained with anti-CREB antibody conjugated with 1:3 and 1:6 molar ratio with Alexa Fluor 488 fluorophore. **(B) Left:** schematic representation of the donor:acceptor (D:A) fluorophore ratios 1:5 and 1:8. **Right:** Percentage of FRET efficiencies corresponding to positive control (D:A ratio of 1:8 and 1:5) and a negative control (D:A ratio of 1:8). Data are mean ± SEM of 2-4 regions of interest (ROIs) per condition. **(C)** Scheme of immunocytochemistry conditions used for FRET analysis of CREB/CRTC1 interaction including positive and negative controls. **(D)** Percentage of FRET efficiencies obtained for CRTC1 and CREB binding in cultured hippocampal neurons. Graph represents data from the positive control, NeuN negative control and treated neurons with vehicle (Veh) or FSK/KCl (20 µM; 55 mM) for 5 min or 15 min. Data represent mean of medians of each coverslip ± SEM, which correspond to analysis of 60 ROIs from 3 coverslips per condition (20-21 ROIs per coverslip) from one independent experiment.

2.5 CRTCs-CREB dependent gene transcription in cortical neurons

To determine the roles of CRTC1 and CRTC2 in CREB-mediated transcription in neurons, *Crtc2* f/f cultured cortical neurons were transduced with lentiviral vectors containing Cre-recombinase (Cre), the inactive Cre-recombinase (ΔCre), short hairpin CRTC1 (shCRTC1) or scramble (Scr) in order to inactivate endogenous *Crtc2* and/or *Crtc1*. Western blot and qRT-PCR analyses were performed to corroborate that lentiviral vectors efficiently reduced CRTC1 and CRTC2 protein and mRNA levels (**Figure 20A**). Western blot analysis revealed a specific reduction of CRTC1 by shCRTC1 and ablation of CRTC2 in Cre-recombinase transduced neurons (**Figure 20A**). Supporting this data, qRT-PCR analysis demonstrated the expected reduction of *Crtc1* ($P < 0.01$) and *Crtc2* ($P < 0.05$) transcripts in neurons transduced with shCRTC1 and Cre lentiviral vectors, respectively (**Figure 20A**).

To study the global effects of CRTC1 and CRTC2 in CREB-mediated transcription, a CRE-luciferase assay was used performing similar experimental conditions but, in this case, neurons were treated with FSK/KCl for 4 h. Neuronal stimulation induced an increase of CREB transcriptional activity in cortical neurons ($P < 0.0001$), which was reduced in shCRTC1-transduced neurons (~75%; $P < 0.001$) but not by *Crtc2* inactivation ($P > 0.05$) (**Figure 20B**). When both CRTCs were inactivated, no additional effects were detected on CREB transcriptional activity compared to shCRTC1-treated neurons (**Figure 20B**). These results indicate that CRTC1 plays a more relevant role in activity-dependent CREB-mediated gene transcription in neurons. Next, we analysed transcript levels of specific CRTC-dependent CREB target genes after treating neurons with FSK/KCl (4 h). Upon neuronal activity, there was an increase in the mRNA levels of the CREB target genes *Nr4a2* (~16 fold) and *c-fos* (~27 fold) (**Figure 20C**). After *Crtc1* silencing, *Nr4a2* presented a significant reduction (~55%; $P < 0.001$) although no effect was detected in *c-fos* levels. By contrast, *Crtc2* deletion had no significant effects on *Nr4a2* and *c-fos* levels ($P > 0.05$) (**Figure 20C**). Moreover, inactivation of both CRTCs had no additional effects on the transcription of these genes than those observed with *Crtc1* silencing.

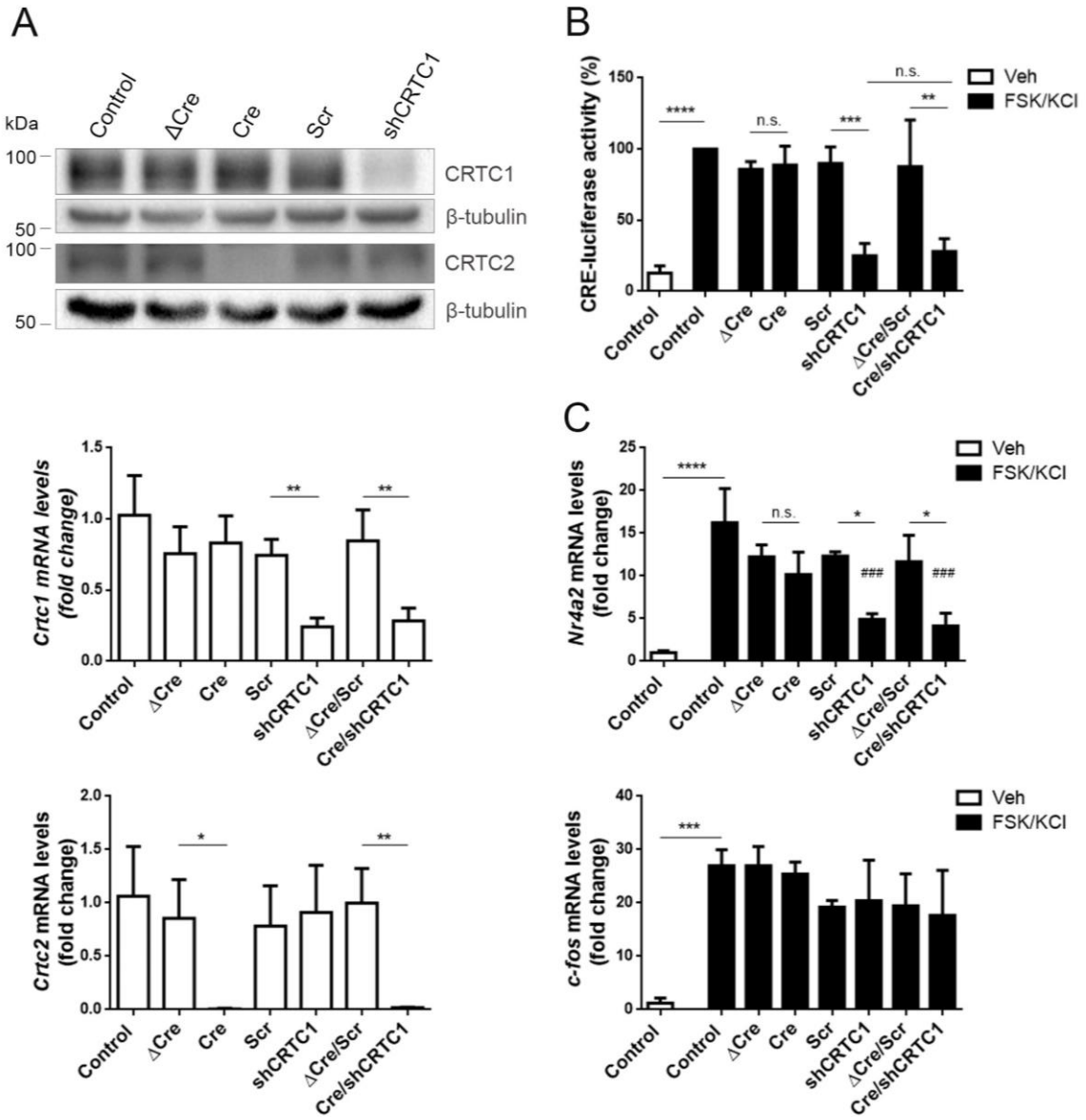

Figure 20. Activity-dependent CRTC1- and CRTC2-mediated CREB transcription in cultured cortical neurons

(A) Western blot (**top**) and qRT-PCR (**bottom**) analysis showing lentiviral-mediated CRTC1 and CRTC2 inactivation in *Crtc2* floxed/floxed (f/f) cultured neurons. Cultured cortical neurons (12 DIV) were non-transduced (control) or transduced with lentiviral vectors containing Cre-recombinase (Cre), a non-active Cre-recombinase mutant (ΔCre), scramble (Scr) or *Crtc1* shRNAs (shCRTC1). Data represent mean ± SD of three independent experiments. *$P < 0.05$, **$P < 0.01$ as determined by one-way ANOVA followed by Tukey's *post hoc* test. **(B)** CREB transcriptional activity analysis in *Crtc2* f/f cortical neurons. Neurons (4 DIV) were non-transduced (control) or transduced with single or combined lentiviral vectors containing ΔCre, Cre, Scr or shCRTC1 and treated at 9 DIV with vehicle (Veh) or FSK/KCl (20 µM; 30 mM) for 4h before analysing the CRE-promoter luciferase activity. Data represent mean ± SD of three independent experiments. **$P < 0.01$, ***$P < 0.001$, ****$P < 0.0001$ as determined by one-way ANOVA followed by Tukey's *post hoc* test. **(C)** *Nr4a2* and *c-fos* mRNA levels after viral-mediated CRTC1 and CRTC2 inactivation in *Crtc2* f/f cultured neurons. Neurons (12 DIV) were non-transduced (control) or transduced with single or combined lentiviral vectors containing ΔCre, Cre, Scr or shCRTC1 and treated with vehicle (Veh) or FSK/KCl (20 µM; 30 mM) for 4h. mRNA levels were quantified by real-time qPCR and normalized to geometric mean of *Ppia, Hprt1* and *Gapdh* genes. Data represent mean ± SD of three independent experiments *$P < 0.05$, **$P < 0.01$, ***$P < 0.001$, ****$P < 0.0001$; # vs. FSK/KCl control as determined by one-way ANOVA followed by Tukey's *post hoc* test.

2.6 Generation and characterization of *Crtc2* cKO mice

To investigate the biological role of neuronal CRTC2 in the adult brain, we generated novel neuron-specific *Crtc2* cKO mice. As described in the results section 1.1, *Crtc2* f/f mutant mice containing two loxP sequences flanking *Crtc2* exon 4 were crossed with CamKIIα-Cre-recombinase transgenic mice to obtain *Crtc2* f/f;CamKII*α*-Cre-recombinase (*Crtc2* cKO) mice lacking *Crtc2* in postmitotic neurons (**Figure 11B**). In *Crtc2* cKO mice, Cre-recombinase expression is under the *CamKIIα* promoter, which is highly expressed in postmitotic neurons during the third postnatal week resulting in neuron-specific *Crtc2* deletion (Yu et al., 2001). We first analysed *Crtc2* mRNA levels in the hippocampus of *Crtc2* f/f (control) and *Crtc2* cKO mice at postnatal days (P)15 and P21, and 4 and 9 months of age (**Figure 21**). *Crtc2* mRNA levels were significantly reduced at P21-9 months in *Crtc2* cKO mice, whereas *Crtc1* and *Crtc3* mRNA levels were similar in both groups at all ages. As control, *Crtc2* mRNA levels were also analysed in liver homogenates of 4 month-old *Crtc2* cKO mice. In agreement with lack of recombination in non-neuronal cells, no significant differences in *Crtc2* mRNAs were detected in the liver of control and *Crtc2* cKO mice (**Figure 21**).

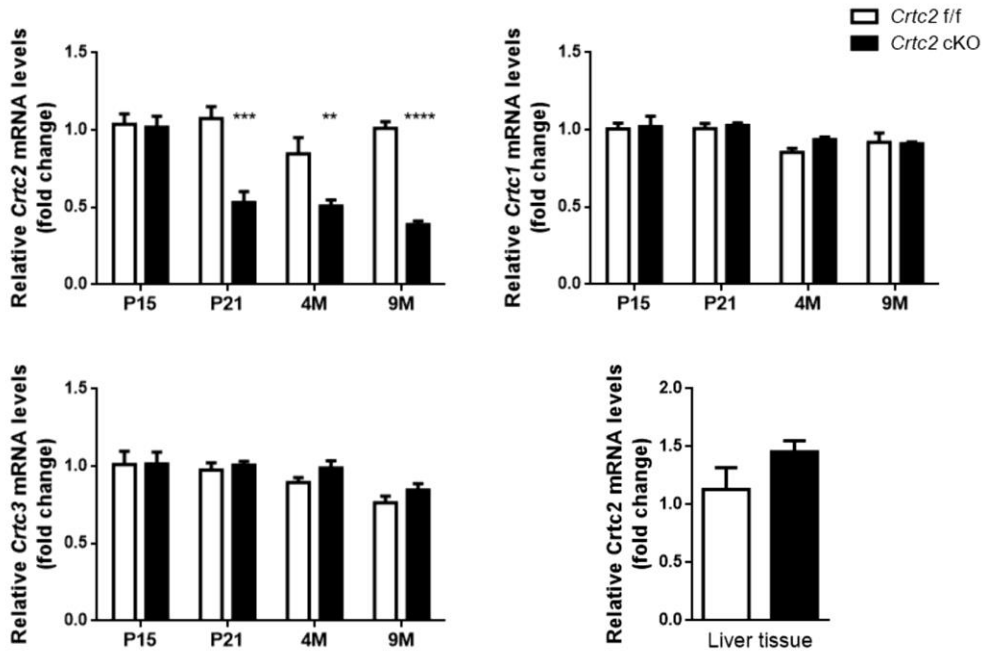

Figure 21. Expression of *Crtcs* in the hippocampus of *Crtc2* cKO mice

Crtc1, Crtc2 and *Crtc3* mRNA levels in hippocampal lysates from *Crtc2* f/f (control) and *Crtc2* cKO mice at different ages: postnatal (P) days 15, 21, 4 months (M) and 9 M. *Crtc2* mRNA levels in liver of *Crtc2* f/f and *Crtc2* cKO mice at 4 months. mRNA levels were quantified by real-time qPCR and normalized to the geometric mean of *Hprt1* and *Gapdh.* Data represent mean ± SEM of 3-6 mice per group. Statistical analysis was determined by two-way ANOVA followed by Sidak's *post hoc* test or by t-test for the liver samples. ***P* < 0.01, ****P* < 0.001, *****P* < 0.0001.

To validate the inactivation of CRTC2 at protein level, hippocampal lysates of *Crtc2* cKO mice were biochemically analysed at different ages. CRTC2 levels were similar in hippocampal lysates of control (*Crtc2* f/f) and *Crtc2* cKO mice at P15, but a significant CRTC2 decrease was found in *Crtc2* cKO mice at P21 and 4 and 9 months (**Figure 22A**). Notably, the maximum reduction of CRTC2 corresponded to a ~50% ($P < 0.0001$) in *Crtc2* cKO mice at 4-9 months, which reinforces the idea that CRTC2 is also expressed in non-neuronal cells in the hippocampus (**Figure 12B and 13**). As a control, we also analysed expression of CRTC1. In this case, no differences in CRTC1 levels were observed in *Crtc2* cKO mice among the different analysed ages (**Figure 22A**).

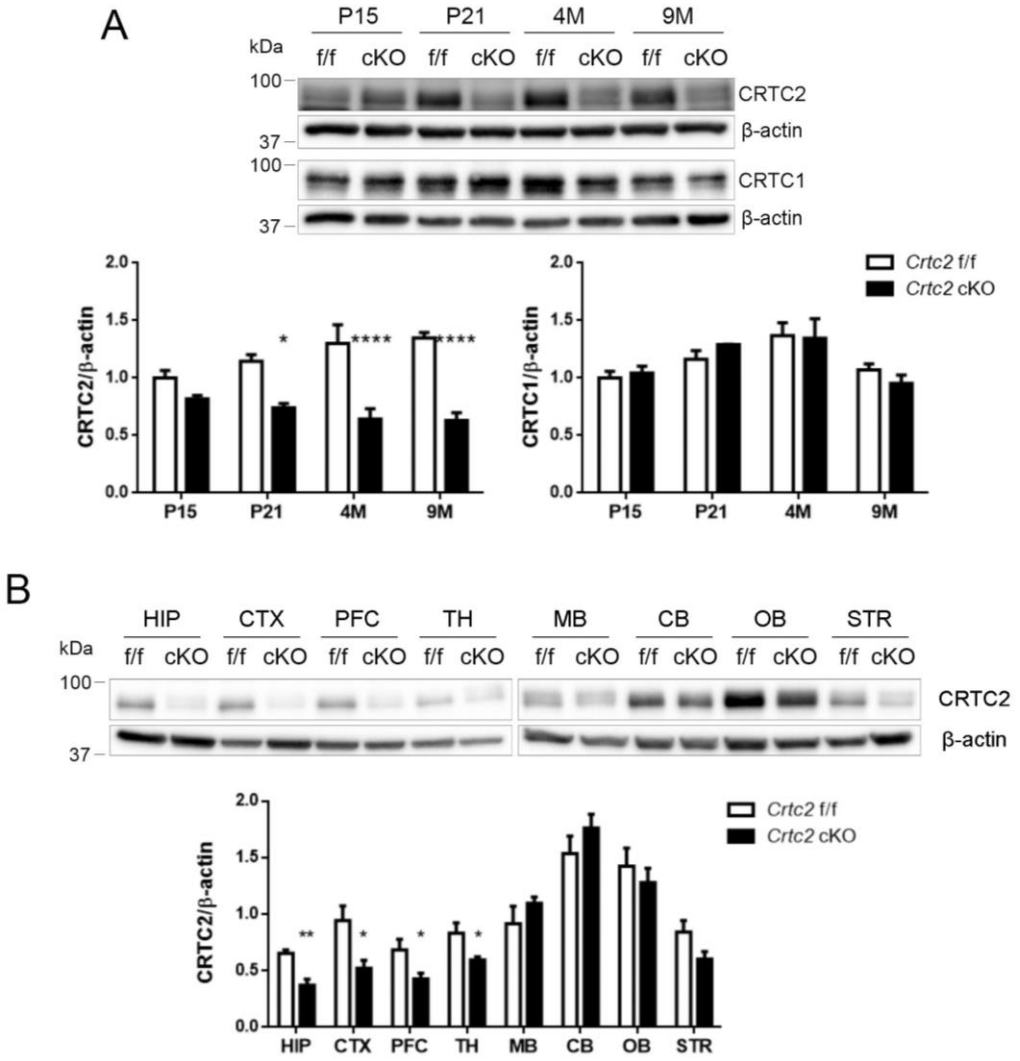

Figure 22. Expression of CRTC1 and CRTC2 in the brain of *Crtc2* cKO mice

(A) Western blot analysis showing CRTC1 and CRTC2 protein levels in hippocampal lysates of *Crtc2* f/f and *Crtc2* cKO mice at postnatal (P) days 15, 21, 4 months (M) and 9 M. Data represent mean ± SEM of 3-6 mice per group. Protein levels were analyzed by two-way ANOVA followed by Sidak's *post hoc* test. *$P < 0.05$, ****$P < 0.0001$. **(B)** Western blot analysis of brains of 4 M-old *Crtc2* f/f and *Crtc2* cKO mice showing CRTC2 protein levels in hippocampus (HIP), total cortex (CTX), prefrontal cortex (PFC), thalamus (TH), midbrain (MB), cerebellum (CB), olfactory bulb (OB) and striatum (STR). Data represent mean ± SEM (n= 5 mice per group). Statistical analysis performed by t-test comparing *Crtc2* f/f vs. *Crtc2* cKO within each brain region. *$P < 0.05$, **$P < 0.01$.

To investigate the brain regions in which CRTC2 is inactivated, we next analysed CRTC2 levels in different brain regions of *Crtc2* cKO mice at 4 months. CRTC2 protein levels were significantly reduced in the hippocampus, cortex, prefrontal cortex and thalamus of *Crtc2* cKO mice. By contrast, CRTC2 protein levels were unchanged in midbrain, cerebellum, olfactory bulb and striatum of *Crtc2* cKO mice (**Figure 22B**). The brain regions with no reduction of CRTC2 strongly correlate with the results of Yu et al., 2001 and Tsien et al., 1996, which reported no major CamKIIα expression in the cerebellum and striatum. These results suggest that CRTC2 is expressed in neurons from hippocampus, cortex and thalamus, whereas ~ 50% of CRTC2 is expressed in non-expressing CamKIIα cells in these regions.

We next analysed transcript levels of well-established CREB target genes, including *Bdnf*, *c-fos*, *Nr4a1* and *Nr4a2* since these genes are regulated by CRTC1 and/or CRTC2 in different cell types (Eberhard et al., 2013; Parra-Damas, Rubió-Ferrarons, et al., 2017; Rodón et al., 2019). qRT-PCR analysis revealed no significant differences of *Bdnf*, *c-fos*, *Nr4a1* and *Nr4a2* levels in hippocampal homogenates of control (*Crtc2* f/f) and *Crtc2* cKO mice from P15 to 4 months (**Figure 23**). These results suggest a minor role of CRTC2 on the transcription of these neuronal CREB target genes.

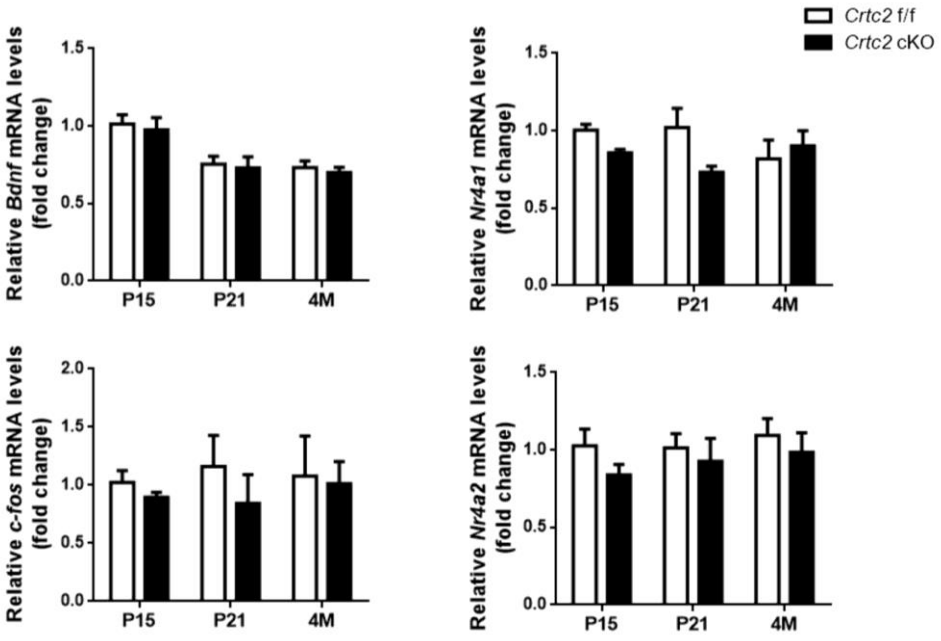

Figure 23. Levels of CREB-target genes in *Crtc2* cKO mice

Bdnf, *Nr4a1, Nr4a2* and *c-fos* mRNA levels in the hippocampus of *Crtc2* f/f and *Crtc2* cKO mice at postnatal (P) days 15, 21 and 4 months (M). All mRNA levels were quantified by real-time qPCR and normalized to the geometric mean of *Hprt1* and *Gapdh* genes. Data represent mean ± SEM of 3-6 mice per group. Statistical analysis was determined by two-way ANOVA followed by Sidak's *post hoc* test.

2.7 Behavioural characterization of *Crtc2* cKO mice

For the behavioural characterization of the *Crtc2* cKO mice a battery of different behavioural tests were performed, starting with general behavioural assays and then performing specific memory tasks. Two different animal groups at 12 months of age were evaluated: males and females. First, male mice were evaluated in a longitudinal study analyzing: 1) observational parameters, 2) Morris Water Maze (MWM) spatial memory, and 3) contextual fear conditioning memory. Then, 12 months-old female mice were evaluated in the MWM and contextual fear conditioning tests.

General behaviour state of 12 month-old male mice were analysed by studying observational parameters mimicking the diagnostic process of general examination in humans (summarized in **Table 8**) (Hatcher et al., 2001). In the majority of the parameters analysed, no significant differences were observed between control *Crtc2* f/f and *Crtc2* cKO mice (**Table 9**). One exception was tremor, in which three out of five *Crtc2* cKO mice showed tremor behaviour compared with six non-trembling *Crtc2* f/f mice. However, when integrating all the different parameters to obtain a general score for evaluating the mice condition, no significant differences were observed. These results indicate no general phenotypic changes in *Crtc2* cKO male mice at 12 months of age.

Next, we analysed spatial reference memory of the same experimental groups in the MWM. Mice were trained (acquisition, ACQ) for 5 days (4 trials each day) and memory retention was studied 2 h after the last training (short-term memory) and 24 h post-training (long-term memory). Results revealed no significant decrease in latencies to find the platform for any group during the acquisition period (**Figure 24A**). Furthermore, when analysing time spent in target quadrant (TG) and opposite quadrant (OP) during the probe trial at 2 h and 24 h after ACQ, no significant differences were observed in any group (**Figure 24B**). We also performed the MWM test in 12 month-old females increasing the number of acquisition days to 8 and the number of trials per day to 6. The results show significant reduction of latencies to find the platform during ACQ indicating that mice learned the task (time effect $P < 0.0001$) (**Figure 24C**). Moreover, probe tests performed at 2 h and 24 h post-acquisition revealed a preference for the TG compared to OP in both groups. However, a significant difference of time spent in TG compared to OP was detected only in the *Crtc2* f/f group at 2 h ($P < 0.05$; **Figure 24D**). In conclusion, female *Crtc2* cKO mice show similar spatial learning and memory than control mice.

Table 9: Scores obtained from the observational parameters

Parameter	Range	*Crtc2* f/f		*Crtc2* cKO		*P* value
		Mean	SD	Mean	SD	
Body Position	0-5	5	0	4,8	0,45	0.3
Spontaneous Activity	0-3	2	0	2	0	n.c.
Tremor	0-2	0	0	0,6	0,55	* 0.02
Urination	0-1	0,17	0,41	0	0	0.39
Defaecation	n	0,5	0,84	1	2,24	0.62
Piloerection	0-1	0	0	0,2	0,45	0.3
Gait	0-3	2,83	0,41	3	0	0.39
Injury	n	0	0	0	0	n.c.
Righting Reflex	0-3	2,3	0,52	2,6	0,55	0.43
Body Tone	0-2	0,5	0,55	0,6	0,89	0.82
Pinna Reflex	0-2	1,67	0,52	1	1	0.19
Fur	0-2	2	0	2	0	n.c.
Whiskers	0-1	0,67	0,52	0,8	0,45	0.66
Lacrimation	0-1	0	0	0	0	n.c.
Tail Elevation	0-2	1	0	1,2	0,45	0.23
Skin Colour	0-2	2	0	1,8	0,45	0.23
Hump	0-1	0	0	0	0	n.c.
Right eye opening	0-2	2	0	2	0	n.c.
Left eye opening	0-2	2	0	2	0	n.c.
Weight	g	51,63	3,73	49,94	4,73	0.52
Total		22,33	2,42	20,6	1,95	0.23

n.c. = no calculated; *Crtc2* f/f n=6; *Crtc2* cKO n=5

Contextual memory was also analysed in the same groups of 12 month-old males and females (España et al., 2010). Results of male (**Figure 24E**) and female (**Figure 24F**) mice show increase in freezing responses at 2 and 24 h, and 7 and 30 days after the training session although no significant differences were found between *Crtc2* f/f and *Crtc2* cKO mice. Altogether, these results suggest that CRTC2 in neurons of the brain does not globally affect spatial and contextual memories in adult mice.

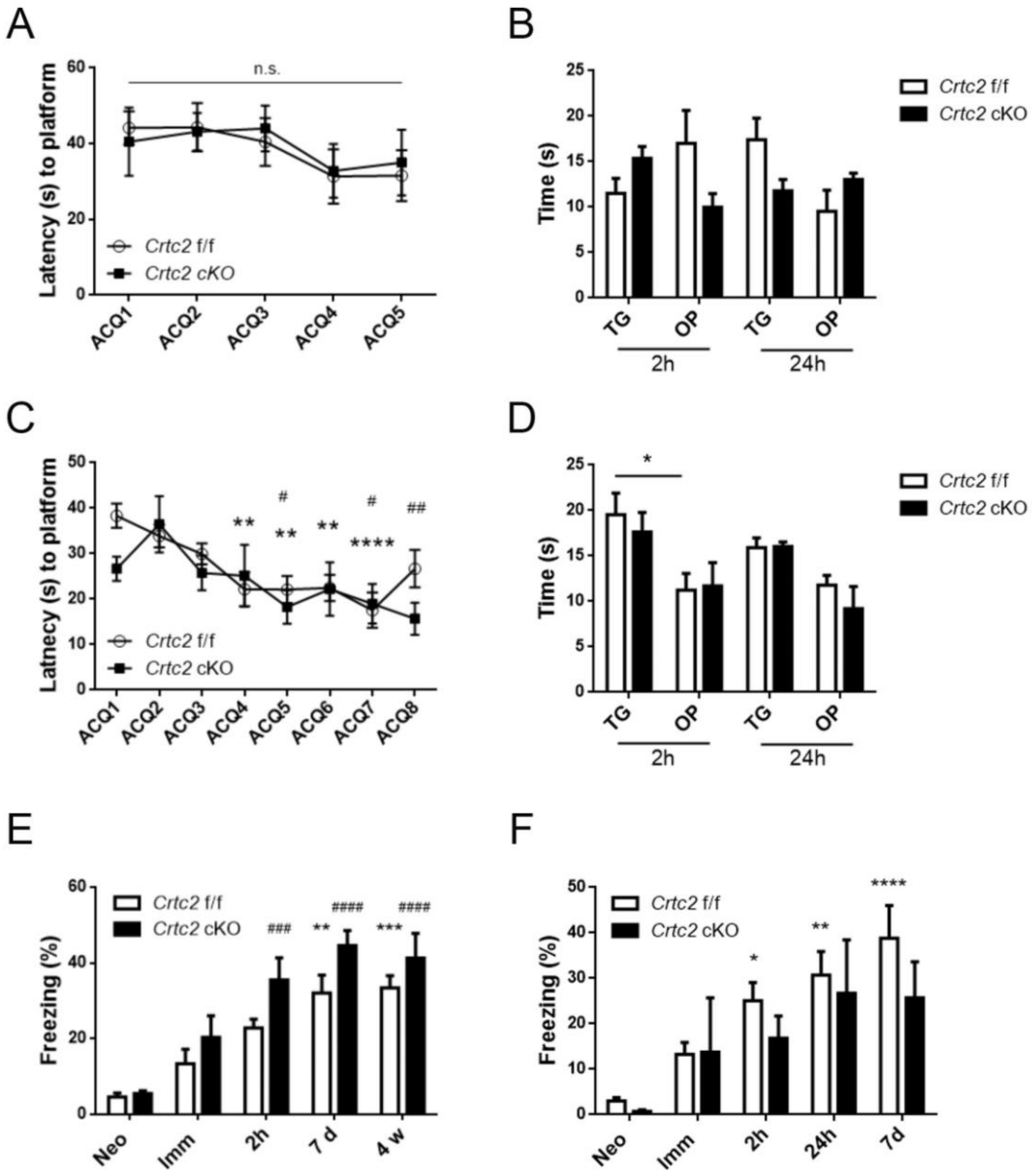

Figure 24. Behavioural characterization of memory in *Crtc2* cKO mice

(A,C) Latencies to platform during the different days of acquisition (ACQ) in the Morris water maze (MWM) test performed in 12 month-old *Crtc2* f/f and cKO male (**A**) and female (**C**) mice. Data represent mean ± SEM of n=5-6 (**A**) and n= 4-7 (**C**) mice per group. Statistical analysis was determined by two-way ANOVA followed by Tukey's *post hoc* test. **P*< 0.05 ***P*< 0.01, *****P*< 0.0001; n.s: non-significant. * represents ACQ1 vs. other ACQs in the *Crtc2* f/f group; # represents ACQ2 vs. other ACQs in the *Crtc2* cKO group. **(B)(D)** Time spent in the target (TG) and opposite (OP) quadrants in the probe trial of the MWM at 2 h and 24 h after training performed in 12 months-old *Crtc2* f/f and cKO male (**B**) and female (**D**) mice. Data represent mean ± SEM of n=5-6 (**B**) and n= 4-7 (**D**) mice per group. Statistical analysis was determined by two-way ANOVA followed by Sidak's *post hoc* test. **P*< 0.05. **(E,F)** Percentage of freezing time of *Crtc2* f/f and *Crtc2* cKO in the contextual fear conditioning (CFC) test in 12 month-old male (**E**) and female (**F**) mice. Freezing was analyzed during neophobia (neo) and after the foot shock immediately (imm) or 2h, 24h, 7 days (d) and 4 weeks (w) after conditioning. Data represent mean ± SEM of n=5-6 males (**E**) or n=4-7 females (**F**). * means significant *vs* Neo in *Crtc2* f/f group; # means significant *vs* Neo in *Crtc2* cKO group. **P* < 0.05, ** *P* < 0.01, *** *P* < 0.001, **** *P* < 0.0001. Statistical analyses were determined by two-way ANOVA followed by Sidak's *post hoc* test.

3 Characterization of CRTC1 and CRTC2 in astrocytes

3.1 Regulation of CRTCs phosphorylation in astrocytes

Our previous studies revealed that CRTC1 and CRTC2 are differentially expressed in astrocytes of the cerebral cortex (**Figure 13**). To determine the molecular mechanisms that regulate CRTC1 and CRTC2 in cortical astrocytes, we evaluated the effects of FSK and NE in CRTCs phosphorylation in the absence or presence of CsA and OkA at doses that inhibit PP2B and PP1, respectively (Cohen et al., 1990). Optimized SDS-PAGE gels revealed two major bands corresponding to phosphorylated and dephosphorylated CRTC1 and CRTC2 forms in cortical astrocytes (**Figure 25, top**). Compared to vehicle or FSK, NE significantly increases the percentage of dephosphorylated CRTC1 ($P < 0.05$) (**Figure 25**). CRTC2 dephosphorylation was also induced by FSK and NE, but the increase in the percentage of dephosphorylated CRTC2 was not significant ($P > 0.05$). Compared to neurons, total CRTC1 and CRTC2 protein levels are not affected by FSK or NE. Interestingly, inhibition of PP2B/CaN with CsA significantly reduced CRTC1 dephosphorylation ($P < 0.01$), whereas PP1 inhibition with OkA did not affect CRTC1 dephosphorylation (**Figure 25**). By contrast, dephosphorylated CRTC2 levels, were not affected by inhibition of PP1 nor PP2B. In cultured astrocytes, CREB phosphorylation was enhanced by NE and/or OkA treatment, indicating that PP1 is the main phosphatase responsible for CREB dephosphorylation in astrocytes (**Figure 25**).

These results suggest that activity-induced CRTC1 dephosphorylation is mainly mediated by PP2B in astrocytes, but CRTC2 dephosphorylation is independent of PP1 and PP2B.

3.2 CRTCs cytosolic-nuclear translocation

We next studied CRTC1/2 cytosolic-nuclear translocation in astrocytes. Subcellular fractionation was performed to obtain total, nuclear and cytosolic fractions (**Figure 26A**). As expected, CRTC1 and CRTC2 were dephosphorylated after NE treatment in all fractions (**Figure 26A**). An increase in nuclear CRTC1 and CRTC2 are detected after NE treatment although, it is only significant for CRTC2 ($P < 0.05$). CRTC1 and CRTC2 in the cytosolic fractions were slightly reduced after NE treatment. Surprisingly, nuclear levels of CRTC1 and CRTC2 are very low compared to cytosolic and total fractions, indicating a very low percentage of CRTC translocation into the nucleus.

Immunocytochemistry analyses were also performed to confirm the above results. Cultured cortical astrocytes were transfected with a pcDNA3-FLAG-TORC2 plasmid to overexpress FLAG-CRTC2 (Screaton et al., 2004) and then were incubated with vehicle or NE and stained with an anti-FLAG antibody (**Figure 26B**). Images were quantified analysing the CRTC2-Flag nuclear/cytosolic intensity ratio (**Figure 26B**). Quantification analysis indicates an increase of CRTC2 in the nucleus after NE treatment.

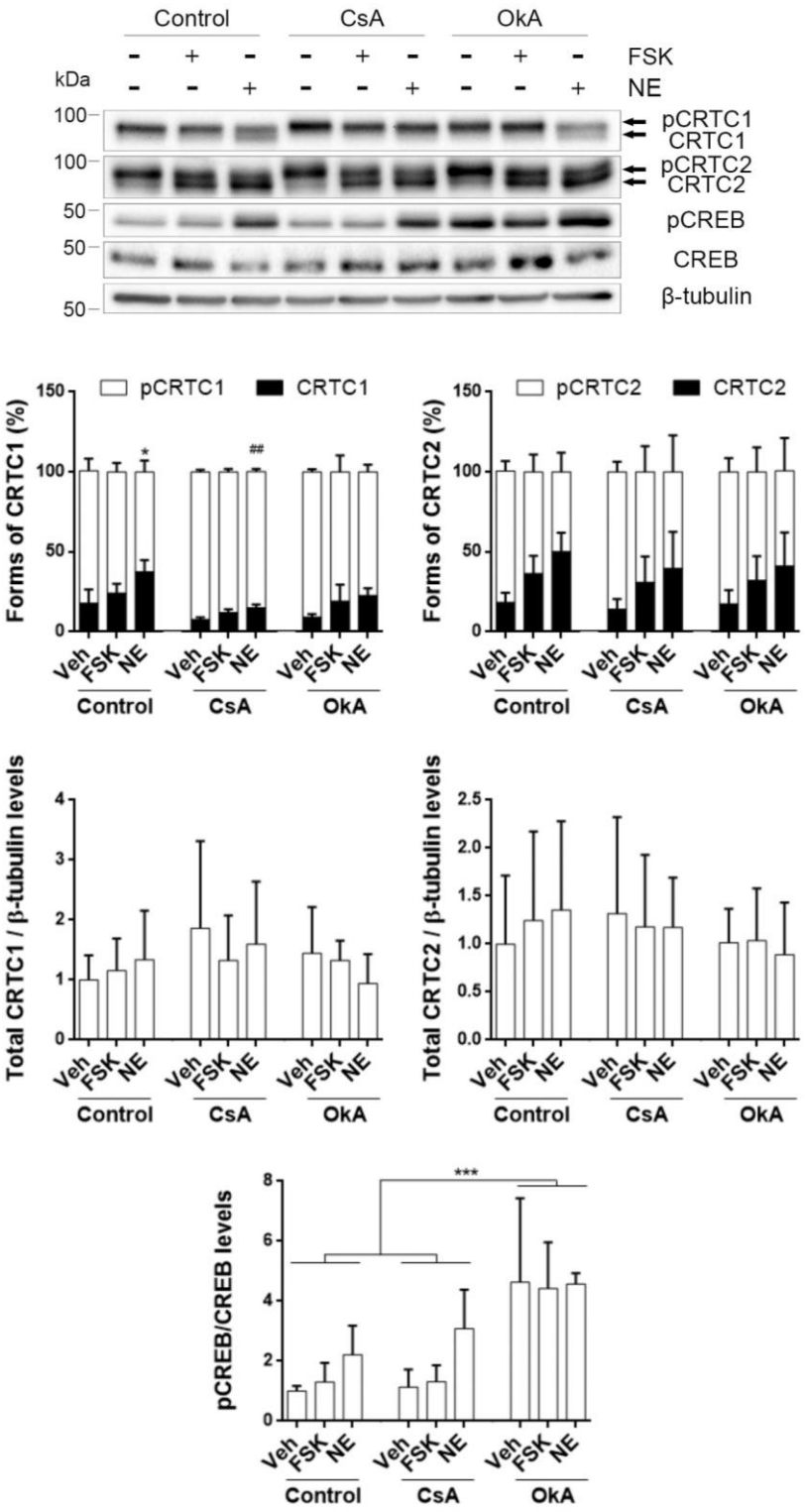

Figure 25. Activity-dependent CRTC1 and CRTC2 dephosphorylation in cultured cortical astrocytes

Western blot analysis showing activity-dependent CRTC1 and CRTC2 dephosphorylation and CREB phosphorylation in cultured mouse cortical astrocytes. Astrocytes were pre-treated for 15 min with vehicle or protein phosphatase inhibitors cyclosporine (CsA, 1 μM) or okadaic acid (OkA, 1 μM) and incubated with vehicle (Veh), FSK (1 μM) or norepinephrine (NE, 10 μM) for 15 min. Data represent the percentage of phosphorylated (p) (white bars) and non-phosphorylated (black bars) forms of CRTC1 and CRTC2, total CRTC1 and CRTC2 protein levels and quantification of pCREB (Ser 133)/CREB levels ratio. Data are mean ± SD of three independent experiments. Data were analyzed by two-way ANOVA followed by Tukey's *post hoc* test. *$P < 0.05$, **$P < 0.01$, ***$P < 0.001$. * *vs* Veh within each group; # *vs* the respective control.

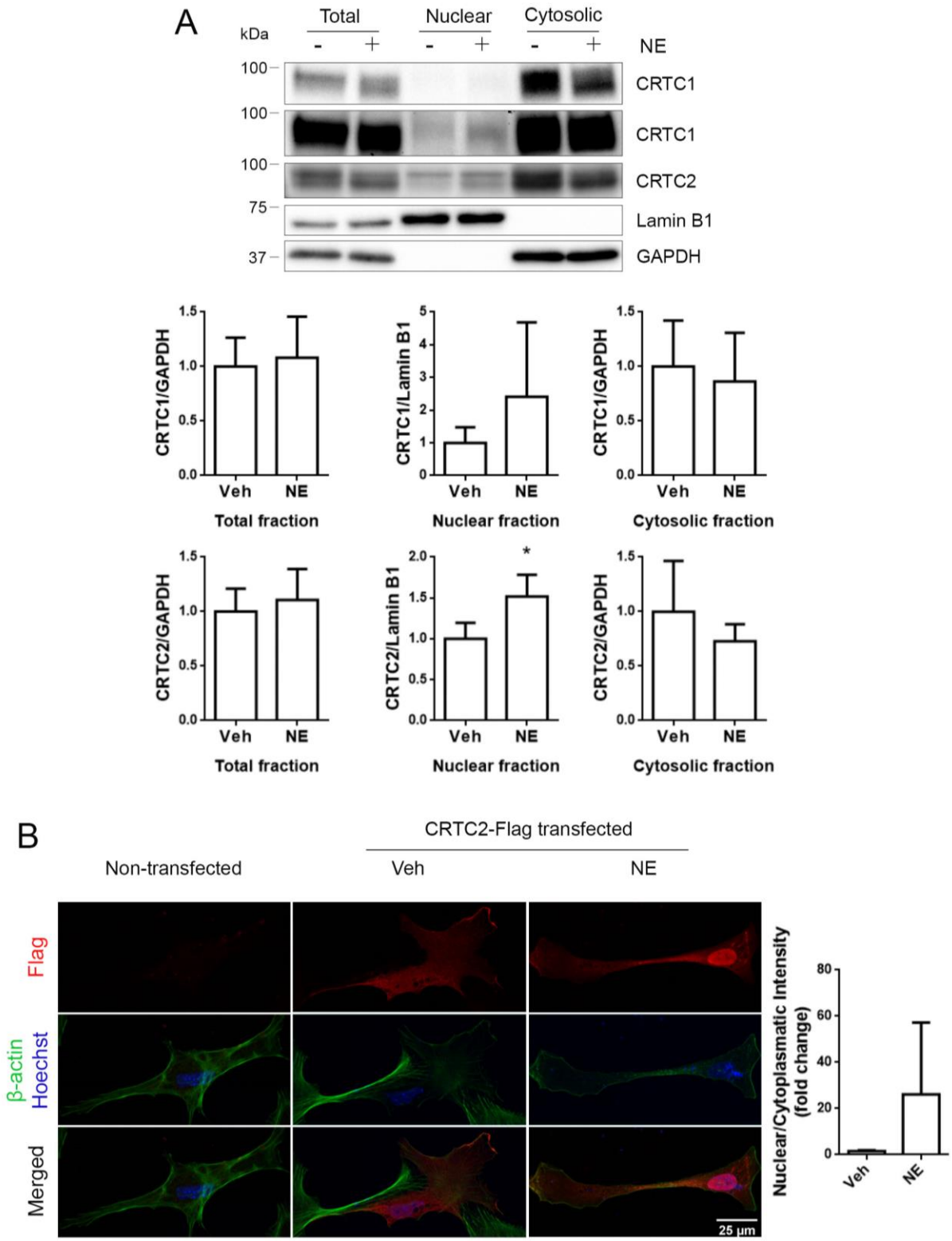

Figure 26. Activity-dependent CRTC1 and CRTC2 nuclear translocation in cultured cortical astrocytes

(A) Subcellular fractionation showing nuclear and cytosolic CRTC1 (two different exposures) and CRTC2 in vehicle (Veh; -) or 15 min norepinephrine-treated (NE; +) cultured astrocytes. Data represent mean ± SD of four independent experiments. **P* < 0.05 as determined by t-test. **(B)** Immunocytochemistry of CRTC2-Flag-transfected astrocytes in vehicle (Veh) and NE-treated conditions. Representative images of astrocytes showing CRTC2 (Flag in red), β-actin (green) and nucleus (Hoechst, blue). Data represent mean ± SD of nuclear/cytosolic Flag intensity (n=4 experiments; 6-12 cells per condition and experiment). Statistical analysis determined by t-test.

3.3 Co-immunoprecipitation of CREB and CRTC2 in astrocytes

I examined the interaction between CRTC2 and CREB in cultured astrocytes using CoIP assays with CREB and CRTC2 antibodies. As shown in **Figure 25**, Western blot analysis demonstrated rapid dephosphorylation of CRTC2 in NE-treated astrocytes (**Figure 27**). Immunoprecipitation with anti-CREB antibody revealed CREB immunoprecipitation plus a band corresponding to dephosphorylated CRTC2 in NE-treated astrocytes. By contrast, CRTC2 antibody immunoprecipitated CRTC2 but not CREB or pCREB. These results suggest a physical interaction between endogenous CRTC2 and CREB induced by activity in astrocytes.

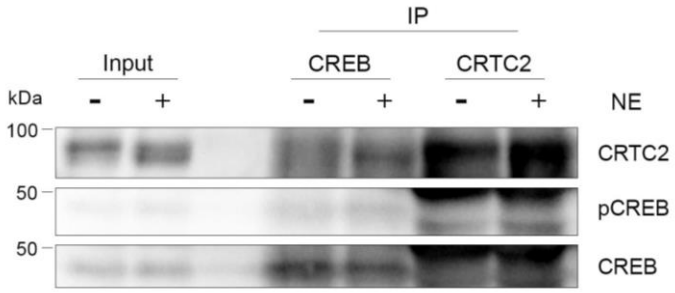

Figure 27. Activity-dependent CRTC2/CREB binding in cortical astrocytes

Co-immunoprecipitation analysis showing NE-induced binding of endogenous CRTC2 to CREB in cultured cortical astrocytes. Western blot showing CRTC2, pCREB and CREB in the lysate (input) and immunoprecipitated (IP) fractions in cultured astrocytes in vehicle (-) and NE (10 μM) treated conditions (15 min). Endogenous CRTC2 is immunoprecipitated with an anti-CREB antibody after NE treatment. Experiment performed once.

3.4 CRTC2/CREB-dependent gene transcription in astrocytes

I next studied the role of CRTC2 on CREB-dependent gene transcription in cortical astrocytes. First, *Crtc2* f/f cultured astrocytes were transduced with adenoviral particles (Ad5) expressing GFP (control of transduction) or Cre-recombinase (Cre) to inactivate endogenous *Crtc2.* Biochemical analysis revealed efficient genetic inactivation of *Crtc2* as demonstrated by decreased CRTC2 protein and mRNA levels in Cre-transduced astrocytes (**Figure 28A**). To study whether CRTC2 regulates CREB transcriptional activity in astrocytes, we performed a CRE-luciferase transcriptional assay in cultured astrocytes treated with vehicle or NE for 8h. NE treatment induced a significant increase of CREB-dependent transcription in cultured astrocytes ($P < 0.0001$; **Figure 28B**). However, compared with control or GFP transduction, Cre-recombinase transduction significantly reduced (~40%; $P < 0.05$) the CREB-dependent gene transcription in NE-treated astrocytes (**Figure 28B**).

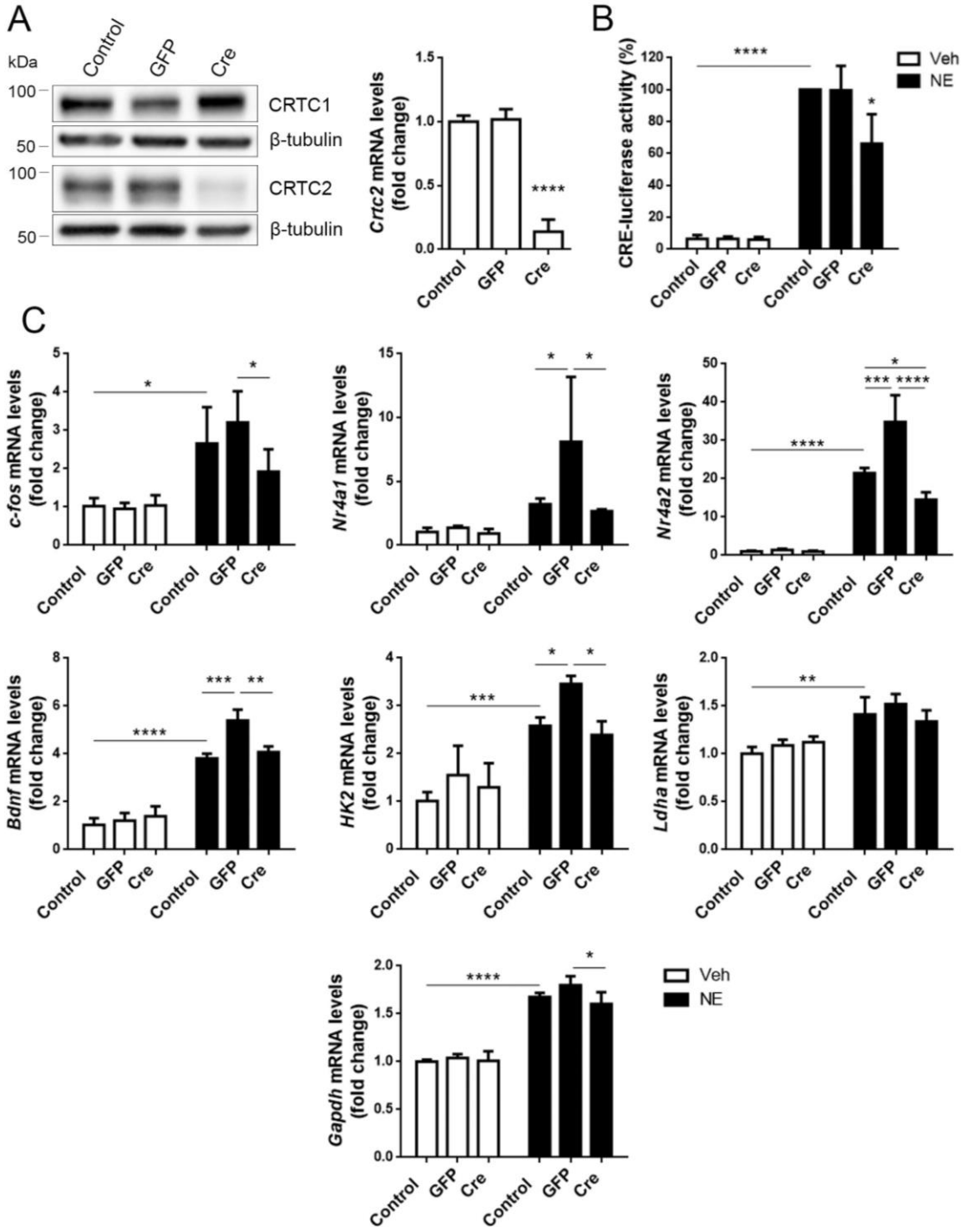

Figure 28. CRTC2 regulates NE-induced CREB-mediated transcription in cortical astrocytes

(A) *Crtc2* f/f cultured astrocytes were non-transduced (control) or transduced with adenoviral particles (Ad5) expressing GFP or Cre-recombinase (Cre). Western blot (**left**) and mRNA (**right**) analyses demonstrate specific reduction of CRTC2 in *Crtc2* f/f astrocytes transduced with Cre-recombinase. Data represent mean ± SD of three independent experiments. ****$P < 0.0001$ as determined by one-way ANOVA followed by Tukey's *post hoc* test. **(B)** CREB transcriptional activity analysis in cultured *Crtc2* f/f cortical astrocytes. Astrocytes were non-transduced (control) or transduced with adenovirus-GFP or -Cre recombinase and treated with NE (10 μM) for 8h before analysis of CRE-luciferase activity. Data represent mean ± SD of three independent experiments. *$P < 0.05$, **** $P < 0.0001$ determined by two-way ANOVA followed by Sidak's *post hoc* test. **(C)** qRT-PCR analysis of *c-fos*, *Nr4a1*, *Nr4a2*, *Bdnf*, *hexokinase2 (HK2)*, *Ldha* and *Gapdh* mRNAs after viral-mediated CRTC2 inactivation in *Crtc2* f/f cultured astrocytes. Astrocytes were non-transduced (control) or transduced with Ad5 adenovirus containing GFP or Cre-

recombinase (Cre) and treated with NE (10 μM) for 4 h. mRNA levels were quantified by real-time qPCR and normalized to geometric mean of *Ppia* and *Actb* genes. Data represent mean ± SD of three independent experiments. **P* < 0.05, ***P* < 0.01, ****P* < 0.001, *****P* < 0.0001 as determined by two-way ANOVA followed by Sidak's *post hoc* test.

I next examined transcript levels of CREB-dependent target genes by qRT-PCR after 4 h of NE treatment. These genes included *c-fos, Nr4a1, Nr4a2* and *Bdnf*. Moreover, I also analysed expression of glycolytic genes (*hexokinase2: HK2; lactate dehydrogenase A: Ldha and Gapdh*) which expression is modulated by neuronal activity (Hasel et al., 2017). Interestingly, and except for *Nr4a1*, all the mentioned gene transcripts increased significantly after NE treatment (*P* < 0.05-0.0001) (**Figure 28B**). Surprisingly, GFP transduction resulted in increased transcription compared with control in NE-induced conditions, which was significant for *Nr4a1* (*P* < 0.05), *Nr4a2* (*P* < 0.001), *Bdnf* (*P* < 0.001) and *HK2* (*P* < 0.05) (**Figure 28C**). These results suggest that Ad5 transduction induces CREB-dependent gene transcription although this increase was not detected in the CRE-luciferase assay (**Figure 28B**). Compared with GFP-transduced astrocytes, NE-treated Ad5-Cre-transduced astrocytes showed a reduction of transcript levels of *Nr4a1* (~70%; *P* < 0.05), *Nr4a2* (~60%; *P* < 0.0001), *c-fos* (~40%; *P* < 0.05), *HK2* (~30%; *P* < 0.05), *Bdnf* (~25%; *P* < 0.01), and *Gapdh* (~10%; *P* < 0.05) (**Figure 28C**). These results suggest that CRTC2 positively regulates activity-dependent CREB transcription in astrocytes.

3.5 CRTC2 recruitment at CREB target genes promoters

The above transcriptional analysis revealed a possible transcriptional regulation of *Nr4a2* and *c-fos* by CRTC2. We then examined whether CRTC2 binds to promoter regions of these genes by performing quantitative chromatin immunoprecipitation (ChIP-qPCR) analysis. CREB and CRTC2 were immunoprecipitated using specific antibodies in astrocytes after vehicle or NE treatment. As a control (beads), no antibody was added for the immunoprecipitation. Immunoprecipitated chromatin was then amplified and quantified by qPCR. For both genes, two different sets of primers were used. P1 primers amplified a proximal promoter region (~ -200 bp of distance to the transcription starting site (TSS)), while P2 primers amplified a distal promoter region (between -1600 to -2000 bp from the TSS) (**Figure 29A**). Quantified immunoprecipitated chromatin was represented as fold enrichment over an irrelevant region. Our results show basal binding of CREB over *Nr4a2* and *c-fos* promoters although, surprisingly, in NE-treated condition, while more CREB is recruited over the *Nr4a2* promoter, less binding of CREB is detected in the *c-fos* proximal region (**Figure 29B**). By contrast, CRTC2 is not bound to the promotor regions of *Nr4a2* or *c-fos* in vehicle conditions, but it is efficiently recruited after NE treatment to the proximal promoter regions of both genes and to the distal region of *c-fos* (*P* <0.0001; **Figure 29B**). These results demonstrate activity-dependent CRTC2 recruitment over *Nr4a2* and *c-fos* promoters in cultured astrocytes.

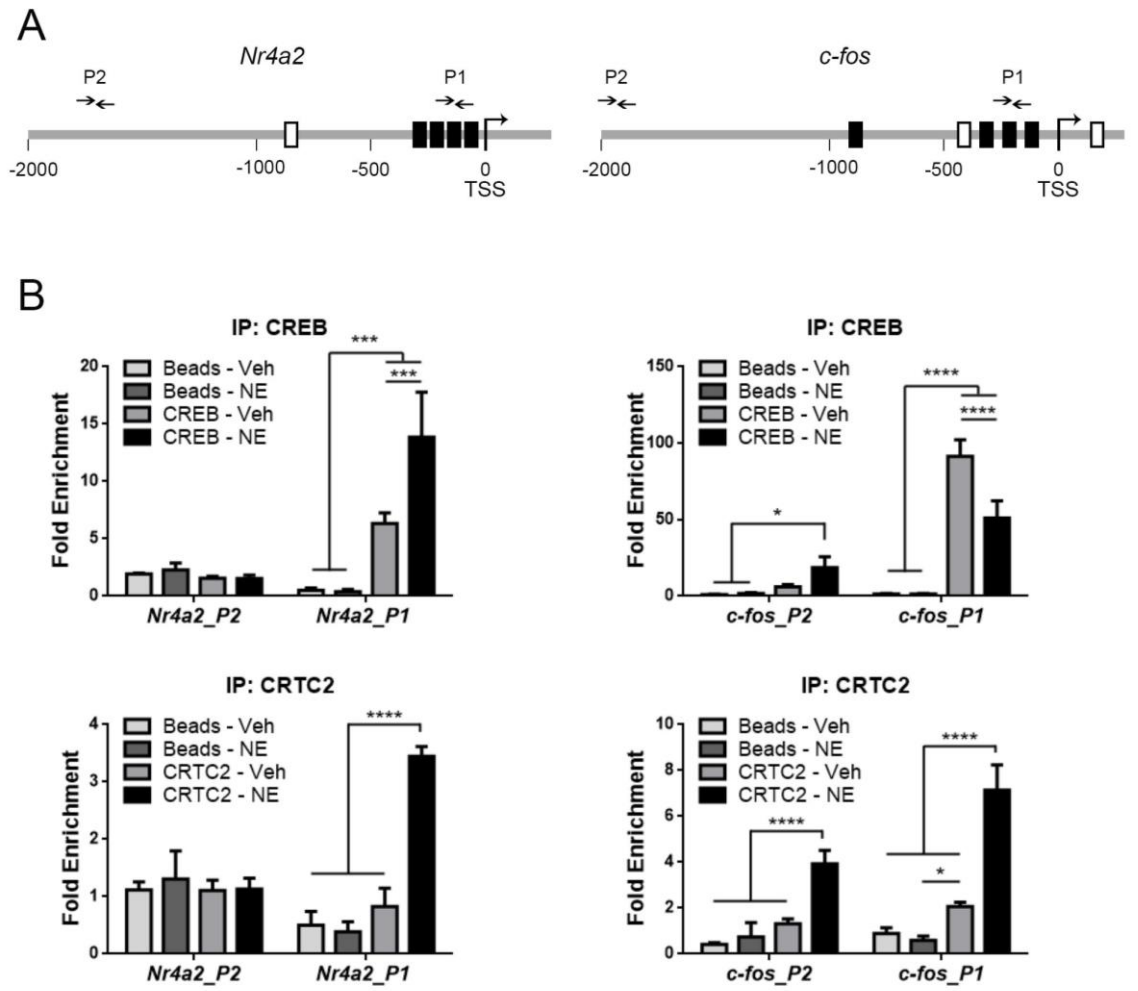

Figure 29. Activity-dependent recruitment of CRTC2 to CREB target gene promoters in cortical astrocytes

(A) Schematic representation of murine *Nr4a2* and *c-fos* gene promoters and position of proximal (P1) and distal (P2) primers for qPCR gene amplification relative to CRE/TATA-less (white boxes) and CRE/TATA (black boxes) sites. TSS: transcription start site. **(B)** Quantitative ChIP analysis showing differential binding of CREB and CRTC2 over *Nr4a2* and *c-fos* promoter regions. ChIP was performed using beads, anti-CREB (top) or CRTC2 (bottom) antibodies in cortical astrocytes treated with vehicle (Veh) or norepinephrine (NE) for 15 min. Data represent fold enrichment ± SD of immunoprecipitation assays from independent cultures (n=3). Statistical analysis determined by two-way ANOVA followed by Sidak's *post hoc* test **P* < 0.05, ****P* < 0.001, *****P* < 0.0001.

VIII Discussion

Brain plasticity is the ability of the brain to reorganize neural connections due to environmental changes and experience. These changes involve structural and functional modifications of neurons and non-neuronal cells allowing continuous physiological adaptation of the nervous system to the dynamics of the environment. The ability of the brain to reorganize itself is mediated, among other mechanisms, through the precise regulation of gene programs. CREB is a transcription factor, abundantly and ubiquitously expressed in all cell types of the brain, that controls a large number of physiological responses after activation through multiple stimuli. CREB transcriptional activity depends on several transcriptional coactivators, including CRTCs. Cerebral CRTCs regulate a wide variety of biological processes, such as memory, synaptic plasticity, circadian rhythm and energy sensing, among others (Saura & Cardinaux, 2017). However, the specific functions of CRTC isoforms and its regulatory mechanisms in different cell types of the brain are largely unknown. This doctoral thesis provides the first comparison of CRTC1 and CRTC2 in neurons and astrocytes focusing on its regulation and function in CREB-dependent transcription. Our results show that CRTC isoforms present differential expression, regulation and contribution to CREB-mediated gene transcription in neurons and astrocytes.

Differential cellular expression of CRTCs in the adult brain

All three CRTC isoforms are differentially expressed in the brain, being CRTC1 the most abundant, followed by CRTC2 and CRTC3 (Watts et al., 2011). However, the relative abundance and cell-type expression patterns of the CRTC isoforms in the adult brain are unclear. In this doctoral thesis, I first investigated the cellular expression pattern of CRTC2 in the brain of *Crtc2-LacZ* reporter mice, a novel *Crtc2* mutant mice generated in the lab. This model allowed us to employ classical histological analysis to follow endogenous *Crtc2* expression instead of using classical immunostaining that relies on the specificity of antibodies. Thus, *Crtc2-LacZ* reporter mice allowed us to examine endogenous CRTC2 expression by analysing β-galactosidase activity controlled under the endogenous *Crtc2* promoter. Our histological analysis showed that CRTC2 is particularly abundant in the hippocampus, more spread in the cortex and hypothalamus, and less abundant in the thalamus. These results agrees with previous reports using *in situ* hybridization that showed low and widely distribution of *Crtc2* mRNAs in distinct rat brain regions (Watts et al., 2011). This *in situ* hybridization analysis revealed high *Crtc2* levels in hippocampus, piriform cortex and different nucleus of the hypothalamus, including paraventricular, supraoptic, suprachiasmatic and ventromedial nuclei. In agreement, immunohistochemical analysis also revealed high CRTC2 protein levels in the adult mouse hippocampus and hypothalamus (Lerner et al., 2009). These results are important considering that the hippocampus is a master region required for learning and memory processes, and the

hypothalamus controls multiple central and peripheral physiological functions, such as circadian rythms, energy balance and the neuroendocrine system.

Interestingly, CRTC2 is expressed in the different brain cell types analyzed: neurons, astrocytes and microglia. CRTC2 is high abundant in pyramidal neurons of the hippocampus in the adult mouse brain. Although the majority of neurons of the pyramidal layer of the hippocampus are glutamatergic excitatory neurons, we cannot exclude the possibility that CRTC2 could be expressed in inhibitory GABAergic neurons. Double immunostaining using markers for particular neuronal subtypes will be necessary to examine the specific neuronal cell types expressing CRTC2. In contrast with previous reports showing restricted expression of CRTC2 in neurons of the adult mouse brain (Lerner et al., 2009), we found that CRTC2 is abundant in astrocytes. These discrepancies on the cellular expression of CRTC2 could be due to the low sensitivity and/or specificity of immunohistochemistry used by Lerner and colleagues compared with our histochemical approach in *Crtc2-LacZ* mice. Our result indeed agrees with a previous report showing expression of both CRTC1 and CRTC2 in cultured cortical astrocytes (Carriba et al., 2012). In contrast to the expression of CRTC2 in the majority of hippocampal and cortical neurons and astrocytes, only few microglia express CRTC2. It is interesting to notice that CRTC2 has not been previously described in microglial cells. Thus, our results demonstrate for the first time expression of CRTC2 in diverse glial cells in the adult mouse brain, including astrocytes and microglia, which may suggest multiple functions of CRTC2 in distinct cell types of the brain.

The above results showing CRTC2 expression in distinct brain cell types agree, in general, with recently published cell-specific transcriptomic analysis of the mouse cerebral cortex (Y. Zhang et al., 2014). When we re-analysed the public available transcriptomic data from Expression Atlas database (Ref. 25186741; E-GEOD-52564; Y. Zhang et al., 2014), we found that CRTC isoforms are differentially expressed in the mouse cerebral cortex (**Figure 13**). *Crtc1* mRNA levels are highly expressed in neurons, oligodendrocytes precursor cells (OPCs) and astrocytes. *Crtc2* is predominantly abundant in all analysed cell types except for oligodendrocytes. Indeed, *Crtc2* transcripts are abundant in microglia, astrocytes, neurons, and endothelial cells, even with higher levels than those observed for *Crtc1*. Contrarily, *Crtc*3 was the less abundant isoform in the mouse cerebral cortex, presenting its higher levels in astrocytes and neurons. These results demonstrate differential cellular expression of CRTC isoforms in the mouse cerebral cortex.

In agreement with the transcriptomic results, we also show that CRTC1 and CRTC2 are differentially expressed in cultured cortical neurons and astrocytes. CRTC1 is particularly abundant in cultured neurons compared to astrocytes, whereas CRTC2 is higher in cultured astrocytes than in neurons. However, the relative expression analysis among different CRTC isoforms were first attempted by *in situ hybridization*, and confirmed by qRT-PCR (Watts et al.,

2011). The results showed that *Crtc1* is the highest expressed isoform in the rat brain, followed by *Crtc2* and *Crtc3.* These results are different from the aforementioned transcriptomic analysis which reveals that *Crtc2* is the main isoform expressed in the mouse cerebral cortex (Y. Zhang et al., 2014). These discrepancies could be due to differences in methodology and animal models used in these two studies. The qRT-PCR analyses were performed in hippocampal and hypothalamus dissected tissues from adult male rats, while the transcriptomic data was obtained by purifying different cell types from P7 or P17 mouse cortices. The results from these two studies are difficult to reconcile since experiments are performed with different species (rat *vs* mouse), different brain regions (hippocampus and hypothalamus *vs* cortex) and different ages (adult *vs* early postnatal). Nonetheless, *Crtc2* levels from cortical cells in young mice are higher than that of *Crtc1*; while *Crtc1* levels are higher than *Crtc2* in adult hippocampus and hypothalamus in the rat brain. Considering the above results, could CRTCs be expressed in an age-dependent manner? We assessed this issue by evaluating CRTC1 and CRTC2 expression in hippocampus of control and *Crtc2* cKO mice at different ages (**Figure 22A**). Our biochemical analysis showed similar levels of CRTC1 and CRTC2 between postnatal day 15 and 9 months of age in control mice. Therefore, we conclude that CRTC1 and CRTC2 levels are constant in the hippocampus during adulthood.

Interestingly, expression of CRTC1 and CRTC2 changes during neuronal differentiation in cultured cortical and hippocampal neurons. CRTC1 increases during neuronal differentiation, showing a peak at 4 DIV and then declines. The maximum expression of CRTC1 is associated with the neuronal stage corresponding to dendritic elongation and arborization, which agrees with the described function of CRTC1 in dendritic development (Li et al., 2009). In the rat brain, CRTC1 levels are high at birth, with a peak at P14, and decline in adulthood correlating with dendritic sprouting (Li et al., 2009). However, these results obtained in rat brain contrast with our CRTC1 expression analysis in mice at postnatal day 15 to 9 months. Both studies differ in the rodent models and ages, which could explain these differences. Nonetheless, when analysing CRTC2 in cultured hippocampal and cortical neurons, we found a dramatic decrease in CRTC2 transcripts and protein levels during neuronal differentiation, in contrast with the sustained CRTC1 levels. Thus, our results suggest that CRTC isoforms may be differentially expressed depending on the cell type and developmental stage. This could be important in particular physiological conditions in which expression of a specific CRTC isoform may play precise biological functions. For instance, CRTC2 expression is constant in the suprachiasmatic nucleus of the hypothalamus, whereas CRTC1 levels change depending of the dark/light cycle (Sakamoto et al., 2013). This modulation of CRTC1 levels in hypothalamus has been postulated to be critical for regulating the circadian rhythm in a CREB-dependent manner (Sakamoto et al., 2013).

Together, these results indicate that CRTC1 and CRTC2 are differentially expressed in neurons and astrocytes in the mouse cerebral cortex. Moreover, the expression of CRTC1 and CRTC2 changes during neuronal differentiation, which can be important for regulating specific physiological functions in particular brain regions.

Differential CRTCs regulation in neurons and astrocytes

Activity-dependent CREB-mediated transcription is regulated by dephosphorylation, nuclear translocation and binding of CRTCs over gene promoters in different cell types, including neurons, hepatocytes and adipocytes (Saura & Cardinaux, 2017). Our results show that cAMP/Ca^{2+} induce CRTC1 and CRTC2 dephosphorylation in neurons, a result that agrees with previous studies demonstrating activity-dependent CRTC1 dephosphorylation in neurons (España et al., 2010; Kovács et al., 2007). The increase of CRTC1 dephosphorylated band observed in different experiments after FSK/KCl treatment (**Figures 15, 16, 17 and 18**) is not reflected when calculating the percentage of dephosphorylated CRTC1 (**Figure 15**). Indeed, Ca^{2+} increase is also accompanied with an increase of total CRTC1, suggesting that it may be the reason of unchanged percentage of CRTC1 dephosphorylation. By contrast, no increase in total CRTC1 levels were detected by increasing cytosolic cAMP levels (i.e., FSK). Thus, increase of CRTC1 after depolarization, could be due to a Ca^{2+}-dependent inhibition of CRTC1 degradation, a possibility reinforced by previous studies indicating ubiquitin-dependent CRTC1 proteasomal degradation (Gao et al., 2018). In summary, while CRTC1 levels rise after a Ca^{2+} increase, the percentage corresponding to the different phosphorylated and unphosphorylated CRTC1 species are constant, indicating that, quantitatively, more unphosphorylated CRTC1 molecules are able to translocate to nucleus to promote CREB-dependent gene transcription. In contrast to CRTC1, total CRTC2 levels are similar in all stimulated conditions, whereas cAMP and Ca^{2+} enhance CRTC2 dephosphorylation.

These results suggest that CRTC1 and CRTC2 could be differently modulated by distinct regulatory mechanisms in cultured neurons affecting their phosphorylation and/or total protein levels through protein stabilization, degradation and/or potentiating translation. In fact, previous studies showed different regulation of total levels and subcellular localization of CRTC1 and CRTC2 during circadian rhythms (Sakamoto et al., 2013). CRTC1 shows a rhythmic expression along the day accompanied with light-evoked nuclear accumulation in the SCN. By contrast, CRTC2 levels are sustained along the different circadian periods without nuclear accumulation after light exposure. These changes in CRTC1 protein levels are not due to changes in transcript levels, which suggests that CRTC1 is regulated through protein translation and/or degradation (Sakamoto et al., 2013). Altogether, these results suggest that both protein levels and regulation of CRTC1 and CRTC2 are differently modulated in cortical neurons.

To evaluate the cellular mechanisms regulating CRTCs dephosphorylation, we employed pharmacological approaches using different protein phosphatase inhibitors. OkA was used to inhibit PP1 and CsA was used as a PP2B inhibitor. We should consider that a limitation of pharmacological inhibitors is the lack of specificity. In this case, OkA treatment can block PP1 and PP2A activity at high doses (1 μM), but it specifically inhibits PP2A at low doses (1 nM) (Cohen et al., 1990). We used 1 μM OkA in most of our experiments, resulting in inhibition of both phosphatases. In order to discard the PP2A implication in the CRTCs dephosphorylation, we also performed assays at lower doses of OkA (< 500 nM) to specifically inhibit PP2A. In this case, we demonstrate that CRTCs dephosphorylation is not compromised after PP2A blockade, indicating that the effects seen in dephosphorylation at 1 μM OkA are dependent on PP1 but not PP2A.

In agreement with previous reports (España et al., 2010; Kovács et al., 2007), our studies indicate that CRTC1 is dephosphorylated mainly by Ca^{2+}-dependent PP2B/CaN after neuronal stimulation. Moreover, CsA, but not OkA, inhibits the increase of CRTC1 levels after cytosolic Ca^{2+} increase, suggesting that changes in CRTC1 levels are dependent on PP2B/CaN. On the contrary, CRTC2 is mainly dephosphorylated by PP1, although PP2B/CaN may also play a residual role in CRTC2 dephosphorylation after FSK/KCl induction. It is possible, however, that in the presence of intracellular Ca^{2+} and cAMP, PP2B/CaN favours the dephosphorylation of one or some CRTC2 specific residues facilitating PP1 activity over the other residues. Nonetheless, the role of PP2B/CaN in CRTC2 dephosphorylation seems to be minimal and cannot achieve CRTC2 dephosphorylation on its own. These results demonstrate that specific downstream signalling mechanisms are involved in specific dephosphorylation and activation of CRTC1 and CRTC2 in neurons (**Figure 30**). Indeed, previous pharmacological studies performed in pinealocytes revealed norepinephrine-induced dephosphorylation of CRTC1 and CRTC2 through Ca^{2+} and cAMP signalling pathways, respectively (McTague et al., 2012). In pinealocytes, CRTC1 nuclear translocation requires PP2B activity, while CRTC2 nuclear translocation requires PP2A. However, it is still possible that CRTC2 could be regulated by both PP1 and PP2A in pinealocytes because the concentration of OkA used in this latter study can block both phosphatases.

Our results demonstrate differential regulation of CRTC1 and CRTC2 in neurons. Particularly, CRTC1 protein levels and CRTC1 dephosphorylation are both regulated by intracellular Ca^{2+}, which promotes a high increase in total CRTC1 levels and enhances the PP2B/CaN activity facilitating CRTC1 dephosphorylation. Intracellular cAMP could also modulate CRTC1 dephosphorylation, for instance, by inhibiting some kinases responsible for CRTCs phosphorylation (Screaton et al., 2004). By contrast, CRTC2 dephosphorylation after neuronal

stimulation is mainly mediated by PP1 after Ca^{2+}/cAMP increase. Regulation of PP1 activity is not well defined. In fact, more than 200 regulatory proteins can modulate its phosphatase activity while promoting substrate specificity (Rebelo et al., 2015). This, adds difficulties in dissecting the specific CRTC2 activation pathway in cultured neurons.

The mechanisms regulating CRTCs in astrocytes has been scarcely investigated. First evidences of CRTC1 and CRTC2 expression and activation in astrocytes were described in 2012 (Carriba et al., 2012). Authors demonstrated CRTCs translocate from cytosol to nucleus in response to ATP or NE treatment and determined CRTC1 phosphorylation is mediated through the PKC-ERK1/2 pathway (Carriba et al., 2012). In this thesis, we attempted to investigate the regulatory mechanisms of CRTC1 and CRTC2 in cultured cortical astrocytes. Interestingly, FSK and NE induce dephosphorylation of both CRTC isoforms. To investigate the phosphatases responsible for CRTCs dephosphorylation, similar pharmacological treatments performed in neurons were employed in cultured astrocytes. Our results show that inhibition of PP2B/CaN after NE treatment resulted in reduced dephosphorylation of CRTC1, which suggests similar regulatory mechanisms of CRTC1 in neurons and astrocytes. Surprisingly, CRTC2 dephosphorylation in astrocytes is not mediated by PP1, PP2A nor PP2B (**Figure 30**). This result is interesting considering that CRTC2 dephosphorylation is mediated by PP1/CaN in COS-7 cells and liver, PP2A/PP1 in pinealocytes or CaN in HEK 293 cells (McTague et al., 2012; Sonntag et al., 2019; Uebi et al., 2010). Thus, the specific phosphatase(s) responsible for CRTC2 dephosphorylation in astrocytes remain still unknown.

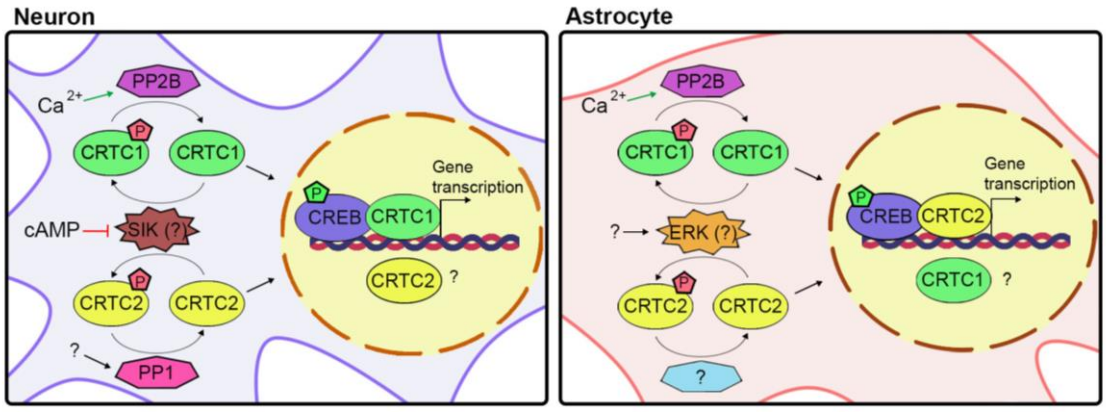

Figure 30: Postulated mechanisms of CRTCs regulation in neurons and astrocytes.

Proposed mechanisms of activity-dependent gene expression mediated by CRTC1 and CRTC2 in neurons (left) and astrocytes (right). **(Left)** Neuronal activity enhances CRTC1 and CRTC2 dephosphorylation mediated by PP2B and PP1, respectively. CRTCs dephosphorylation favours its nuclear localization. Nuclear translocation of CRTC1 promotes CREB-dependent gene transcription in neurons. **(Right)** Astrocytic treatment with NE favours CRTC1 and CRTC2 dephosphorylation and nuclear translocation. CRTC1 dephosphorylation is PP2B dependent, while CRTC2 dephosphorylation is independent of PP1, PP2A and PP2B. Activity-dependent CRTC2 nuclear localization enhances its binding over CRE-containing promoters and CREB-mediated transcription.

Altogether, our results clearly indicate differential regulatory mechanisms of brain CRTC1 and CRTC2 isoforms depending on the cellular context. Indeed, the same intracellular signalling pathway may lead to differential activation of specific CRTC isoforms resulting in selective CREB recruitment over gene promoters (Ravnskjaer et al., 2007). Future studies are necessary to fully understand the regulatory mechanisms of CRTC isoforms in the different cell types of the brain.

CRTCs cytosolic-nuclear translocation

As previously reported, CRTC dephosphorylation induces nuclear translocation and CREB-mediated transcription (Li et al., 2009; Screaton et al., 2004). Supporting this data, our results also revealed increase of CRTCs in the nucleus of neurons and astrocytes after cellular stimulation. Surprisingly, our biochemical assays performed by cellular fractionation show very low CRTCs nuclear levels, both in basal and treated conditions, while cytosolic levels are very high. These results are surprising and slightly different to the obtained by immunocytochemical methods. Abundant cytosolic localization of CRTCs may suggest relevant roles of these factors in the cytosolic compartment in neurons and astrocytes. One of these cytosolic CRTC functions seems to be the regulation of RNA splicing by the interaction of spliceosome factors and vesicle trafficking from endoplasmic reticulum to Golgi by directly binding with COPII (Amelio et al., 2009; Han et al., 2015).

These small discrepancies in the results, obtained by the two methods, may reflect some particularities of the procedures. For instance, as immunocytochemistry require cell fixation, we can obtain a real picture of the CRTCs distribution 15 min after treatment in cultured cells. On the contrary, the cellular fractionation procedure requires homogenization and centrifugation steps and, although samples were kept on ice along the procedure, it takes longer to obtain the final samples corresponding to nucleus and cytosolic fractions, and therefore it may cause changes in the final results. Indeed, it is possible that low nuclear CRTCs levels may be due to CRTCs nuclear export that could happen during cell fractionation. An alternative could be using an inhibitor for the nuclear export, such as leptomycin B, during the cell treatment. In agreement with this hypothesis, the study performed by Kovács et al., 2007 used leptomycin B prior to stimulation to detect overexpressed CRTC1 nuclear accumulation in neurons. On the other hand, Kovács and colleagues stated that leptomycin B treatment was not required for detecting overexpressed CRTC2 in the nucleus, suggesting also, distinct regulation of nuclear export for CRTC1 and CRTC2 in neurons. This may result in differences on its nuclear persistance while compromising CREB transcriptional activity.

In summary, our results suggest that upon neuronal or astrocytic stimulation, the increase in dephosphorylated CRTCs leads to a cytosolic-nuclear shuttling resulting in CRTCs nuclear accumulation. In agreement with these results, previous studies showed CRTC1 shuttling from synapse to nucleus in response to synaptic activity in cultured neurons (Ch'Ng et al., 2012), but also in hippocampal neurons after exposing mice to stimulus in spatial and associative memory tasks (Parra-Damas et al., 2014; Parra-Damas, Chen, et al., 2017). Astrocytic CRTCs nuclear translocation was also previoulsy determined in cultured rat astrocytes as an increase in the number of CRTC1 and CRTC2-positive nuclei after ATP and NE treatment (Carriba et al., 2012). This nuclear import of CRTCs could be mediated through importins. The CRTCs NLS become unmasked after its dephosphorylation, which could be recognized by importins to facilitate the nuclear entrance of medium and large proteins (Yun et al., 2019).

On the other hand, CRTCs subcellular localization changes depending on the stimulus, but also depending on the brain region. For instance, after feeding, CRTC2 is located in the nucleus in specific hypothalamic regions, such as the arcuate or paraventricular nuclei, whereas it localizes in the cytoplasm in the lateral hypothalamus (Lerner et al., 2009). Thus, although it is relevant to investigate the CRTCs nuclear translocation in cultured cells, it is also necessary to translate these experimental conditions into *in vivo* models to further deep into the CRTCs physiological roles.

Differential contribution of CRTCs to CREB-mediated gene expression

Binding of CRTCs to CREB to mediate CREB-dependent gene expression has already been described (Conkright, Canettieri, et al., 2003; Luo et al., 2012). Here, we corroborate the binding of endogenous dephosphorylated CRTC1 to CREB upon neuronal cAMP/Ca^{2+} induction, as demonstrated by co-immunoprecipitation assays. Similar conclusions were obtained using FRET techniques, as demonstrated by increase of FRET efficiency after neuronal stimulation. FRET is a challenging method and, although the obtained results are not conclusive due to the small sample size, results are encouraging. Difficulties in the setting up of FRET can be controlled with good positive and negative controls, which would delimit the range of FRET efficiency for the experimental conditions (Snapp & Hegde, 2006). But, getting experimental values similar to those obtained with the positive control is complicated due to experimental limitations that cannot be controlled. For instance, the distance between the fluorophores as well as their orientation are critical for obtaining good FRET efficiencies. A small variation in the distance between the two fluorophores is translated in big changes in the FRET efficiency, as efficiency depends on the distance at sixth power ($E=1/[1+(r/R_0)^6]$) (Snapp & Hegde, 2006). Second, for the correct transference of energy between the two fluorophores, apart from being less than 10 nm apart, they have to be well-orientated since perpendicular orientation results in no energy transfer (Broussard et al., 2013). These scenarios, a part of contributing to increase the variability of the FRET

efficiencies, would raise the possibility of acquiring false negatives results. Thus, obtaining low FRET efficiency values do not exclude the possibility for CREB/CRTC1 interaction. The presence of false positives could also be possible, although they can be controlled with good negative controls. The mean of FRET efficiencies obtained with the NeuN negative control was almost zero, although the deviation indicates wide distribution of the different obtained FRET efficiencies suggesting the presence of few false positive measurements. Altogether, the preliminary results obtained with FRET in combination with the biochemical methods, confirm CREB-CRTC1 interaction upon stimulation in neurons as a mechanism involved in CREB-dependent gene transcription.

The distinct expression and regulatory mechanisms of CRTCs in neurons may, in part, explain their differential effects on CREB-mediated transcription. In agreement with previous studies (Kovács et al., 2007; Parra-Damas, Rubió-Ferrarons, et al., 2017; Uchida et al., 2017), our data indicate that CRTC1 is a critical regulator of the CREB-dependent transcription in neurons. By contrast, the role of CRTC2 in CREB-mediated gene transcription in cortical neurons is minimal. However, CRTC2 participates in CREB-dependent transcription in hypothalamic neurons, where mediates glucose sensing (Lerner et al., 2009). In fact, being CRTC1 the main CRTC isoform expressed in neurons it is not surprising that the contribution of CRTC1 to CREB transcriptional activity is around 75%. The low contribution of CRTC2 to CREB-dependent gene transcription can be explained by the reduced expression of CRTC2 in neurons. Nonetheless, CRTCs can also potentiate gene transcription by interacting with other transcription factors belonging to the bZIP family (Canettieri et al., 2009; M. W. Lee et al., 2010). We, then, cannot exclude the possibility that CRTC2 could mediate gene transcription in neurons. Moreover, although both CRTCs cofactors are dephosphorylated in response to cAMP/Ca^{2+} signalling and translocated to the nucleus, their diverse regulation could also be translated to different transcriptional properties, resulting in delayed nuclear import or export or even retarded transcription in the case of CRTC2. The idea that CRTC2 transcriptional activity can be delayed compared to CRTC1 was previously mentioned by Kovács and colleagues. They show CRTC2 persistence in the nucleus seem to be higher than CRTC1 in neurons (Kovács et al., 2007) which could indicate differential transcriptional timing depending on the CRTC isoform.

Further evidences for the role of CRTC1 on CREB-dependent gene transcription in cultured neurons were demonstrated analysing the transcription of *Nr4a2,* a CRTC1 target gene (Parra-Damas, Rubió-Ferrarons, et al., 2017), which mRNA levels were reduced after *Crtc1* silencing. Nonetheless, when analysing *c-fos* transcription, another classical CRTC1/CREB target gene, our results reflected no alteration on its transcription in the absence of CRTC1. This result is surprising considering that several studies have showed that CRTC1 binds to *c-fos* gene promoter

and regulates its transcription in neurons (Nonaka et al., 2014; Parra-Damas et al., 2014; Parra-Damas, Rubió-Ferrarons, et al., 2017). Although *Nr4a2* and *c-fos* genes are regulated by CRTC2 in other cell types (Eberhard et al., 2013; Hernandez et al., 2015; Rodón et al., 2019), our results show no effect of CRTC2 inactivation in the transcription of these genes in neurons. These results reflect that CRTC1 and CRTC2 may play no redundant roles in cultured cortical neurons. In agreement, CRTC2 does not show compensatory effects when CRTC1 is silenced, since no increase in CRTC2 mRNA or protein levels are detected in shCRTC1-transduced neurons, neither CRTC1 compensates the loss of CRTC2 in Cre-transduced neurons or in *Crtc2* cKO mice. In fact, although *Crtc2* cKO mice present significant CRTC2 reduction without showing any compensatory effects on CRTC1 or CRTC3 expression, the transcriptional results obtained for the *Crtc2* cKO mice agrees with data obtained from cultured neurons. CRTC2 neuronal deletion does not result either in reduced hippocampal transcription of CREB target genes nor deficits in spatial and contextual memory in *Crtc2* cKO mice.

In astrocytes, CRTC2 it rapidly dephosphorylated and translocated to the nucleus to mediate CREB-dependent gene transcription. In agreement, overexpression of a dominant negative mutant for CRTC2 resulted in 50% reduction of CREB transcriptional activity in cultured rat astrocytes (Carriba et al., 2012). Carriba and colleagues also analysed the CRTC1-CREB dependent gene transcription concluding that a 50% of the CREB transcriptional activity was CRTC1-dependent. Although CRTC1 is dephosphorylated and translocated to nucleus in astrocytes, we could not evaluate its implication in CREB-dependent gene transcription since no specific viral-mediated CRTC1 approaches for astrocytes were available. Nonetheless, it is quite surprising that 50% of CREB activity in astrocytes is CRTC1-dependent when protein levels of CRTC1 are low in cultured astrocytes. Surprisingly, Carriba at al. showed that treatment with CsA does not affect CREB transcriptional activity in cultured astrocytes which, from one hand, supports the idea that after calcium signalling there is a lack of CREB transcriptional activity in astrocytes (Murray et al., 2009). But, on the other hand, and taking into consideration that our results show that CRTC1 dephosphorylation is mediated by PP2B, if 50% of the CREB transcription depends on CRTC1, CsA treatment should also alter the transcriptional activity of CREB.

In contrast to neurons, astrocytic CRTC2 plays a prominent role in the transcription of *c-fos*, *Nr4a1*, *Nr4a2*, *Bdnf*, *hexokinase* (*HK2*) or *Gapdh*. Chromatin immunoprecipitation assays demonstrated CRTC2 and CREB recruitment over the promoter regions of *Nr4a2* and *c-fos* genes after NE treatment in cultured astrocytes. However, CREB is constitutively bound to CRE sites independently of NE-treatment while CRTC2 binding is activity-dependent. These results are similar with data obtained in cultured neurons when evaluating CRTC1 interaction in the promoter region (Parra-Damas, Rubió-Ferrarons, et al., 2017). Notably, CRTC2-dependent

regulation of *HK2* and *Gapdh* may have important physiological implications considering that these genes are directly involved in glycolysis and its transcription is regulated by neuronal activity (Hasel et al., 2017). HK2 is a rate-limiting enzyme which activity mediates the first glycolytic step, while GAPDH is an enzyme that catalyzes a reversible oxidative phosphorylation step in the glycolytic pathway. These results, thus, open the door to investigate the involvement of CRTC2 in the glycolytic pathway in astrocytes. Considering that astrocytes are the cell masters of brain homeostasis, and that CRTC2 participates in glucose balance in the liver and glucose sensing in the hypothalamus, it is plausible that CRTC2 could participate in astrocytic glucose metabolism.

In **conclusion**, our results indicate that CRTC1 and CRTC2 are differentially expressed, regulated and contribute to CREB-dependent gene transcription in a cell type-specific manner in the cerebral cortex (**Figure 30**), which suggest non-redundant roles of CRTC isoforms in the brain.

IX Conclusions

- **CRTC2 is expressed in neurons, astrocytes and microglia in the hippocampus, hypothalamus and cortex in the adult mouse brain.**
- **CRTC1 and CRTC2 are differentially expressed and regulated in cortical neurons and astrocytes.**
  - CRTC1 is highly expressed in neurons, whereas CRTC2 is mainly expressed in astrocytes.
  - CRTC1 dephosphorylation and activation depend on PP2B/CaN in neurons and astrocytes.
  - CRTC2 dephosphorylation depends on PP1 in neurons but is independent of PP2B/CaN, PP1 and PP2A in astrocytes.
- **CRTCs contribute differentially to CREB-mediated gene transcription in neurons and astrocytes.**
  - CRTC1 is the main CRTC isoform that regulates CREB-dependent gene transcription in neurons.
  - CRTC2 regulates CREB-dependent gene transcription in astrocytes.

X References

Alberini, C. M. (2009). Transcription factors in long-term memory and synaptic plasticity. In *Physiological Reviews*. https://doi.org/10.1152/physrev.00017.2008

Alberts, A. S., Montminy, M., Shenolikar, S., & Feramisco, J. R. (1994). Expression of a peptide inhibitor of protein phosphatase 1 increases phosphorylation and activity of CREB in NIH 3T3 fibroblasts. *Molecular and Cellular Biology*. https://doi.org/10.1128/mcb.14.7.4398

Allen, N. J. (2014). Astrocyte Regulation of Synaptic Behavior. *Annual Review of Cell and Developmental Biology*. https://doi.org/10.1146/annurev-cellbio-100913-013053

Altarejos, J. Y., Goebel, N., Conkright, M. D., Inoue, H., Xie, J., Arias, C. M., Sawchenko, P. E., & Montminy, M. (2008). The Creb1 coactivator Crtc1 is required for energy balance and fertility. *Nature Medicine*. https://doi.org/10.1038/nm.1866

Altarejos, J. Y., & Montminy, M. (2011). CREB and the CRTC co-activators: Sensors for hormonal and metabolic signals. In *Nature Reviews Molecular Cell Biology*. https://doi.org/10.1038/nrm3072

Amelio, A. L., Caputi, M., & Conkright, M. D. (2009). Bipartite functions of the CREB co-activators selectively direct alternative splicing or transcriptional activation. *EMBO Journal*. https://doi.org/10.1038/emboj.2009.216

Amelio, A. L., Miraglia, L. J., Conkright, J. J., Mercer, B. A., Batalov, S., Cavett, V., Orth, A. P., Busby, J., Hogenesch, J. B., & Conkright, M. D. (2007). A coactivator trap identifies NONO (p54nrb) as a component of the cAMP-signaling pathway. *Proceedings of the National Academy of Sciences of the United States of America*. https://doi.org/10.1073/pnas.0707999105

Ao, H., Ko, S. W., & Zhuo, M. (2006). CREB activity maintains the survival of cingulate cortical pyramidal neurons in the adult mouse brain. *Molecular Pain*. https://doi.org/10.1186/1744-8069-2-15

Araque, A., Parpura, V., Sanzgiri, R. P., & Haydon, P. G. (1999). Tripartite synapses: Glia, the unacknowledged partner. In *Trends in Neurosciences*. https://doi.org/10.1016/S0166-2236(98)01349-6

Asahara, H., Santoso, B., Guzman, E., Du, K., Cole, P. A., Davidson, I., & Montminy, M. (2001). Chromatin-Dependent Cooperativity between Constitutive and Inducible Activation Domains in CREB. *Molecular and Cellular Biology*. https://doi.org/10.1128/mcb.21.23.7892-7900.2001

Baltaci, S. B., Mogulkoc, R., & Baltaci, A. K. (2019). Molecular Mechanisms of Early and Late LTP. In *Neurochemical Research*. https://doi.org/10.1007/s11064-018-2695-4

Barco, A., Patterson, S., Alarcon, J. M., Gromova, P., Mata-Roig, M., Morozov, A., & Kandel, E. R. (2005). Gene expression profiling of facilitated L-LTP in VP16-CREB mice reveals that BDNF is critical for the maintenance of LTP and its synaptic capture. *Neuron*. https://doi.org/10.1016/j.neuron.2005.09.005

Benarroch, E. E. (2014). Brain glucose transporters: Implications for neurologic disease. *Neurology*. https://doi.org/10.1212/WNL.0000000000000328

Benito, E., & Barco, A. (2010). CREB's control of intrinsic and synaptic plasticity: implications for CREB-dependent memory models. In *Trends in Neurosciences*. https://doi.org/10.1016/j.tins.2010.02.001

Berdeaux, R. (2011). Metabolic regulation by salt inducible kinases. *Frontiers in Biology*. https://doi.org/10.1007/s11515-011-1148-0

Bito, H., Deisseroth, K., & Tsien, R. W. (1996). CREB phosphorylation and dephosphorylation: A Ca2+- and stimulus duration-dependent switch for hippocampal gene expression. *Cell*. https://doi.org/10.1016/S0092-8674(00)81816-4

Bittinger, M. A., McWhinnie, E., Meltzer, J., Iourgenko, V., Latario, B., Liu, X., Chen, C. H., Song, C., Garza, D., & Labow, M. (2004). Activation of cAMP response element-mediated gene expression by regulated nuclear transport of TORC Proteins. *Current Biology*. https://doi.org/10.1016/j.cub.2004.11.002

Bliss, T. V. P., & Collingridge, G. L. (2013). Expression of NMDA receptor-dependent LTP in the hippocampus: bridging the divide. In *Molecular brain*. https://doi.org/10.1186/1756-6606-6-5

Bosch, M., Castro, J., Saneyoshi, T., Matsuno, H., Sur, M., & Hayashi, Y. (2014). Structural and molecular remodeling of dendritic spine substructures during long-term potentiation. *Neuron*. https://doi.org/10.1016/j.neuron.2014.03.021

Bourtchuladze, R., Frenguelli, B., Blendy, J., Cioffi, D., Schutz, G., & Silva, A. J. (1994). Deficient long-term memory in mice with a targeted mutation of the cAMP-responsive element-binding protein. *Cell*. https://doi.org/10.1016/0092-8674(94)90400-6

Breit, A., Wicht, K., Boekhoff, I., Glas, E., Lauffer, L., Mückter, H., & Gudermann, T. (2016). Glucose enhances basal or melanocortin-induced cAMP-response element activity in hypothalamic cells. *Molecular Endocrinology*. https://doi.org/10.1210/me.2016-1001

Briand, L. A., Lee, B. G., Lelay, J., Kaestner, K. H., & Blendy, J. A. (2015). Serine 133 phosphorylation is not required for hippocampal CREB-mediated transcription and behavior. *Learning and Memory*. https://doi.org/10.1101/lm.037044.114

Broussard, J. A., Rappaz, B., Webb, D. J., & Brown, C. M. (2013). Fluorescence resonance energy transfer microscopy as demonstrated by measuring the activation of the serine/threonine kinase Akt. *Nature Protocols*. https://doi.org/10.1038/nprot.2012.147

Burkewitz, K., Morantte, I., Weir, H. J. M., Yeo, R., Zhang, Y., Huynh, F. K., Ilkayeva, O. R., Hirschey, M. D., Grant, A. R., & Mair, W. B. (2015). Neuronal CRTC-1 Governs Systemic Mitochondrial Metabolism and Lifespan via a Catecholamine Signal. *Cell*. https://doi.org/10.1016/j.cell.2015.02.004

Canettieri, G., Coni, S., Guardia, M. D., Nocerino, V., Antonucci, L., Di Magno, L. D., Screaton, R., Screpanti, I., Giannini, G., & Gulino, A. (2009). The coactivator CRTC1 promotes cell proliferation and transformation via AP-1. *Proceedings of the National Academy of Sciences of the United States of America*. https://doi.org/10.1073/pnas.0808749106

Cardinaux, J.-R., Notis, J. C., Zhang, Q., Vo, N., Craig, J. C., Fass, D. M., Brennan, R. G., & Goodman, R. H. (2000). Recruitment of CREB Binding Protein Is Sufficient for CREB-Mediated Gene Activation. *Molecular and Cellular Biology*. https://doi.org/10.1128/mcb.20.5.1546-1552.2000

Carriba, P., Pardo, L., Parra-Damas, A., Lichtenstein, M. P., Saura, C. A., Pujol, A., Masgrau, R., & Galea, E. (2012). ATP and noradrenaline activate CREB in astrocytes via noncanonical Ca2+ and cyclic AMP independent pathways. *GLIA*. https://doi.org/10.1002/glia.22352

Ch'ng, T. H., DeSalvo, M., Lin, P., Vashisht, A., Wohlschlegel, J. A., & Martin, K. C. (2015). Cell biological mechanisms of activity-dependent synapse to nucleus translocation of CRTC1 in neurons. *Frontiers in Molecular Neuroscience*. https://doi.org/10.3389/fnmol.2015.00048

Ch'Ng, T. H., Uzgil, B., Lin, P., Avliyakulov, N. K., O'Dell, T. J., & Martin, K. C. (2012). Activity-dependent transport of the transcriptional coactivator CRTC1 from synapse to nucleus. *Cell*. https://doi.org/10.1016/j.cell.2012.05.027

Cheng, A., Wan, R., Yang, J. L., Kamimura, N., Son, T. G., Ouyang, X., Luo, Y., Okun, E., & Mattson, M. P. (2012). Involvement of PGC-1α in the formation and maintenance of neuronal dendritic spines. *Nature Communications*. https://doi.org/10.1038/ncomms2238

Chrivia, J. C., Kwok, R. P. S., Lamb, N., Hagiwara, M., Montminy, M. R., & Goodman, R. H. (1993). Phosphorylated CREB binds specifically to the nuclear protein CBP. *Nature*. https://doi.org/10.1038/365855a0

Clark, K., MacKenzie, K. F., Petkevicius, K., Kristariyanto, Y., Zhang, J., Choi, H. G., Peggie, M., Plater, L., Pedrioli, P. G. A., McIver, E., Gray, N. S., Arthur, J. S. C., & Cohen, P. (2012). Phosphorylation of CRTC3 by the salt-inducible kinases controls the

interconversion of classically activated and regulatory macrophages. *Proceedings of the National Academy of Sciences of the United States of America*. https://doi.org/10.1073/pnas.1215450109

Cohen, P., Holmes, C. F. B., & Tsukitani, Y. (1990). Okadaic acid: a new probe for the study of cellular regulation. In *Trends in Biochemical Sciences*. https://doi.org/10.1016/0968-0004(90)90192-E

Comerford, K. M., Leonard, M. O., Karhausen, J., Carey, R., Colgan, S. P., & Taylor, C. T. (2003). Small ubiquitin-related modifier-1 modification mediates resolution of CREB-dependent responses to hypoxia. *Proceedings of the National Academy of Sciences of the United States of America*. https://doi.org/10.1073/pnas.0337412100

Conkright, M. D., Canettieri, G., Screaton, R., Guzman, E., Miraglia, L., Hogenesch, J. B., Montminy, M., & Jolla, L. (2003). *TORCs : Transducers of Regulated CREB Activity The Salk Institute for Biological Studies*. *12*, 413–423.

Conkright, M. D., Guzmán, E., Flechner, L., Su, A. I., Hogenesch, J. B., & Montminy, M. (2003). Genome-wide analysis of CREB target genes reveals a core promoter requirement for cAMP responsiveness. *Molecular Cell*. https://doi.org/10.1016/S1097-2765(03)00134-5

Dash, P. K., Hochner, B., & Kandel, E. R. (1990). Injection of the cAMP-responsive element into the nucleus of Aplysia sensory neurons blocks long-term facilitation. *Nature*. https://doi.org/10.1038/345718a0

De Armentia, M. L., Jancic, D., Olivares, R., Alarcon, J. M., Kandel, E. R., & Barco, A. (2007). cAMP response element-binding protein-mediated gene expression increases the intrinsic excitability of CA1 pyramidal neurons. *Journal of Neuroscience*. https://doi.org/10.1523/JNEUROSCI.3850-07.2007

Deak, M., Clifton, A. D., Lucocq, J. M., & Alessi, D. R. (1998). Mitogen- and stress-activated protein kinase-1 (MSK1) is directly activated by MAPK and SAPK2/p38, and may mediate activation of CREB. *EMBO Journal*. https://doi.org/10.1093/emboj/17.15.4426

Dentin, R., Hedrick, S., Xie, J., Yates, J., & Montminy, M. (2008). Hepatic glucose sensing via the CREB coactivator CRTC2. *Science*. https://doi.org/10.1126/science.1151363

Dentin, R., Liu, Y., Koo, S. H., Hedrick, S., Vargas, T., Heredia, J., Yates, J., & Montminy, M. (2007). Insulin modulates gluconeogenesis by inhibition of the coactivator TORC2. *Nature*. https://doi.org/10.1038/nature06128

Ding, G., Gong, Y., Eckel-Mahan, K. L., & Sun, Z. (2018). Central circadian clock regulates energy metabolism. In *Advances in Experimental Medicine and Biology*. https://doi.org/10.1007/978-981-13-1286-1_5

Du, K., & Montminy, M. (1998). CREB is a regulatory target for the protein kinase Akt/PKB. *Journal of Biological Chemistry*. https://doi.org/10.1074/jbc.273.49.32377

Eberhard, C. E., Fu, A., Reeks, C., & Screaton, R. A. (2013). CRTC2 is required for β-cell function and proliferation. *Endocrinology*. https://doi.org/10.1210/en.2012-2088

Eraso-Pichot, A., Larramona-Arcas, R., Vicario-Orri, E., Villalonga, R., Pardo, L., Galea, E., & Masgrau, R. (2017). CREB decreases astrocytic excitability by modifying subcellular calcium fluxes via the sigma-1 receptor. *Cellular and Molecular Life Sciences*. https://doi.org/10.1007/s00018-016-2397-5

España, J., Valero, J., Miñano-Molina, A. J., Masgrau, R., Martín, E., Guardia-Laguarta, C., Lleó, A., Giménez-Llort, L., Rodríguez-Alvarez, J., & Saura, C. A. (2010). β-amyloid disrupts activity-dependent gene transcription required for memory through the CREB coactivator CRTC1. *Journal of Neuroscience*. https://doi.org/10.1523/JNEUROSCI.2154-10.2010

Felinski, E. A., & Quinn, P. G. (2001). The coactivator dTAFII110/hTAFII135 is sufficient to recruit a polymerase complex and activate basal transcription mediated by CREB. *Proceedings of the National Academy of Sciences of the United States of America*. https://doi.org/10.1073/pnas.241337698

Ferreri, K., Gill, G., & Montminy, M. (1994). The cAMP-regulated transcription factor CREB interacts with a component of the TFIID complex. *Proceedings of the National Academy of Sciences of the United States of America*. https://doi.org/10.1073/pnas.91.4.1210

Finsterwald, C., Fiumelli, H., Cardinaux, J. R., & Martin, J. L. (2010). Regulation of dendritic development by BDNF requires activation of CRTC1 by glutamate. *Journal of Biological Chemistry*. https://doi.org/10.1074/jbc.M110.125740

Gao, W. W., Tang, H. M. V., Cheng, Y., Chan, C. P., Chan, C. P., & Jin, D. Y. (2018). Suppression of gluconeogenic gene transcription by SIK1-induced ubiquitination and degradation of CRTC1. *Biochimica et Biophysica Acta - Gene Regulatory Mechanisms*. https://doi.org/10.1016/j.bbagrm.2018.01.021

Ginty, D. D., Bonni, A., & Greenberg, M. E. (1994). Nerve growth factor activates a Ras-dependent protein kinase that stimulates c-fos transcription via phosphorylation of CREB. *Cell*. https://doi.org/10.1016/0092-8674(94)90055-8

Gonzalez, G. A., & Montminy, M. R. (1989). Cyclic AMP stimulates somatostatin gene transcription by phosphorylation of CREB at serine 133. *Cell*. https://doi.org/10.1016/0092-8674(89)90013-5

Group, E. S., & Microsystems, L. (2006). FRET Acceptor PhotoBleaching (AB) in LASAF. *Confocal Application Notes*.

Hagiwara, M., Alberts, A., Brindle, P., Meinkoth, J., Feramisco, J., Deng, T., Karin, M., Shenolikar, S., & Montminy, M. (1992). Transcriptional attenuation following cAMP induction requires PP-1-mediated dephosphorylation of CREB. *Cell*. https://doi.org/10.1016/0092-8674(92)90537-M

Han, H. S., Jung, C. Y., Yoon, Y. S., Choi, S., Choi, D., Kang, G., Park, K. G., Kim, S. T., & Koo, S. H. (2014). Arginine methylation of CRTC2 is critical in the transcriptional control of hepatic glucose metabolism. *Science Signaling*. https://doi.org/10.1126/scisignal.2004479

Han, J., Li, E., Chen, L., Zhang, Y., Wei, F., Liu, J., Deng, H., & Wang, Y. (2015). The CREB coactivator CRTC2 controls hepatic lipid metabolism by regulating SREBP1. *Nature*. https://doi.org/10.1038/nature14557

Hasel, P., Dando, O., Jiwaji, Z., Baxter, P., Todd, A. C., Heron, S., Márkus, N. M., McQueen, J., Hampton, D. W., Torvell, M., Tiwari, S. S., McKay, S., Eraso-Pichot, A., Zorzano, A., Masgrau, R., Galea, E., Chandran, S., Wyllie, D. J. A., Simpson, T. I., & Hardingham, G. E. (2017). Neurons and neuronal activity control gene expression in astrocytes to regulate their development and metabolism. *Nature Communications*. https://doi.org/10.1038/ncomms15132

Hatcher, J. P., Jones, D. N. C., Rogers, D. C., Hatcher, P. D., Reavill, C., Hagan, J. J., & Hunter, A. J. (2001). Development of SHIRPA to characterise the phenotype of gene-targeted mice. *Behavioural Brain Research*. https://doi.org/10.1016/S0166-4328(01)00275-3

Henneberger, C., Papouin, T., Oliet, S. H. R., & Rusakov, D. A. (2010). Long-term potentiation depends on release of d-serine from astrocytes. *Nature*. https://doi.org/10.1038/nature08673

Henriksson, E., Säll, J., Gormand, A., Wasserstrom, S., Morrice, N. A., Fritzen, A. M., Foretz, M., Campbell, D. G., Sakamoto, K., Ekelund, M., Degerman, E., Stenkula, K. G., & Göransson, O. (2015). SIK2 regulates CRTCs, HDAC4 and glucose uptake in adipocytes. *Journal of Cell Science*. https://doi.org/10.1242/jcs.153932

Hernandez, J. B., Chang, C., Leblanc, M., Grimm, D., Le Lay, J., Kaestner, K. H., Zheng, Y., & Montminy, M. (2015). The CREB/CRTC2 pathway modulates autoimmune disease by promoting Th17 differentiation. *Nature Communications*. https://doi.org/10.1038/ncomms8216

Herzig, S., Long, F., Jhala, U. S., Hedrick, S., Quinn, R., Bauer, A., Rudolph, D., Schutz, G., Yoon, C., Puigserver, P., Spiegelman, B., & Montminy, M. (2001). CREB regulates hepatic gluconeogenesis through the coactivator PGC-1. *Nature*. https://doi.org/10.1038/35093131

Hill, M. J., Suzuki, S., Segars, J. H., & Kino, T. (2016). CRTC2 is a coactivator of GR and couples

GR and CREB in the regulation of hepatic gluconeogenesis. *Molecular Endocrinology*. https://doi.org/10.1210/me.2015-1237

Ho, A., Morishita, W., Atasoy, D., Liu, X., Tabuchi, K., Hammer, R. E., Malenka, R. C., & Südhof, T. C. (2006). Genetic analysis of Mint/X11 proteins: Essential presynaptic functions of a neuronal adaptor protein family. *Journal of Neuroscience*. https://doi.org/10.1523/JNEUROSCI.2855-06.2006

Hogan, M. F., Ravnskjaer, K., Matsumura, S., Huising, M. O., Hull, R. L., Kahn, S. E., & Montminy, M. (2015). Hepatic insulin resistance following chronic activation of the CREB coactivator CRTC2. *Journal of Biological Chemistry*. https://doi.org/10.1074/jbc.M115.679266

Horton, J. D., Goldstein, J. L., & Brown, M. S. (2002). SREBPs: activators of the complete program of cholesterol and fatty acid synthesis in the liver. *Journal of Clinical Investigation*. https://doi.org/10.1172/jci15593

Iguchi-Ariga, S. M., & Schaffner, W. (1989). CpG methylation of the cAMP-responsive enhancer/promoter sequence TGACGTCA abolishes specific factor binding as well as transcriptional activation. *Genes & Development*. https://doi.org/10.1101/gad.3.5.612

Iijima, K., Zhao, L., Shenton, C., & Iijima-Ando, K. (2009). Regulation of energy stores and feeding by neuronal and peripheral CREB activity in Drosophila. *PLoS ONE*. https://doi.org/10.1371/journal.pone.0008498

Iourgenko, V., Zhang, W., Mickanin, C., Daly, I., Jiang, C., Hexham, J. M., Orth, A. P., Miraglia, L., Meltzer, J., Garza, D., Chirn, G. W., McWhinnie, E., Cohen, D., Skelton, J., Terry, R., Yu, Y., Bodian, D., Buxton, F. P., Zhu, J., … Labow, M. A. (2003). Identification of a family of cAMP response element-binding protein coactivators by genome-scale functional analysis in mammalian cells. *Proceedings of the National Academy of Sciences of the United States of America*. https://doi.org/10.1073/pnas.1932773100

Jagannath, A., Butler, R., Godinho, S. I. H., Couch, Y., Brown, L. A., Vasudevan, S. R., Flanagan, K. C., Anthony, D., Churchill, G. C., Wood, M. J. A., Steiner, G., Ebeling, M., Hossbach, M., Wettstein, J. G., Duffield, G. E., Gatti, S., Hankins, M. W., Foster, R. G., & Peirson, S. N. (2013). The CRTC1-SIK1 pathway regulates entrainment of the circadian clock. *Cell*. https://doi.org/10.1016/j.cell.2013.08.004

Jansson, D., Ng, A. C. H., Fu, A., Depatie, C., Al Azzabi, M., & Screaton, R. A. (2008). Glucose controls CREB activity in islet cells via regulated phosphorylation of TORC2. *Proceedings of the National Academy of Sciences of the United States of America*. https://doi.org/10.1073/pnas.0800796105

Jeong, H., Cohen, D. E., Cui, L., Supinski, A., Savas, J. N., Mazzulli, J. R., Yates, J. R., Bordone, L., Guarente, L., & Krainc, D. (2012). Sirt1 mediates neuroprotection from mutant huntingtin by activation of the TORC1 and CREB transcriptional pathway. *Nature Medicine*. https://doi.org/10.1038/nm.2559

Johannessen, M., Delghandi, M. P., & Moens, U. (2004). What turns CREB on? In *Cellular Signalling*. https://doi.org/10.1016/j.cellsig.2004.05.001

Jurek, B., Slattery, D. A., Hiraoka, Y., Liu, Y., Nishimori, K., Aguilera, G., Neumann, I. D., & Van Den Burg, E. H. (2015). Oxytocin regulates stress-induced Crf gene transcription through creb-regulated transcription coactivator 3. *Journal of Neuroscience*. https://doi.org/10.1523/JNEUROSCI.1345-14.2015

Kageyama, K., & Suda, T. (2010). Transcriptional regulation of hypothalamic corticotropin-releasing factor gene. In *Vitamins and hormones*. https://doi.org/10.1016/S0083-6729(10)82016-3

Katoh, Y., Takemori, H., Lin, X. Z., Tamura, M., Muraoka, M., Satoh, T., Tsuchiya, Y., Min, L., Doi, J., Miyauchi, A., Witters, L. A., Nakamura, H., & Okamoto, M. (2006). Silencing the constitutive active transcription factor CREB by the LKB1-SIK signaling cascade. *FEBS Journal*. https://doi.org/10.1111/j.1742-4658.2006.05291.x

Kaushik, R., Grochowska, K. M., Butnaru, I., & Kreutz, M. R. (2014). Protein trafficking from synapse to nucleus in control of activity-dependent gene expression. In *Neuroscience*. https://doi.org/10.1016/j.neuroscience.2014.09.011

Kee, B. L., Arias, J., & Montminy, M. R. (1996). Adaptor-mediated recruitment of RNA polymerase II to a signal-dependent activator. *Journal of Biological Chemistry*. https://doi.org/10.1074/jbc.271.5.2373

Kenworthy, A. K. (2001). Imaging protein-protein interactions using fluorescence resonance energy transfer microscopy. *Methods*. https://doi.org/10.1006/meth.2001.1189

Kim, S.-J., Nian, C., Widenmaier, S., & McIntosh, C. H. S. (2008). Glucose-Dependent Insulinotropic Polypeptide-Mediated Up-Regulation of -Cell Antiapoptotic Bcl-2 Gene Expression Is Coordinated by Cyclic AMP (cAMP) Response Element Binding Protein (CREB) and cAMP-Responsive CREB Coactivator 2. *Molecular and Cellular Biology*. https://doi.org/10.1128/mcb.00325-07

Kim, Y. H., Yoo, H., Hong, A. R., Kwon, M., Kang, S. W., Kim, K., & Song, Y. (2018). NEDD4L limits cAMP signaling through ubiquitination of CREB-regulated transcription coactivator 3. *FASEB Journal*. https://doi.org/10.1096/fj.201701406R

Kogan, J. H., Frankland, P. W., Blendy, J. A., Coblentz, J., Marowitz, Z., Schütz, G., & Silva, A.

J. (1997). Spaced training induces normal long-term memory in CREB mutant mice. *Current Biology*. https://doi.org/10.1016/S0960-9822(06)00022-4

Kogan, J. H., Frankland, P. W., & Silva, A. J. (2000). Long-term memory underlying hippocampus-dependent social recognition in mice. *Hippocampus*. https://doi.org/10.1002/(SICI)1098-1063(2000)10:1<47::AID-HIPO5>3.0.CO;2-6

Koo, S. H., Flechner, L., Qi, L., Zhang, X., Screaton, R. A., Jeffries, S., Hedrick, S., Xu, W., Boussouar, F., Brindle, P., Takemori, H., & Montminy, M. (2005). The CREB coactivator TORC2 is a key regulator of fasting glucose metabolism. *Nature*. https://doi.org/10.1038/nature03967

Koppel, I., Jaanson, K., Klasche, A., Tuvikene, J., Tiirik, T., Pärn, A., & Timmusk, T. (2018). Dopamine cross-reacts with adrenoreceptors in cortical astrocytes to induce BDNF expression, CREB signaling and morphological transformation. *GLIA*. https://doi.org/10.1002/glia.23238

Kornhauser, J. M., Cowan, C. W., Shaywitz, A. J., Dolmetsch, R. E., Griffith, E. C., Hu, L. S., Haddad, C., Xia, Z., & Greenberg, M. E. (2002). CREB transcriptional activity in neurons is regulated by multiple, calcium-specific phosphorylation events. *Neuron*. https://doi.org/10.1016/S0896-6273(02)00655-4

Kovács, K. A., Steullet, P., Steinmann, M., Do, K. Q., Magistretti, P. J., Halfon, O., & Cardinaux, J. R. (2007). TORC1 is a calcium- and cAMP-sensitive coincidence detector involved in hippocampal long-term synaptic plasticity. *Proceedings of the National Academy of Sciences of the United States of America*. https://doi.org/10.1073/pnas.0607524104

Kwok, R. P. S., Lundblad, J. R., Chrivia, J. C., Richards, J. P., Bächinger, H. P., Brennan, R. G., Roberts, S. G. E., Green, M. R., & Goodman, R. H. (1994). Nuclear protein CBP is a coactivator for the transcription factor CREB. *Nature*. https://doi.org/10.1038/370223a0

Lamarre-Vincent, N., & Hsieh-Wilson, L. C. (2003). Dynamic glycosylation of the transcription factor CREB: A potential role in gene regulation. *Journal of the American Chemical Society*. https://doi.org/10.1021/ja028200t

Lamprecht, R., Hazvi, S., & Dudai, Y. (1997). cAMP response element-binding protein in the amygdala is required for long- but not short-term conditioned taste aversion memory. *Journal of Neuroscience*. https://doi.org/10.1523/jneurosci.17-21-08443.1997

Le Lay, J., Tuteja, G., White, P., Dhir, R., Ahima, R., & Kaestner, K. H. (2009). CRTC2 (TORC2) Contributes to the Transcriptional Response to Fasting in the Liver but Is Not Required for the Maintenance of Glucose Homeostasis. *Cell Metabolism*. https://doi.org/10.1016/j.cmet.2009.06.006

Lee, B., Aiqing Li, Hansen, K. F., Ruifeng Cao, Jae Hwa Yoon, & Obrietan, K. (2010). CREB influences timing and entrainment of the SCN circadian clock. *Journal of Biological Rhythms*. https://doi.org/10.1177/0748730410381229

Lee, M. W., Chanda, D., Yang, J., Oh, H., Kim, S. S., Yoon, Y. S., Hong, S., Park, K. G., Lee, I. K., Choi, C. S., Hanson, R. W., Choi, H. S., & Koo, S. H. (2010). Regulation of Hepatic Gluconeogenesis by an ER-Bound Transcription Factor, CREBH. *Cell Metabolism*. https://doi.org/10.1016/j.cmet.2010.02.016

Lerner, R. G., Depatie, C., Rutter, G. A., Screaton, R. A., & Balthasar, N. (2009). A role for the CREB co-activator CRTC2 in the hypothalamic mechanisms linking glucose sensing with gene regulation. *EMBO Reports*. https://doi.org/10.1038/embor.2009.177

Li, S., Zhang, C., Takemori, H., Zhou, Y., & Xiong, Z.-Q. (2009). TORC1 regulates activity-dependent CREB-target gene transcription and dendritic growth of developing cortical neurons. *The Journal of Neuroscience : The Official Journal of the Society for Neuroscience*, *29*(8), 2334–2343. https://doi.org/10.1523/JNEUROSCI.2296-08.2009

Lisman, J., Cooper, K., Sehgal, M., & Silva, A. J. (2018). Memory formation depends on both synapse-specific modifications of synaptic strength and cell-specific increases in excitability. In *Nature Neuroscience*. https://doi.org/10.1038/s41593-018-0076-6

Liu, Y., Dentin, R., Chen, D., Hedrick, S., Ravnskjaer, K., Schenk, S., Milne, J., Meyers, D. J., Cole, P., Yates, J., Olefsky, J., Guarente, L., & Montminy, M. (2008). A fasting inducible switch modulates gluconeogenesis via activator/coactivator exchange. *Nature*. https://doi.org/10.1038/nature07349

Lonze, B. E., & Ginty, D. D. (2002). Function and regulation of CREB family transcription factors in the nervous system. In *Neuron*. https://doi.org/10.1016/S0896-6273(02)00828-0

Lonze, B. E., Riccio, A., Cohen, S., & Ginty, D. D. (2002). Apoptosis, axonal growth defects, and degeneration of peripheral neurons in mice lacking CREB. *Neuron*. https://doi.org/10.1016/S0896-6273(02)00686-4

Lu, B., Nagappan, G., & Lu, Y. (2015). BDNF and synaptic plasticity, cognitive function, and dysfunction. *Handbook of Experimental Pharmacology*. https://doi.org/10.1007/978-3-642-45106-5_9

Lu, Q., Hutchins, A. E., Doyle, C. M., Lundblad, J. R., & Kwok, R. P. S. (2003). Acetylation of cAMP-responsive element-binding protein (CREB) by CREB-binding protein enhances CREB-dependent transcription. *Journal of Biological Chemistry*. https://doi.org/10.1074/jbc.M300546200

Luo, Q., Viste, K., Urday-Zaa, J. C., Kumar, G. S., Tsai, W. W., Talai, A., Mayo, K. E.,

Montminy, M., & Radhakrishnan, I. (2012). Mechanism of CREB recognition and coactivation by the CREB-regulated transcriptional coactivator CRTC2. *Proceedings of the National Academy of Sciences of the United States of America*. https://doi.org/10.1073/pnas.1219028109

Lv, S., Qiu, X., Li, J., Li, W., Zhang, C., Zhang, Z. N., & Luan, B. (2016). Suppression of CRTC2-mediated hepatic gluconeogenesis by TRAF6 contributes to hypoglycemia in septic shock. *Cell Discovery*. https://doi.org/10.1038/celldisc.2016.46

MacKenzie, K. F., Clark, K., Naqvi, S., McGuire, V. A., Nöehren, G., Kristariyanto, Y., van den Bosch, M., Mudaliar, M., McCarthy, P. C., Pattison, M. J., Pedrioli, P. G. A., Barton, G. J., Toth, R., Prescott, A., & Arthur, J. S. C. (2013). PGE 2 Induces Macrophage IL-10 Production and a Regulatory-like Phenotype via a Protein Kinase A–SIK–CRTC3 Pathway . *The Journal of Immunology*. https://doi.org/10.4049/jimmunol.1202462

Magistretti, P. J., & Pellerin, L. (1996). Cellular Bases of Brain Energy Metabolism and Their Relevance to Functional Brain Imaging: Evidence for a Prominent Role of Astrocytes. *Cerebral Cortex*. https://doi.org/10.1093/cercor/6.1.50

Mahmoud, S., Gharagozloo, M., Simard, C., & Gris, D. (2019). Astrocytes Maintain Glutamate Homeostasis in the CNS by Controlling the Balance between Glutamate Uptake and Release. *Cells*. https://doi.org/10.3390/cells8020184

Mair, W., Morantte, I., Rodrigues, A. P. C., Manning, G., Montminy, M., Shaw, R. J., & Dillin, A. (2011). Lifespan extension induced by AMPK and calcineurin is mediated by CRTC-1 and CREB. *Nature*. https://doi.org/10.1038/nature09706

Matsumoto, K., Yamamoto, T., Kurachi, H., Nishio, Y., Takeda, T., Homma, H., Morishige, K. I., Miyake, A., & Murata, Y. (1998). Human chorionic gonadotropin-α gene is transcriptionally activated by epidermal growth factor through cAMP response element in trophoblast cells. *Journal of Biological Chemistry*. https://doi.org/10.1074/jbc.273.14.7800

Mattson, M. P. (2008). Glutamate and neurotrophic factors in neuronal plasticity and disease. *Annals of the New York Academy of Sciences*. https://doi.org/10.1196/annals.1418.005

Mátyus, L. (1992). New trends in photobiology. Fluorescence resonance energy transfer measurements on cell surfaces. A spectroscopic tool for determining protein interactions. In *Journal of Photochemistry and Photobiology, B: Biology*. https://doi.org/10.1016/1011-1344(92)85039-W

Mayr, B., & Montminy, M. (2001). Transcriptional regulation by the phosphorylation-dependent factor creb. In *Nature Reviews Molecular Cell Biology*. https://doi.org/10.1038/35085068

McTague, J., Amyotte, N., Kanyo, R., Ferguson, M., Chik, C. L., & Ho, A. K. (2012). Different

signaling mechanisms are involved in the norepinephrine- stimulated TORC1 and TORC2 nuclear translocation in rat pinealocytes. *Endocrinology*. https://doi.org/10.1210/en.2012-1315

Mengus, G., Fadloun, A., Kobi, D., Thibault, C., Perletti, L., Michel, I., & Davidson, I. (2005). TAF4 inactivation in embryonic fibroblasts activates TGFβ signalling and autocrine growth. *EMBO Journal*. https://doi.org/10.1038/sj.emboj.7600748

Murray, P. D., Kingsbury, T. J., & Krueger, B. K. (2009). Failure of Ca2+-activated, CREB-dependent transcription in astrocytes. *GLIA*. https://doi.org/10.1002/glia.20809

Navarrete, M., & Araque, A. (2010). Endocannabinoids potentiate synaptic transmission through stimulation of astrocytes. *Neuron*. https://doi.org/10.1016/j.neuron.2010.08.043

Newman, L. A., Korol, D. L., & Gold, P. E. (2011). Lactate produced by glycogenolysis in astrocytes regulates memory processing. *PLoS ONE*. https://doi.org/10.1371/journal.pone.0028427

Nonaka, M., Kim, R., Fukushima, H., Sasaki, K., Suzuki, K., Okamura, M., Ishii, Y., Kawashima, T., Kamijo, S., Takemoto-Kimura, S., Okuno, H., Kida, S., & Bito, H. (2014). Region-specific activation of CRTC1-CREB signaling mediates long-term fear memory. *Neuron*, *84*(1), 92–106. https://doi.org/10.1016/j.neuron.2014.08.049

Ogryzko, V. V., Schiltz, R. L., Russanova, V., Howard, B. H., & Nakatani, Y. (1996). The transcriptional coactivators p300 and CBP are histone acetyltransferases. *Cell*. https://doi.org/10.1016/S0092-8674(00)82001-2

Pardo, L., Schlüter, A., Valor, L. M., Barco, A., Giralt, M., Golbano, A., Hidalgo, J., Jia, P., Zhao, Z., Jové, M., Portero-Otin, M., Ruiz, M., Giménez-Llort, L., Masgrau, R., Pujol, A., & Galea, E. (2016). Targeted activation of CREB in reactive astrocytes is neuroprotective in focal acute cortical injury. *GLIA*. https://doi.org/10.1002/glia.22969

Pardo, L., Valor, L. M., Eraso-Pichot, A., Barco, A., Golbano, A., Hardingham, G. E., Masgrau, R., & Galea, E. (2017). CREB Regulates Distinct Adaptive Transcriptional Programs in Astrocytes and Neurons. *Scientific Reports*. https://doi.org/10.1038/s41598-017-06231-x

Park, J., Yoon, Y. S., Han, H. S., Kim, Y. H., Ogawa, Y., Park, K. G., Lee, C. H., Kim, S. T., & Koo, S. H. (2014). SIK2 is critical in the regulation of lipid homeostasis and adipogenesis in vivo. *Diabetes*. https://doi.org/10.2337/db13-1423

Park, P., Volianskis, A., Sanderson, T. M., Bortolotto, Z. A., Jane, D. E., Zhuo, M., Kaang, B. K., & Collingridge, G. L. (2014). NMDA receptor-dependent long-term potentiation comprises a family of temporally overlapping forms of synaptic plasticity that are induced by different patterns of stimulation. In *Philosophical Transactions of the Royal Society B: Biological*

Sciences. https://doi.org/10.1098/rstb.2013.0131

Parker, D., Jhala, U. S., Radhakrishnan, I., Yaffe, M. B., Reyes, C., Shulman, A. I., Cantley, L. C., Wright, P. E., & Montminy, M. (1998). Analysis of an activator:Coactivator complex reveals an essential role for secondary structure in transcriptional activation. *Molecular Cell*. https://doi.org/10.1016/S1097-2765(00)80279-8

Parpura, V., Basarsky, T. A., Liu, F., Jeftinija, K., Jeftinija, S., & Haydon, P. G. (1994). Glutamate-mediated astrocyte-neuron signalling. *Nature*. https://doi.org/10.1038/369744a0

Parra-Damas, A., Chen, M., Enriquez-Barreto, L., Ortega, L., Acosta, S., Perna, J. C., Fullana, M. N., Aguilera, J., Rodríguez-Alvarez, J., & Saura, C. A. (2017). CRTC1 Function During Memory Encoding Is Disrupted in Neurodegeneration. *Biological Psychiatry*. https://doi.org/10.1016/j.biopsych.2016.06.025

Parra-Damas, A., Rubió-Ferrarons, L., Shen, J., & Saura, C. A. (2017). CRTC1 mediates preferential transcription at neuronal activity-regulated CRE/TATA promoters. *Scientific Reports*. https://doi.org/10.1038/s41598-017-18215-y

Parra-Damas, A., & Saura, C. A. (2019). Synapse-to-Nucleus Signaling in Neurodegenerative and Neuropsychiatric Disorders. In *Biological Psychiatry*. https://doi.org/10.1016/j.biopsych.2019.01.006

Parra-Damas, A., Valero, J., Chen, M., España, J., Martín, E., Ferrer, I., Rodríguez-Alvarez, J., & Saura, C. a. (2014). Crtc1 activates a transcriptional program deregulated at early Alzheimer's disease-related stages. *The Journal of Neuroscience : The Official Journal of the Society for Neuroscience*, *34*(17), 5776–5787. https://doi.org/10.1523/JNEUROSCI.5288-13.2014

Patel, K., Foretz, M., Marion, A., Campbell, D. G., Gourlay, R., Boudaba, N., Tournier, E., Titchenell, P., Peggie, M., Deak, M., Wan, M., Kaestner, K. H., Göransson, O., Viollet, B., Gray, N. S., Birnbaum, M. J., Sutherland, C., & Sakamoto, K. (2014). The LKB1-salt-inducible kinase pathway functions as a key gluconeogenic suppressor in the liver. *Nature Communications*. https://doi.org/10.1038/ncomms5535

Pettitt, S. J., Liang, Q., Rairdan, X. Y., Moran, J. L., Prosser, H. M., Beier, D. R., Lloyd, K. C., Bradley, A., & Skarnes, W. C. (2009). Agouti C57BL/6N embryonic stem cells for mouse genetic resources. *Nature Methods*. https://doi.org/10.1038/nmeth.1342

Pfaffl, M. W. (2001). A new mathematical model for relative quantification in real-time RT-PCR. *Nucleic Acids Research*. https://doi.org/10.1093/nar/29.9.e45

Pierrat, B., Da Silva Correia, J., Mary, J. L., Tomás-Zuber, M., & Lesslauer, W. (1998). RSK-B, a novel ribosomal S6 kinase family member, is a CREB kinase under dominant control of

p38α mitogen-activated protein kinase (p38α(MAPK)). *Journal of Biological Chemistry*. https://doi.org/10.1074/jbc.273.45.29661

Pittenger, C., Huang, Y. Y., Paletzki, R. F., Bourtchouladze, R., Scanlin, H., Vronskaya, S., & Kandel, E. R. (2002). Reversible inhibition of CREB/ATF transcription factors in region CA1 of the dorsal hippocampus disrupts hippocampus-dependent spatial memory. *Neuron*. https://doi.org/10.1016/S0896-6273(02)00684-0

Prats-Puig, A., Soriano-Rodríguez, P., Oliveras, G., Carreras-Badosa, G., Espuña, S., Díaz-Roldán, F., De Zegher, F., Ibáñez, L., Bassols, J., Puig, T., & López-Bermejo, A. (2016). Soluble CRTC3: A newly identified protein released by adipose tissue that is associated with childhood obesity. *Clinical Chemistry*. https://doi.org/10.1373/clinchem.2015.249136

Ravnskjaer, K., Kester, H., Liu, Y., Zhang, X., Lee, D., Yates, J. R., & Montminy, M. (2007). Cooperative interactions between CBP and TORC2 confer selectivity to CREB target gene expression. *EMBO Journal*. https://doi.org/10.1038/sj.emboj.7601715

Rebelo, S., Santos, M., Martins, F., da Cruz e Silva, E. F., & da Cruz e Silva, O. A. B. (2015). Protein phosphatase 1 is a key player in nuclear events. In *Cellular Signalling*. https://doi.org/10.1016/j.cellsig.2015.08.007

Ricarte, F. R., Le Henaff, C., Kolupaeva, V. G., Gardella, T. J., & Partridge, N. C. (2018). Parathyroid hormone(1–34) and its analogs differentially modulate osteoblastic Rankl expression via PKA/SIK2/SIK3 and PP1/PP2A–CRTC3 signaling. *Journal of Biological Chemistry*. https://doi.org/10.1074/jbc.RA118.004751

Riccio, A., Ahn, S., Davenport, C. M., Blendy, J. A., & Ginty, D. D. (1999). Mediation by a CREB family transcription factor of NGF-dependent survival of sympathetic neurons. *Science*. https://doi.org/10.1126/science.286.5448.2358

Riera, C. E., Huising, M. O., Follett, P., Leblanc, M., Halloran, J., Van Andel, R., De Magalhaes Filho, C. D., Merkwirth, C., & Dillin, A. (2014). TRPV1 pain receptors regulate longevity and metabolism by neuropeptide signaling. *Cell*. https://doi.org/10.1016/j.cell.2014.03.051

Rodón, L., Svensson, R. U., Wiater, E., Chun, M. G. H., Tsai, W. W., Eichner, L. J., Shaw, R. J., & Montminy, M. (2019). The CREB coactivator CRTC2 promotes oncogenesis in LKB1-mutant non–small cell lung cancer. *Science Advances*. https://doi.org/10.1126/sciadv.aaw6455

Rudolph, D., Tafuri, A., Gass, P., Hämmerling, G. J., Arnold, B., & Schütz, G. (1998). Impaired fetal T cell development and perinatal lethality in mice lacking the cAMP response element binding protein. *Proceedings of the National Academy of Sciences of the United States of America*. https://doi.org/10.1073/pnas.95.8.4481

Ruijter, J. M., Ramakers, C., Hoogaars, W. M. H., Karlen, Y., Bakker, O., van den hoff, M. J. B., & Moorman, A. F. M. (2009). Amplification efficiency: Linking baseline and bias in the analysis of quantitative PCR data. *Nucleic Acids Research*. https://doi.org/10.1093/nar/gkp045

Sakamoto, K., Norona, F. E., Alzate-Correa, D., Scarberry, D., Hoyt, K. R., & Obrietan, K. (2013). Clock and light regulation of the CREB coactivator CRTC1 in the suprachiasmatic circadian clock. *Journal of Neuroscience*. https://doi.org/10.1523/JNEUROSCI.4202-12.2013

Saluja, D., Vassallo, M. F., & Tanese, N. (1998). Distinct Subdomains of Human TAF II 130 Are Required for Interactions with Glutamine-Rich Transcriptional Activators . *Molecular and Cellular Biology*. https://doi.org/10.1128/mcb.18.10.5734

Saura, C. A., & Cardinaux, J. R. (2017). Emerging Roles of CREB-Regulated Transcription Coactivators in Brain Physiology and Pathology. In *Trends in Neurosciences*. https://doi.org/10.1016/j.tins.2017.10.002

Saura, C. a, & Valero, J. (2011). The role of CREB signaling in Alzheimer's disease and other cognitive disorders. *Reviews in the Neurosciences*, *22*(2), 153–169. https://doi.org/10.1515/RNS.2011.018

Schlag, B. D., Vondrasek, J. R., Munir, M., Kalandadze, A., Zelenaia, O. A., Rothstein, J. D., & Robinson, M. B. (1998). Regulation of the glial Na+-dependent glutamate transporters by cyclic AMP analogs and neurons. *Molecular Pharmacology*. https://doi.org/10.1124/mol.53.3.355

Schumacher, M. A., Goodman, R. H., & Brennan, R. G. (2000). The structure of a CREB bZIP·somatostatin CRE complex reveals the basis for selective dimerization and divalent cation-enhanced DNA binding. *Journal of Biological Chemistry*. https://doi.org/10.1074/jbc.M007293200

Screaton, R. A., Conkright, M. D., Katoh, Y., Best, J. L., Canettieri, G., Jeffries, S., Guzman, E., Niessen, S., Yates, J. R., Takemori, H., Okamoto, M., & Montminy, M. (2004). The CREB coactivator TORC2 functions as a calcium- and cAMP-sensitive coincidence detector. *Cell*. https://doi.org/10.1016/j.cell.2004.09.015

Segarra-Mondejar, M., Casellas-Díaz, S., Ramiro-Pareta, M., Müller-Sánchez, C., Martorell-Riera, A., Hermelo, I., Reina, M., Aragonés, J., Martínez-Estrada, O. M., & Soriano, F. X. (2018). Synaptic activity-induced glycolysis facilitates membrane lipid provision and neurite outgrowth. *The EMBO Journal*. https://doi.org/10.15252/embj.201797368

Serrano, A., Haddjeri, N., Lacaille, J. C., & Robitaille, R. (2006). GABAergic network activation

of glial cells underlies hippocampal heterosynaptic depression. *Journal of Neuroscience*. https://doi.org/10.1523/JNEUROSCI.5255-05.2006

Shan, T., Xiong, Y., Zhang, P., Li, Z., Jiang, Q., Bi, P., Yue, F., Yang, G., Wang, Y., Liu, X., & Kuang, S. (2016). Lkb1 controls brown adipose tissue growth and thermogenesis by regulating the intracellular localization of CRTC3. *Nature Communications*. https://doi.org/10.1038/ncomms12205

Shanware, N. P., Trinh, A. T., Williams, L. M., & Tibbetts, R. S. (2007). Coregulated ataxia telangiectasia-mutated and casein kinase sites modulate cAMP-response element-binding protein-coactivator interactions in response to DNA damage. *Journal of Biological Chemistry*. https://doi.org/10.1074/jbc.M610674200

Shaywitz, A. J., Dove, S. L., Kornhauser, J. M., Hochschild, A., & Greenberg, M. E. (2000). Magnitude of the CREB-Dependent Transcriptional Response Is Determined by the Strength of the Interaction between the Kinase-Inducible Domain of CREB and the KIX Domain of CREB-Binding Protein. *Molecular and Cellular Biology*. https://doi.org/10.1128/mcb.20.24.9409-9422.2000

Shen, R., Wang, B., Giribaldi, M. G., Ayres, J., Thomas, J. B., & Montminy, M. (2016). Neuronal energy-sensing pathway promotes energy balance by modulating disease tolerance. *Proceedings of the National Academy of Sciences of the United States of America*. https://doi.org/10.1073/pnas.1606106113

Sheng, M., Thompson, M. A., & Greenberg, M. E. (1991). CREB: A Ca2+-regulated transcription factor phosphorylated by calmodulin-dependent kinases. *Science*. https://doi.org/10.1126/science.1646483

Shi, Y., Venkataraman, S. L., Dodson, G. E., Mabb, A. M., LeBlanc, S., & Tibbetts, R. S. (2004). Direct regulation of CREB transcriptional activity by ATM in response to genotoxic stress. *Proceedings of the National Academy of Sciences of the United States of America*. https://doi.org/10.1073/pnas.0307718101

Simpson, I. A., Chundu, K. R., Davies-Hill, T., Honer, W. G., & Davies, P. (1994). Decreased concentrations of GLUT1 and GLUT3 glucose transporters in the brains of patients with Alzheimer's disease. *Annals of Neurology*. https://doi.org/10.1002/ana.410350507

Snapp, E. L., & Hegde, R. S. (2006). Rational Design and Evaluation of FRET Experiments to Measure Protein Proximities in Cells. *Current Protocols in Cell Biology*. https://doi.org/10.1002/0471143030.cb1709s32

Song, Yihui, Zhai, L., Valencia Swain, J., Chen, Y., Wang, P., Chen, L., Liu, Y., & Xiang, S. (2018). Structural Insights into the CRTC2–CREB Complex Assembly on CRE. *Journal of*

Molecular Biology. https://doi.org/10.1016/j.jmb.2018.04.038

Song, Youngsup, Altarejos, J., Goodarzi, M. O., Inoue, H., Guo, X., Berdeaux, R., Kim, J. H., Goode, J., Igata, M., Paz, J. C., Hogan, M. F., Singh, P. K., Goebel, N., Vera, L., Miller, N., Cui, J., Jones, M. R., Chen, Y. D. I., Taylor, K. D., … Montminy, M. (2010). CRTC3 links catecholamine signalling to energy balance. *Nature*. https://doi.org/10.1038/nature09564

Sonntag, T., Moresco, J. J., Vaughan, J. M., Matsumura, S., Yates, J. R., & Montminy, M. (2017). Analysis of a cAMP regulated coactivator family reveals an alternative phosphorylation motif for AMPK family members. *PLoS ONE*. https://doi.org/10.1371/journal.pone.0173013

Sonntag, T., Ostojić, J., Vaughan, J. M., Moresco, J. J., Yoon, Y. S., Yates, J. R., & Montminy, M. (2019). Mitogenic Signals Stimulate the CREB Coactivator CRTC3 through PP2A Recruitment. *IScience*. https://doi.org/10.1016/j.isci.2018.12.012

St-Pierre, J., Drori, S., Uldry, M., Silvaggi, J. M., Rhee, J., Jäger, S., Handschin, C., Zheng, K., Lin, J., Yang, W., Simon, D. K., Bachoo, R., & Spiegelman, B. M. (2006). Suppression of Reactive Oxygen Species and Neurodegeneration by the PGC-1 Transcriptional Coactivators. *Cell*. https://doi.org/10.1016/j.cell.2006.09.024

Steinman, M. Q., Gao, V., & Alberini, C. M. (2016). The role of lactate-mediated metabolic coupling between astrocytes and neurons in long-term memory formation. In *Frontiers in Integrative Neuroscience*. https://doi.org/10.3389/fnint.2016.00010

Stepensky, D. (2007). FRETcalc plugin for calculation of FRET in non-continuous intracellular compartments. *Biochemical and Biophysical Research Communications*. https://doi.org/10.1016/j.bbrc.2007.05.180

Sun, P., Enslen, H., Myung, P. S., & Maurer, R. A. (1994). Differential activation of CREB by Ca2+/calmodulin-dependent protein kinases type II and type IV involves phosphorylation of a site that negatively regulates activity. *Genes and Development*. https://doi.org/10.1101/gad.8.21.2527

Suzuki, A., Stern, S. A., Bozdagi, O., Huntley, G. W., Walker, R. H., Magistretti, P. J., & Alberini, C. M. (2011). Astrocyte-neuron lactate transport is required for long-term memory formation. *Cell*. https://doi.org/10.1016/j.cell.2011.02.018

Takasaki, I., Takarada, S., Tatsumi, S., Azegami, A., Yasuda, M., Fukuchi, M., Tabuchi, A., Kondo, T., Tabuchi, Y., & Tsuda, M. (2008). Extracellular adenosine 5′-triphosphate elicits the expression of brain-derived neurotrophic factor exon IV mRNA in rat astrocytes. *GLIA*. https://doi.org/10.1002/glia.20704

Tan, Y., Rouse, J., Zhang, A., Cariati, S., Cohen, P., & Comb, M. J. (1996). FGF and stress

regulate CREB and ATF-1 via a pathway involving p38 MAP kinase and MAPKAP kinase-2. *The EMBO Journal*. https://doi.org/10.1002/j.1460-2075.1996.tb00840.x

Tasoulas, J., Rodon, L., Kaye, F. J., Montminy, M., & Amelio, A. L. (2019). Adaptive Transcriptional Responses by CRTC Coactivators in Cancer. In *Trends in Cancer*. https://doi.org/10.1016/j.trecan.2018.12.002

Taylor, C. T., Furuta, G. T., Synnestvedt, K., & Colgan, S. P. (2000). Phosphorylation-dependent targeting of cAMP response element binding protein to the ubiquitin/proteasome pathway in hypoxia. *Proceedings of the National Academy of Sciences of the United States of America*. https://doi.org/10.1073/pnas.220211797

Than, T. A., Lou, H., Ji, C., Win, S., & Kaplowitz, N. (2011). Role of cAMP-responsive Element-binding Protein (CREB)-regulated Transcription Coactivator 3 (CRTC3) in the initiation of mitochondrial biogenesis and stress response in liver cells. *Journal of Biological Chemistry*. https://doi.org/10.1074/jbc.M111.240481

Tsien, J. Z., Chen, D. F., Gerber, D., Tom, C., Mercer, E. H., Anderson, D. J., Mayford, M., Kandel, E. R., & Tonegawa, S. (1996). Subregion- and cell type-restricted gene knockout in mouse brain. *Cell*. https://doi.org/10.1016/S0092-8674(00)81826-7

Uchida, S., Teubner, B. J. W., Hevi, C., Hara, K., Kobayashi, A., Dave, R. M., Shintaku, T., Jaikhan, P., Yamagata, H., Suzuki, T., Watanabe, Y., Zakharenko, S. S., & Shumyatsky, G. P. (2017). CRTC1 Nuclear Translocation Following Learning Modulates Memory Strength via Exchange of Chromatin Remodeling Complexes on the Fgf1 Gene. *Cell Reports*. https://doi.org/10.1016/j.celrep.2016.12.052

Uebi, T., Tamura, M., Horike, N., Hashimoto, Y. K., & Takemori, H. (2010). Phosphorylation of the CREB-specific coactivator TORC2 at Ser307 regulates its intracellular localization in COS-7 cells and in the mouse liver. *American Journal of Physiology - Endocrinology and Metabolism*. https://doi.org/10.1152/ajpendo.00525.2009

Viosca, J., De Armentia, M. L., Jancic, D., & Barco, A. (2009). Enhanced CREB-dependent gene expression increases the excitability of neurons in the basal amygdala and primes the consolidation of contextual and cued fear memory. *Learning and Memory*. https://doi.org/10.1101/lm.1254209

Viosca, J., Malleret, G., Bourtchouladze, R., Benito, E., Vronskava, S., Kandel, E. R., & Barco, A. (2009). Chronic enhancement of CREB activity in the hippocampus interferes with the retrieval of spatial information. *Learning and Memory*. https://doi.org/10.1101/lm.1220309

Volkenhoff, A., Weiler, A., Letzel, M., Stehling, M., Klämbt, C., & Schirmeier, S. (2015). Glial glycolysis is essential for neuronal survival in drosophila. *Cell Metabolism*.

https://doi.org/10.1016/j.cmet.2015.07.006

Wadzinski, B. E., Wheat, W. H., Jaspers, S., Peruski, L. F., Lickteig, R. L., Johnson, G. L., & Klemm, D. J. (1993). Nuclear protein phosphatase 2A dephosphorylates protein kinase A-phosphorylated CREB and regulates CREB transcriptional stimulation. *Molecular and Cellular Biology*. https://doi.org/10.1128/mcb.13.5.2822

Wang, Y., Inoue, H., Ravnskjaer, K., Viste, K., Miller, N., Liu, Y., Hedrick, S., Vera, L., & Montminy, M. (2010). Targeted disruption of the CREB coactivator Crtc2 increases insulin sensitivity. *Proceedings of the National Academy of Sciences of the United States of America*. https://doi.org/10.1073/pnas.0914897107

Wang, Y., Vera, L., Fischer, W. H., & Montminy, M. (2009). The CREB coactivator CRTC2 links hepatic ER stress and fasting gluconeogenesis. *Nature*. https://doi.org/10.1038/nature08111

Watts, A. G., Sanchez-Watts, G., Liu, Y., & Aguilera, G. (2011). The distribution of messenger rnas encoding the three isoforms of the transducer of regulated camp responsive element binding protein activity in the rat forebrain. *Journal of Neuroendocrinology*. https://doi.org/10.1111/j.1365-2826.2011.02178.x

Wen, A. Y., Sakamoto, K. M., & Miller, L. S. (2010). The Role of the Transcription Factor CREB in Immune Function. *The Journal of Immunology*. https://doi.org/10.4049/jimmunol.1001829

Wilson, E. N., Abela, A. R., Do Carmo, S., Allard, S., Marks, A. R., Welikovitch, L. A., Ducatenzeiler, A., Chudasama, Y., & Cuello, A. C. (2017). Intraneuronal Amyloid Beta Accumulation Disrupts Hippocampal CRTC1-Dependent Gene Expression and Cognitive Function in a Rat Model of Alzheimer Disease. *Cerebral Cortex (New York, N.Y. : 1991)*. https://doi.org/10.1093/cercor/bhv332

Wouters, F. S., Verveer, P. J., & Bastiaens, P. I. H. (2001). Imaging biochemistry inside cells. In *Trends in Cell Biology*. https://doi.org/10.1016/S0962-8924(01)01982-1

Wu, Z., Huang, X., Feng, Y., Handschin, C., Feng, Y., Gullicksen, P. S., Bare, O., Labow, M., Spiegelman, B., & Stevenson, S. C. (2006). Transducer of regulated CREB-binding proteins (TORCs) induce PGC-1α transcription and mitochondrial biogenesis in muscle cells. *Proceedings of the National Academy of Sciences of the United States of America*. https://doi.org/10.1073/pnas.0606714103

Xing, J., Ginty, D. D., & Greenberg, M. E. (1996). Coupling of the RAS-MAPK pathway to gene activation by RSK2, a growth factor-regulated CREB kinase. *Science*. https://doi.org/10.1126/science.273.5277.959

Xu, Z., Liu, J., You, W., Wang, Y., & Shan, T. (2019). Cold exposure induces nuclear translocation of CRTC3 in brown adipose tissue. *Journal of Cellular Biochemistry*. https://doi.org/10.1002/jcb.28189

Yin, J. C. P., Del Vecchio, M., Zhou, H., & Tully, T. (1995). CREB as a Memory Modulator: induced expression of a dCREB2 activator isoform enhances long-term memory in drosophila. *Cell*. https://doi.org/10.1016/0092-8674(95)90375-5

Yin, J. C. P., Wallach, J. S., Del Vecchio, M., Wilder, E. L., Zhou, H., Quinn, W. G., & Tully, T. (1994). Induction of a dominant negative CREB transgene specifically blocks long-term memory in Drosophila. *Cell*. https://doi.org/10.1016/0092-8674(94)90399-9

Yoon, Y. S., Lee, M. W., Ryu, D., Kim, J. H., Ma, H., Seo, W. Y., Kim, Y. N., Kim, S. S., Lee, C. H., Hunter, T., Choi, C. S., Montminy, M. R., & Koo, S. H. (2010). Suppressor of MEK null (SMEK)/protein phosphatase 4 catalytic subunit (PP4C) is a key regulator of hepatic gluconeogenesis. *Proceedings of the National Academy of Sciences of the United States of America*. https://doi.org/10.1073/pnas.1012665107

Yoon, Y. S., Tsai, W. W., De Velde, S. Van, Chen, Z., Lee, K. F., Morgan, D. A., Rahmouni, K., Matsumura, S., Wiater, E., Song, Y., & Montminy, M. (2018). cAMP-inducible coactivator CRTC3 attenuates brown adipose tissue thermogenesis. *Proceedings of the National Academy of Sciences of the United States of America*. https://doi.org/10.1073/pnas.1805257115

Yu, H., Saura, C. A., Choi, S. Y., Sun, L. D., Yang, X., Handler, M., Kawarabayashi, T., Younkin, L., Fedeles, B., Wilson, M. A., Younkin, S., Kandel, E. R., Kirkwood, A., & Shen, J. (2001). APP processing and synaptic plasticity in presenilin-1 conditional knockout mice. *Neuron*. https://doi.org/10.1016/S0896-6273(01)00417-2

Yun, C. Y., Hong, S. D., Lee, Y. H., Lee, J., Jung, D. E., Kim, G. H., Kim, S. H., Jung, J. K., Kim, K. H., Lee, H., Hong, J. T., Han, S. B., & Kim, Y. (2019). Nuclear entry of CRTC1 as druggable target of acquired pigmentary disorder. *Theranostics*. https://doi.org/10.7150/thno.30276

Zhang, X., Odom, D. T., Koo, S. H., Conkright, M. D., Canettieri, G., Best, J., Chen, H., Jenner, R., Herbolsheimer, E., Jacobsen, E., Kadam, S., Ecker, J. R., Emerson, B., Hogenesch, J. B., Unterman, T., Young, R. A., & Montminy, M. (2005). Genome-wide analysis of cAMP-response element binding protein occupancy, phosphorylation, and target gene activation in human tissues. *Proceedings of the National Academy of Sciences of the United States of America*. https://doi.org/10.1073/pnas.0501076102

Zhang, Y., Chen, K., Sloan, S. A., Bennett, M. L., Scholze, A. R., O'Keeffe, S., Phatnani, H. P.,

Guarnieri, P., Caneda, C., Ruderisch, N., Deng, S., Liddelow, S. A., Zhang, C., Daneman, R., Maniatis, T., Barres, B. A., & Wu, J. Q. (2014). An RNA-sequencing transcriptome and splicing database of glia, neurons, and vascular cells of the cerebral cortex. *Journal of Neuroscience*. https://doi.org/10.1523/JNEUROSCI.1860-14.2014

Zhou, Y., Wu, H., Li, S., Chen, Q., Cheng, X. W., Zheng, J., Takemori, H., & Xiong, Z. Q. (2006). Requirement of TORC1 for late-phase long-term potentiation in the hippocampus. *PLoS ONE*. https://doi.org/10.1371/journal.pone.0000016

XI Acknowledgements

I ja per acabar, m'agradaria dedicar unes paraules a totes les persones que he anat trobant al llarg d'aquest camí i m'han anat guiant i ajudant perquè aquesta tesi arribés a bon port.

Començaré donant les gràcies al responsable de tot plegat, a en Carles. Moltes gràcies per la oportunitat que em vas donar al obrir-me les portes del teu laboratori. Per invertir temps i diners perquè m'anés formant i anés aprenent a investigar i per tot el coneixement que m'has transmès. Durant tots aquests anys he après moltíssim! Moltes gràcies.

Tota aquesta feina també ha estat possible gràcies als companys que han anat passant pel laboratori al llarg d'aquests anys. Lílian, Muriel, Míriam i Arnaldo, gràcies per haver-me ajudat a donar els primers passos en el món dels westerns i les immunos. Lluny queden els primers blots on tot el film sortia negre! Gracias también por la paciencia cuando os preguntaba mil cosas y la ayuda con la optimización de protocolos. Carlos, Anna, Lola, Ángel, un brindis por los aaaaaaix, los pim pim pims y las risas tontas de cansancio. Os deseo toda la suerte del mundo con vuestras tesis y que podáis seguir endulzando los varios "atropellos" científicos con un montón de croissants de chocolate! També m'agradaria donar les gràcies a les estudiants de màster Paula, Laura i Noelia que m'han ajudat (i molt!) en alguns experiments d'aquesta tesi. També a la feina feta per tots els tècnics que han passat pel laboratori, per fer moltes tasques essencials que sovint són invisibilitzades. M'agradaria fer una menció especial per l'Òscar, per passar-se hores i hores tallant fins a aconseguir unes llesques impossibles amb el criòstat. La teva energia matinal era un xut d'alegria i optimisme per encarar el dia.

També un agraïment infinit a tots els Pepe's (Alfredo, Dolo, Judit, Cris i els diversos masterands) per l'ajuda durant els moments obscurs de generació lentiviral i per haver permès el robatori descarat i reiterat de còrtex. Als membres del laboratori veí: Abel, Arantxa i Raquel, amb els vostres consells va ser més fàcil fer el salt de neurones a astròcits! I a la resta de professors i companys de l'INc, per l'ajuda i els moments compartits. També a tot el personal tècnic. M'agradaria agrair especialment a la Tzvetana, pels seus coneixements i experiència en l'anàlisi de FRET, i a la Núria, per haver-nos ajudat tant amb la posada a punt de tots els *settings* quan no sabíem ni per on començar. A en Jaume, per tota la orientació i l'ajuda rebuda per fer els experiments conductuals. També al personal d'administració. Gràcies per facilitar-me tot el *papeleo*, sobretot durant aquesta última etapa!

Judit, Cris, moltes gràcies per tots els moments compartits tant dins com fora del departament. Ja sabeu que totes aquestes pàgines no haguessin estat possibles sense vosaltres. Així que, ara que acabo aquesta etapa, us ho agraeixo de cor. Mil gràcies per l'ajuda, per aguantar el meu discurs *cansino*, pels *planassus* i per les aventures sense maleta! Espero que la vida no ens allunyi gaire.

Ja fora del departament, també m'agradaria donar les gràcies a tota la gent que m'ha acompanyat al llarg d'aquesta etapa, que m'ha ajudat a desconnectar de la feina i que, malauradament, també ha hagut de patit les frustracions.

Per tot això, infinites gràcies a la família. Mama, papa, Xevi, per tot el suport, acompanyament i ànims durant tots aquests anys que han vingut carregats de reptes. Per aguantar-me, mimar-me i musicar els difícils mesos d'escriptura confinada. No voldria acabar aquest paràgraf sense fer notori el nivell d'implicació familiar en aquest projecte. I és que l'angoixa i l'interès per rebre un mail de l'estabulari avisant-me d'un possible part, ha acabat essent compartit a nivell familiar.

Als companys de pis, per ser la segona família i poder compartir vida en diversos xalets a Sarda. Ari, Leyre, Mireia, Eric, Anna. Gràcies per tots els Catans però també per escoltar amb cara d'interès tots els assajos de les presentacions! Al final us heu tornat uns experts en CREB i CRTCs, i crec que ja hi teniu cert domini!

A la penya croquetaire: Cris, Vicente, Clara, Guillem, Manu, Aleix, Marta i, ja quasi londinencs, Gisela i Carlos. Per tots els moments de desconnexió que ens han portat mil anècdotes, a vegades inversemblants, en companyia de la cabra Pelé, els petards, les avellanes i la pinça! Per tots aquests moments de felicitat, mil gràcies!

A la Kati, per totes les quedades on hem pogut compartir tant! Ets una gran referent i et desitjo tota la sort del món en aquesta nova etapa. A la Laura, per tot el suport i ànims rebuts des de la distància a través de parrafades i podcasts. Molts ànims i sort amb les teves mosquetes. A la Mireia, per tot l'optimisme i per ensenyar-me a treure ferro a qualsevol problema. Quan tot això acabi ho celebrarem amb un bon "sucre"!

I per últim, als garrotxins. Blanca, Ari, Serrat, Andreu, Martin, Núria, Eric, Quel, Albert i els expatriats Ula, Sílvia i Eli. Per tots els sopars improvisats, les tardes de jocs, les gimcanes i les farres de poble pre-covid. Els *findes* sense vosaltres no haguessin estat el mateix.

A tots vosaltres, MIL GRÀCIES!